THESIS DISSERTATION

TOWARDS OPTIMAL POWER DISTRIBUTION STRATEGIES FOR MODULAR BATTERIES

Ageing-aware predictive management

XABIER DORRONSORO MARTINEZ

2024

PHD PROGRAM IN

APPLIED ENGINEERING

TOWARDS OPTIMAL POWER DISTRIBUTION STRATEGIES FOR MODULAR BATTERIES: Ageing-aware predictive management

PhD Dissertation Presented in

MONDRAGON UNIBERTSITATEA

as Part of the PhD Program in

APPLIED ENGINEERING

Presented by

XABIER DORRONSORO MARTINEZ

Directed by

DR. UNAI IRAOLA

Codirected by

DR. ERIK GARAYALDE

In HERNANI, December 2024

ABSTRACT

Over the last few years, the battery system industry has shown a steady growth, largely as a consequence of a pressing energy transition that calls for sustainable alternatives to conventional energetic model. Despite areas for improvement, Li-ion batteries have emerged as a leading storage system, outperforming numerous competing options. In the development of these systems, multiple scales are evident, which complicates their integration in practice. Spanning from the small scale, with portable electronic devices, to the large scale, with storage systems fulfilling grid level functions, via the medium scale, with private or commercial means of transport.

This research focuses on medium and large storage systems, which are characterised by a design, control and security that transcends a single or few cells. Such systems assemble independent modules and make serial and/or parallel connections, scaling up to the dimensions required by the application. Notwithstanding an increase in the adoption of these systems, it is relevant to note that both the asymmetries between the different cells and modules, as well as the growing interest of some applications in second life batteries, dictate the need for maximising the potential of modular configurations. In this context, this thesis aims to design a predictive control, based on the electro-thermal and degradation model of the battery, to determine the power distribution across different modules, in order to optimise the performance and lifetime of the battery.

Results illustrate, on the one hand, the feasibility of implementing this control strategy to obtain better quantitative results than those met with a control that distributes the power demand, based on the nominal capacity of each module. On the other hand, obtained operating dynamics reveal that reducing divergences between state variables of different modules, such as temperature or state of charge, need not always be the optimal solution. Therefore, the formulated control strategy supports the initial hypothesis and confirms the fulfilment of the main objective.

LABURPENA

Azken urteotan, bateria sistemen garapenean diarduen industriak hazkunde etengabea izan du, ohiko energia eredua aukera jasangarriagoengatik ordezkatu nahiaren edo beharraren ondorioz, hein handi baten. Biltegiratze sistema horien hedapen prozesuan, bereziki, Li-ioetan oinarrituriko teknologiak hartu dute aurrea, gaur egungo sistemek hobekuntza esanguratsuak behar izan arren. Sistema horien garapenean, hainbat aplikazio maila sailkatzen dira, bakoitza ezaugarri bereizgarriekin, eta horrek, azken finean, BESSen integratzea zailtzen du. Aplikazio maila horren adibide dira, eskala txikiko gailu elektroniko mugikorrak, eskala ertaineko garraiobideak (pribatuak naiz merkataritzako izan) edota sare elektrikoarekin elkarlanean aritzen diren eskala handiko biltegiratze sistemak.

Lan honen ikerketa lerroa tamaina ertain naiz handiko biltegiratze sistemetara mugatzen da, horien diseinu, kontrol eta segurtasun neurriak bateria unitate bakar batetik edo gutxi batzutatik haratago eramanaz. Era horretako sistemen diseinu prozesuan, aukera zabalduena, hainbat bateria unitatez osaturiko modulu independienteen muntaitik abiatzen da, ostean, horien arteko serie eta paralelo konexio aukeren bitartez aplikazioak zehazturiko ezaugarrietara egokituz. Hala baina, ekidin ezin diren bateria unitateen edota moduluen arteko funtzionamendu desorekatuek, baita baterien bigarren bizitza bultzatzen duten aplikazioek, lehen mailako behar bilakatu dute egitura modular aurreratuagoen garapena. Erronka horri erantzuna emateko, tesi honen heleburua, moduluen arteko potentzia banaketa baterien eredu elektro-termikoaren eta degradazioaren arabera egingo duen iragarpen bidezko kontrol estrategia baten garapena da. Era honetan, bai bateriaren errendimendua, baita bateriaren bizitza luzatzea ahalbidetzea lortu nahi da.

Ikerketa amaitzeko, alde batetik, proposaturiko kontrol estrategia emaitza kuantitatiboak hobetzeko erabili daitekeela ondorioztatu da, modulu bakoitzaren funtzionamendu potentzia, dagozkion Ah kopuruaren arabera proportzionalki banatzen duen kontrolarekin alderatuz. Bestalde, funtzionamendu dinamiken analisiaren bitartez, baldintza desberdinetan dauden baterien egoera aldagaien (tenperatura edo karga-egoera, esaterako) orekatzeak ez duela zertan irtenbide egokiena izan erakutsi da. Beraz, proposaturiko kontrol-estrategiak hasierako hipotesia babesten du eta helburu nagusia betetzen dela erakusten du.

RESUMEN

Durante los últimos años la industria de los sistemas de baterías ha mostrado un crecimiento continuo, en gran medida, como consecuencia de una acuciante transición energética que reclama modelos sostenibles y alternativos al convencional. A pesar de presentar áreas de mejora, las baterías de Li-ion han emergido como líderes en el desarrollo de estos sistemas de almacenamiento, superando a numerosas soluciones competitivas. En el desarrollo de estos sistemas, se evidencian múltiples escalas de aplicación, cada una con distintas características, lo cual complica su integración. Desde la pequeña escala, con dispositivos electrónicos portátiles, hasta la gran escala, con sistemas de almacenamiento que cumplen funciones a nivel de red eléctrica, pasando por la media escala, con medios de transporte particulares o comerciales.

Esta investigación se centra en los sistemas de almacenamiento de medio y gran tamaño, los cuales se caracterizan por un diseño, control y seguridad que trascienden de una única o pocas celdas. Este tipo de sistemas ensambla módulos independientes y realiza conexiones en serie y/o paralelo, hasta escalar a las dimensiones requeridas por la aplicación. A pesar de un aumento en la adopción de estos sistemas, resulta oportuno evidenciar que tanto las asimetrías entre las distintas celdas y módulos, como el creciente interés de algunas aplicaciones en las baterías de segunda vida, demanda maximizar el potencial de las configuraciones modulares. Ante esta realidad, esta tesis busca formular un control predictivo, basado en el modelo electro-térmico y de degradación de la batería, para determinar la distribución de potencia entre los distintos módulos, con el fin de optimizar el rendimiento y la vida útil de la batería.

Los resultados muestran, por un lado, la viabilidad de emplear esta estrategia de control para obtener resultados cuantitativos mejores que los logrados con un control que distribuye la demanda de potencia, en base a la capacidad nominal de cada módulo. Por otro lado, las dinámicas de funcionamiento obtenidas muestran que disminuir las divergencias entre las variables de estados de los distintos módulos, como pueden ser la temperatura o el estado de carga, no tienen porqué ser siempre la solución óptima. Por lo tanto, la estrategia de control formulada apoya la hipótesis inicial y muestra el cumplimiento del objetivo principal.

ACKNOWLEDGMENTS

I must, first of all, express my deepest gratitude to my supervisors, Unai Iraola Iriondo and Erik Garayalde Perez, for their invaluable guidance and encouragement throughout the course of this PhD thesis. Your feedback and dedication have been critical in completing this research.

I would also like to thank you Centro Tecnológico de Automoción de Galicia (CTAG) and the University of California Merced (UCM) for granting me the opportunity to undertake my pre-doctoral research experience at their institutions. I wish to give distinguished acknowledgement to Jorge Varela Barreras and Ricardo de Castro for their mentorship during my doctoral academic placements. Your invaluable input and expertise have enhanced the depth and quality of my work.

Further in my acknowledgment, I extend my sincere appreciation to my Galarreta colleagues, close friends, UCM fellow PhD candidates, handball teammates, Mondragon University professors, as well as to each and every one of you who have accompanied me on this academic journey. Special thanks are due to Manex Aizpurua, Iker Lopetegi and Josu Yeregui. Being able to share the daily experiences of this doctoral thesis with you has turned what could have been a daunting process into something I have found joy in.

Azkenik, eskerrak eman nahi dizkiot familiari. Gurasoei, harturiko erabaki bakoitzean emandako babesagatik; anaiari, burugogor galanta izan arren, laguntza etengabea eskaintzeagatik; eta bidelagunari, beste behin ere partekatzean erronkak eramangarriagoak eta une zoriontsuak are bereziagoak direla erakusteagatik.

CONTENTS

ABBREVIATIONS

AI	**A**rtificial **I**ntelligence
BESS	**B**attery **E**nergy **S**torage **S**ystem
BMS	**B**attery **M**anagement **S**ystem
BoL	**B**eginning **o**f **L**ife
C-rate	**C**urrent **R**ate
CBM	**C**ontrollable **B**attery **M**odules
CAPEX	**C**apital **E**xpenditure
CC	**C**onstant-**C**urrent
CC-CV	**C**onstant-**C**urrent **C**onstant-**V**oltage
CV	**C**onstant-**V**oltage
DC	**D**irect **C**urrent
DoD	**D**epth **o**f **D**ischarge
ECM	**E**quivalent **C**ircuit **M**odel
EoL	**E**nd **o**f **L**ife
ESS	**E**nergy **S**torage **S**ystem
EV	**E**lectric **V**ehicle
FCR	**F**requency **C**ontainment **R**eserve
FEC	**F**ull **E**quivalent **C**ycles
IPOPT	**I**nterior **P**oint **O**ptimisation
KPI	**K**ey **P**erformance **I**ndicator
ML	**M**achine **L**earning
MOO	**M**ulti-**O**bjective **O**ptimisation
MPC	**M**odel **P**redictive **C**ontrol
OCV	**O**pen-**C**ircuit **V**oltage
OPEX	**C**perating **E**xpenditure
P2D	**P**seudo-two **D**imensional model
PBM	**P**hysics **B**ased **M**odel
PV	**P**hoto**V**oltaic
RCP	**R**apid **C**ontrol **P**rototyping
RMS	**R**oot **M**ean **S**quare
SDG	**S**ustainable **D**evelopment **G**oals
SEI	**S**olid **E**lectrolyte **I**nterphase
SOA	**S**afe **O**perating **A**rea

SoC	**S**tate **o**f **C**harge
SoH	**S**tate **o**f **H**ealth
SOO	**S**ingle-**O**bjective **O**ptimisation
UN	**U**nited **N**ations

GLOSSARY

Parameters

c_{BM} (\$)	Total battery module cost
$\mathrm{C_p}(\mathrm{J \cdot K^{-1}})$	Specific heat capacity
$\mathrm{C_{th}}(\mathrm{J \cdot K^{-1}})$	Thermal capacity
$\mathrm{h_t}(\mathrm{J \cdot kg^{-1} \cdot K^{-1}})$	Heat transfer coefficient
$\mathbb{C}_{\mathrm{SoH}}^{\mathrm{ageing}}$ (\$)	Operating cost of the battery
λ (-)	Cost function tuning factor
$\mathrm{m_{cell}}$ (g)	Cell mass
$\mathrm{M_p}$ (-)	Number of parallel modules
$\mathrm{M_s}$ (-)	Number of series modules
N_c (-)	Control horizon
N_p (-)	Prediction horizon
$\mathrm{Q_{cell}}$ (Ah)	Nominal capacity of the cell
$\overline{q_{\mathrm{cell}}}$ (-)	Maximum cell SoC
$\underline{q_{\mathrm{cell}}}$ (-)	Minimum cell SoC
σ (-)	v_{ocv} tuning parameter
$\overline{T_{\mathrm{cell}}}$ (K)	Maximum cell temperature
$\underline{T_{\mathrm{cell}}}$ (K)	Minimum cell temperature
τ (s)	Discrete time-step
v_{ocv} (V)	Open circuit voltage
$\overline{V_{\mathrm{cell}}}$ (V)	Maximum cell voltage
$\underline{V_{\mathrm{cell}}}$ (V)	Minimum cell voltage

Subscripts

m_s	Series module index
m_p	Parallel module index
Tot	Overall capacity
Ch	Charged capacity
cell	Cell scale
BM	Battery module scale

Variables

$\mathbb{C}_{\text{grid}}\ (t)$ (\$)	Momentary grid cost
$J_{BM}(Q_{\text{Loss}})$ (\$)	BM cost value
$J_{\text{supply}}(\tau,\ P_{\text{grid}})$ (\$)	Supply cost value
$P_{\text{cell}}(u,\ V)$ (W)	Cell power
$P_{\text{PV}}(t)$ (W)	PV power
$P_{\text{load}}(t)$ (W)	Demand power
$P_{\text{grid}}(t)$ (W)	Grid power
$P_{\text{loss,cell}}(t)$ (W)	Power losses in the cell
$q_{\text{cell}}(u,\ t)$ (-)	Cell capacity
$Q_{\text{Loss}}(u,\ T,\ q,\ t)$ (Ah)	Lost capacity
$R_{\text{cell}}(u,\ T,\ q)$ (Ω)	Internal resistance of the cell
$SoH(Q_{\text{Loss}})$ (-)	State of Health
t(-) (s)	Time
$T_{\text{amb}}(t)$ (K)	Ambient temperature
$T_{\text{cell}}(u,\ R_{\text{cell}},\ t)$ (K)	Average temperature of the cell
$u(\mathbf{x})$ (A)	Applied current to the cell
$V\ (u,\ R_{\text{cell}},\ T_{\text{cell}})$ (V)	Voltage
$\alpha, \beta\ (u,\ t)$ (-)	Adaptive cost weights
$\gamma\ (u,\ t)$ (-)	Module scaling factor
$\phi\ (V,\ u)$ (-)	Power sharing factor
$\varphi\ (u,\ t)$ (Ah)	Capacity variation factor

Chapter 1

INTRODUCTION

With the presentation of this thesis' framework as its main goal, this chapter begins by introducing the background concerning battery systems. This is followed by the dissertation's contribution to the field and concluded with a brief description of the outline to be followed.

1.1 BACKGROUND

In 2015 the UN approved the 2030 Agenda for Sustainable Development Goals (SDG) committed to the building of a better future [1]. Comprising seventeen objectives, this Agenda is aimed at eradicating poverty, combating climate change, promoting education, advocating women's equality and fostering the preservation of the environment. In meeting these SDGs, new energetic models have burst into the scene, pledging to facilitate reform and contributing to the compliance of sustainable energy related goals. Indeed, under the threat of a climate crisis, the need for responsible production and thoughtful consumption is gaining momentum, urging the industry to align its research and production plans with these targets.

As a response to market needs, social demands and legal commitments, energy storage systems (ESSs) come to the forefront. Notwithstanding its advances, renewable energy, including solar and wind energy, has proven to fall short given its stochastic nature [2]. The shortcomings of these sources comes along with the opening up of new opportunities for the development of completely new systems, namely, the transition of vehicles from a combustion engine to an electric motor [3]. In addressing this shift to new solutions, medium and large-size ESSs, such as electrochemical battery energy storage systems (BESSs), are becoming key means for change [4]. Their portability and high energy density, as well as their efficiency, reliability, and flexibility, make these solutions highly interesting and appealing [2].

Beyond its defining features, battery cost per kWh has dropped during the last few years [5], while the energy density of the latest battery-packs has increased due to advances made in this research field [6]. Dynamics transcending defining characteristics of emerging battery systems allow widespread deployment of electrochemical batteries, including Li-ion batteries. Nevertheless, improvement opportunities and windows for action persist (see Figure 1.1). For instance, upon generally established performance and safety criteria, part of the stored energy remains unavailable. This limitation demands more efficient solutions in fulfilment of the SDGs.

With calls for innovation growing louder, advances in the cells' technologies were not long to come into light. As an example, new materials, such as sodium (Na) [7], were incorporated and the development of revolutionary alternatives, particularly, solid-state batteries, emerged as a path to new and more interesting technologies [8]. Both solutions

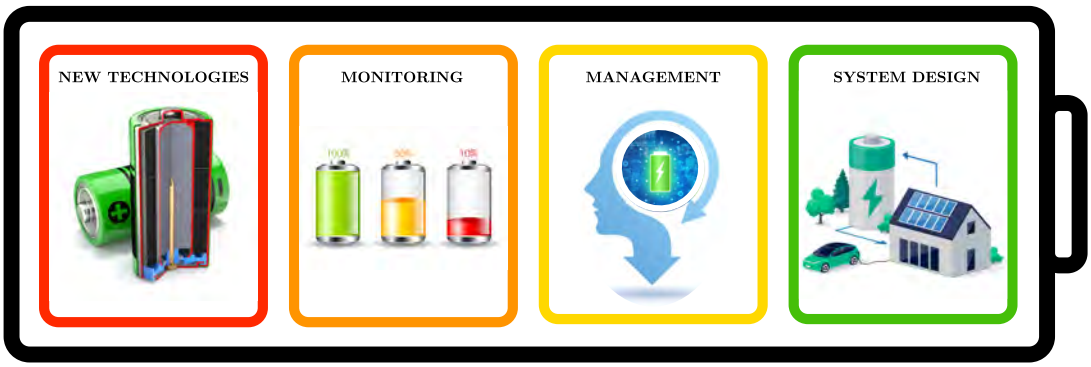

Figure 1.1: Battery-related main research areas.

show promising qualities, although further work is still needed before commercial products can be developed.

Further exploring innovative alternatives, in terms of monitoring, it is worth noting progress made in physics-based models (PBM) or advanced estimators [9–12]. Contemporary hardware equipment allows measuring the majority of the cell-related observable information, for example cell voltage. That being said, today's battery models and algorithms provide no feasible means to take full advantage of data related to cell states. This is where breakthroughs on physics-based and data-driven models or advanced estimators come into play.

Elaborating in previous two lines of research, there is a third investigation path that affects preceding advancements and enables their functioning and effective implementation: the control strategy. Given its partaking in their well-perform, advanced control strategies that are based on better battery characterisations, estimators, and models may increase the computational load, while facilitating better outcomes. Eventually, these management solutions will result in a higher quality system, as well as an increased safety [11, 13].

Concluding with developments, the BESS design deserves attention from system perspectives, since it is decisive for the proper sizing and performance of the energy storage unit. Aspects, such as, the cell technology – new or second life – and the type of architecture to be used – conventional large battery systems or controllable battery modules (CBM) – are to be taken in close regard. Along these lines, the type of battery management system (BMS) communication – centralised, decentralised or distributed – and the power electronic hardware to be employed, are, as well, some of the many variables worthy of notice. Finally, in completing the process of system design, it is key selecting the better suited sizing strategy, among which different alternatives can be distinguished [14].

Drawing upon outlined research topics, a common problem across them is that of the "weakest cell problem" [15]. Resulting from the connection of cells with slightly different

characteristics, this problem is inevitable considering its manufacturing and ageing processes. By virtue of this limitation, the performance of the battery-pack is constrained by the weakest cell. This phenomenon goes back to the beginning of life (BoL) of the battery operation, and asymmetries can reach values around 5% in state of health (SoH) at the end of life (EoL) [16]. To date, the suggested solution mainly consists of developing balancing systems, with the aim of reducing divergences between connected cells. This alternative emphasises voltage balancing in many applications, since this has long been determined as the critical cut-off constraint for safety throughout charging and discharging process. New options have, however, arisen, with the balancing of the state of charge (SoC) and operating temperature standing out [17]. In exploring these alternatives, two kinds of hardware systems are distinguished, each with its advantages and disadvantages [11]. On the one hand, passive/dissipative balancing systems aim to stabilise the system based on excess energy dissipation. On the other hand, active/nondissipative circuits target transferring energy between cells, having regard to the balancing objective.

Efforts made in the battery field have been further complemented by power electronics and control software. Joint endeavours of these distinct, yet related, domains have provided greater improvements, by facilitating the reconsideration of the BESS from a system perspective. Such a comprehensive outlook enables mitigating the "weakest cell problem" beyond balancing at the cell level, by allowing control systems to be implemented at different layers of the BESS, for example at the module level [18]. It is thus possible to control individual units on the basis of their operating state, including isolating them in case of failure, without affecting the entire system. This approach to BESS further facilitates the integration of second-life batteries. Accordingly, a shift from conventional non-controllable modules-based architecture to a new individually controllable and scalable modular battery system layout seems to be promising [19].

1.2 DISSERTATION CONTRIBUTION

With the dissertation topic already defined, the following hypotheses have been formulated:

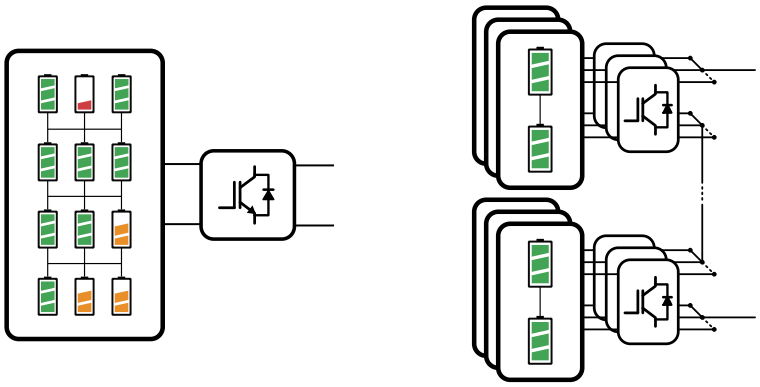

(a) (b)

Figure 1.2: BESS architectures: a) conventional large battery system b) modular BESS.

1.2.1 Hypothesis and objectives

- **H1**. A storage system based on modular batteries, which allows to regulate the operating power of each CBM individually, can enhance the characteristics of a traditional BESS from a qualitative standpoint.
- **H2**. From a control perspective, a solution that modulates the current of each module, based on predictions and optimisations, can present better results, in terms of lifetime and operating cost, than a conventional modular system, where all units operate under fixed operating rules.
- **H3**. When developing a control for modular batteries, the use of information from a battery model, as well as the quality of adapting the control to different battery ageing points, allows for the formulation of a more flexible control which, in turn, results in better battery management.
- **H4**. In controlling modules that differ from one another, or that rely on non-battery agents to regulate module current, consistent results can be obtained, by avoiding a multi-variable optimisation control and opting for a economic cost based single-objective control problem.

These hypotheses underline, on the one hand, that the modular BESS configurations can enhance the qualitative characteristics of a storage system, and, on the other hand, the option of optimising the management of each module as well as the whole system. On this premise, the main objective of the thesis is formulated: to develop a model-based predictive

control algorithm for the power distribution of modular battery systems. In addressing this main goal, various sub-objectives are specified:

- **O1**. To analyse the various advantages and disadvantages of modular systems, with a view to determine whether these turn out to be qualitatively more interesting options than a conventional battery system.
- **O2**. To evaluate the impact of different control variables, namely, the SoC, temperature, current and capacity loss, as well as different control algorithms.
- **O3**. To develop a control strategy that leverages the electro-thermal and ageing model of each module. This algorithm shall feature the flexibility to adapt to the different operating points of the battery throughout its lifetime.
- **O4**. To devise a single-goal optimisation based control strategy, instead of a multi-variable problem, with the aim of building on a multi-agent system, where each module, as any other element in the system, can be regarded as an agent.

This thesis encompasses both qualitative and quantitative methodologies. The herein research begins with an exploratory investigation of the relevant literature and a contextual interpretation of current BESS solutions, to later on proceed to the formulation of a research question that seeks to test the different hypotheses that correspond to the specific objectives. Once the central structure that guides and upholds the whole research process has been laid down, the quantitative and experimental methods are applied to develop a control algorithm that allows the optimisation of the operating characteristics of a BESS. In particular, modelling and simulating tools, such as MATLAB/Simulink® and YALMIP [20], are employed.

1.2.2 Literature contribution

Journal articles

[1] X. Dorronsoro, E. Garayalde, U. Iraola and M. Aizpurua, "Modular battery energy storage system design factors analysis to improve battery-pack reliability", *Journal of Energy Storage*, vol. 54, 2022, p. 105256, doi: 10.1016/j.est.2022.105256. [21]

[2] X. Dorronsoro, R. De Castro, J. V. Barreras, E. Garayalde and U. Iraola, "Battery aging-aware adaptive MPC based on coupled semi-empirical electro-thermal and aging models", *Journal of Energy Storage*". **Submitted for publication**

Conferance papers

[1] X. Dorronsoro, E. Garayalde, U. Iraola and M. Aizpurua, "Modular Battery Systems' Accessible Energy Analysis", *2022 Seminario Anual de Automática, Electrónica Industrial e Instrumentación*, 2022. [22]

[2] X. Dorronsoro, I. Lopetegi, E. Garayalde, U. Iraola and J. Yeregui, "Modular Battery Energy Storage Systems for Available Energy Increase", *2022 IEEE Vehicle Power and Propulsion Conference (VPPC)*, Merced, CA, USA, 2022, pp. 1-7, doi: 10.1109/VPPC55846.2022.10003430. [23]

[3] X. Dorronsoro, R. De Castro, J. V. Barreras, E. Garayalde and U. Iraola, "Model Predictive Control for EV Chargers Coupling Electro-Thermal and Degradation Battery Models", *2023 IEEE Vehicle Power and Propulsion Conference (VPPC)*, Milan, Italy, 2023, pp. 1-8, , doi: 10.1109/VPPC60535.2023.10403342. [24]

[4] M. Aizpurua, E. Garayalde, I. Lopetegi, J. Yeregui, X. Dorronsoro and U. Iraola, "Modular BESS architecture for enhanced performance and extended lifetime", *ECCE 2024*. **Submitted for publication**

1.3 DISSERTATION OUTLINE

This thesis begins by studying the background and addressing the relevance of the chosen research area. Having contextualised the subject matter and justified the reason for its object of study, this thesis continues by setting out the different hypotheses and research purposes. Building on these goals, this chapter presents the methodology used and the structure followed to meet the specific objectives and to provide an adequate response to the main research question.

Charpter 2

Once the methodological and structural foundations have been laid, Chapter 2 summarises the literature review with regard to, first, the various battery design architectures and, second, the different energy management strategies to be considered in the implementation of a battery storage system. With the architectures presented and the basics of battery control defined, this chapter recalls the research proposal on how modular BESSs can be optimally controlled.

Charpter 3

This chapter briefly introduces the different battery models that currently prevail. Upon

the different alternatives, this thesis opts for a semi-empirical model, coupled with an electro-thermal and ageing model, as well as a cost model for each cell. To conclude, this chapter sets out the modular structure to be tested.

Charpter 4

Departing from the semi-empirical battery models and the predictive control algorithm chosen in previous chapters, a first approximation of their implementation is made. For this purpose, a simplified system with a single module in a grid-connected residential dwelling, including a battery and a photovoltaic (PV) system, is employed. In this context, the feasibility of the problem is looked into, both from the model and the control strategy perspectives. Once launched in simulations and in a rapid control prototyping (RCP) system, the results are presented and the possibility of extrapolating the whole system to modular batteries is examined.

Charpter 5

This chapter takes the knowledge gained in previous section and adapts earlier insights with the aim of optimally controlling the modular BESS, through the use of predictive control. The aim is to ensure that the control algorithm formulated determines the operating current of each agent, in order to reduce the total cost of the system's use, while extending the useful life of the battery.

Charpter 6

The last chapter outlines the most significant findings obtained, via the analysis of initial hypotheses, and summarises key conclusions in accordance to the research question posed. Beyond discussing the aftermath, this chapter draws possible future lines of research, building on the outcomes obtained in this thesis.

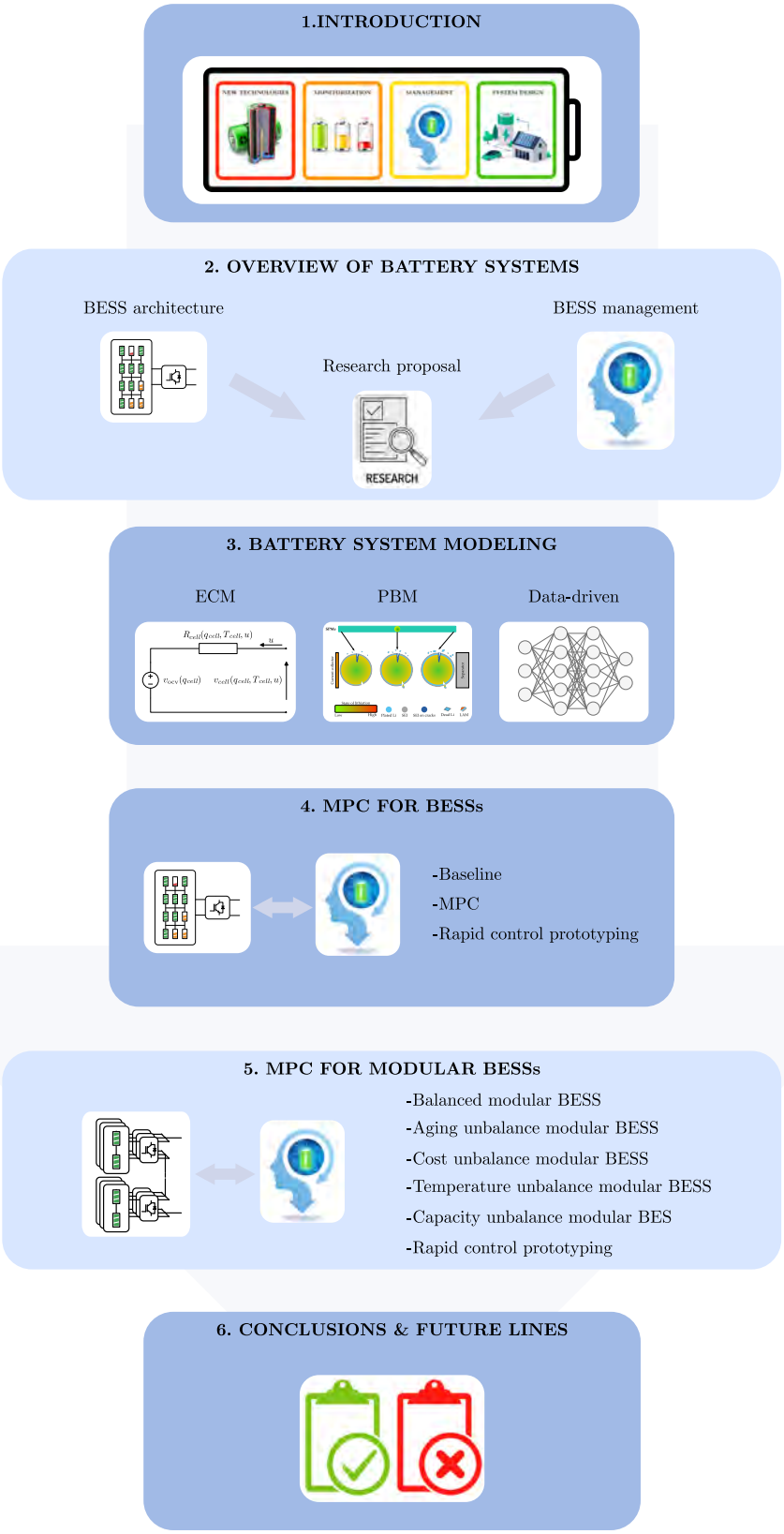

Figure 1.3: Dissertation outline.

Chapter 2

OVERVIEW OF BATTERY SYSTEMS

In further exploring batteries, Lithium-ion BESSs have gained ground. This storage technology consists of developing configurations that connect cells in series/parallel with a BMS for monitoring, estimation, balancing and safety tasks. The rationale behind connecting these battery cells/modules in series and parallel is to be able to adapt the sizing to specific application requirements. Despite their utility, new hardware and control designs appear to promote new concepts of reconfiguration and modularity, with the aim of reducing the heterogeneity of the cells generated during their lifetime, and, ultimately, to maximise the performance of any battery. Through this analysis it is possible to formulate a research question for improvement of the BESSs.

2.1 BATTERY ARCHITECTURE DESIGN

A BESS is a complex system that calls upon knowledge from multiple engineering fields for its development. In this section, a hardware-oriented analysis is considered. Under this perspective, the details related to conventional batteries are first introduced, yet thermal design is not contemplated. Next, emerging trends, such as reconfigurable batteries and modular BESSs, are presented. Through this appraisal, it is possible to determine which alternative has the greatest potential to improve current battery systems.

2.1.1 Conventional battery systems

In designing a medium to large storage system for applications, namely, electric vehicle (EV) or stationary systems, a single cell does not meet the application requirements. Their voltage, current and capacity specifications demand a more complex solution. Consequently, battery-packs are traditionally formed by grouping a large set of cells, a BMS for monitoring and control purposes, along with a power converter system that connects the battery to the application. To group these cells together, the series connection is used to increase the voltage of the battery-pack, while parallel connection is required for scenarios with higher current and capacity demand. In light of the above, the decision to determine the number of cells in series and parallel is generally based on a design process that considers layout factors including power, efficiency, safety and cost. For instance, the latest EV designs employ batteries with a cell-to-pack structure by connecting cells in series reaching a nominal voltage of e.g. 800 V [25], while energy can vary from 20 up to 118 kWh [26]. Another example could be a large-scale BESS, where thousands of cells are necessary to meet appliance requirements. Joining all these cells together, however, is not feasible. Therefore, the industry considers the alternative of assembling modules that are independent - with their BMS for cell level tasks -, but not controllable - as they do not have individual converters at module level -, which are serialised/parallelised in the final configuration as deemed appropriate [11].

In determining the BESS specifications, cells with equal characteristics are presumed. This implies, for example, that a 16P16S module configuration (16 cells in parallel and 16 cells in series) has approximately 256 times more power and energy than a single cell. That being said, during operation, a battery-pack with cells connected in series is prone to different initial state and parameter values [27]. There are several underlying drivers for

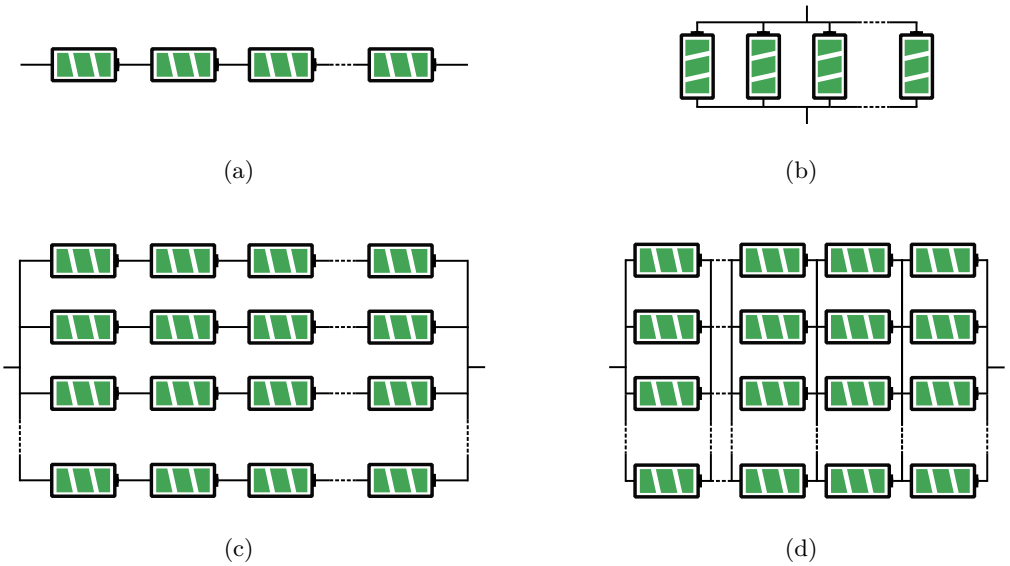

Figure 2.1: Cell-to-cell connection in conventional BESSs: a) Series, b) Parallel, c) Series-parallel, and d) Parallel-series. The connection strategy can be applied at module-to-module level in the same way.

these differences. On the one hand, cell mismatch is a common practice in manufacturing and can vary from 1% to 10% at the inception of the battery's life [28, 29]. On the other hand, cells do not degrade identically throughout lifespan because of initial differences and other physical asymmetries, such as temperature distribution inside the battery-pack [30]. Consequently, the remaining capacity and SoC diverges between cells, and the value of updating the state of the cells in each sampling interval gains ground. As an example of such relevance asymmetries in a series string is that, whenever the same current is drawn through each individual cell, accessible energy is limited by the weakest cell. This effect is depicted in Figure 2.2, which illustrates the discharge of a battery string composed of two unbalanced cells.

As far as heterogeneity of cells connected in parallel is regarded, the voltage differences are automatically balanced by the nature of the electrical connection pattern. This does not, however, ensure that these are balanced in all other battery states. Further, it should be noted that, due to these differences, recirculating currents arise between the cells connected in parallel, which results in uneven degradation [31]. Although this is a phenomenon already identified by the industry, there is still no standard solution to address this challenge.

When these inconsistencies are poorly managed and redundant controls are not possible, the chance of overall system failure increases as a result of the weakest cell. Additionally, with an increase in the number of cells, there is a corresponding rise in the quantity of electronic components, which impacts the probability of malfunctions. In the event of

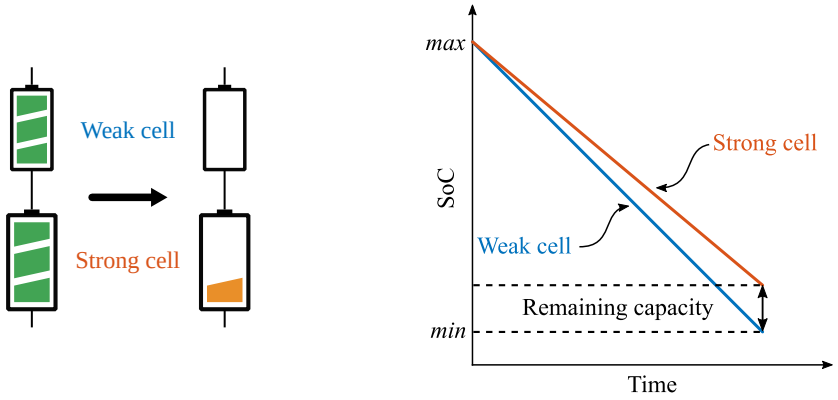

Figure 2.2: Impact of cell-to-cell asymmetries during the discharge of two cells in series: a) Initial and final state of the cells, illustrating remaining capacity, and b) The discharging process, where the weak cell reaches minimum SoC before the strong cell [18].

an internal failure, the BMS is not capable of isolating just the source of the problem, which ends up shutting down the entire BESS. New trends, introduced in Section 2.1.2, are drawing attention in order to address this issue. Nevertheless, by the time the design process, the feasibility analysis and the implementation stage are conducted, the industry has already a functional solution in place. This alternative counteracts the effect of cell asymmetries, including additional hardware to the BMS, in order to enable battery variable equalisation, for example voltage or SoC balancing, of all cells inside a battery-pack. The following subsections will examine frequent cell balancing methods and their associated hardware circuits.

2.1.1.1 *Cell balancing method*

The integration of a BMS is necessary when it comes to monitoring, estimating, controlling and ensuring the safety of battery cells. At unit level, this BMS must also integrate a balancing system to modify the state of each cell in order to find the balance point. This balancing can differ depending on the control variables and objectives, with SoC or voltage being the most standard options. Besides these options, another alternative is the reduction of thermal dispersion between cells as a control target. Considering the aforementioned, and aiming to address the equilibrium issue mentioned earlier, this section outlines the following classification.

On the one hand, there is the balancing method known as the *passive* or *dissipative balancing* [11]. In order to illustrate this typology with an example, consideration can be given to SoC balancing. Its functioning is based on draining the energy from those cells

that have a higher capacity than the setpoint established by the controller [32]. Although, traditionally, these circuits only used passive components, current solutions include active components and controls to face the cell unbalance. Consequently, the more appropriate terminology to refer to this balancing method nowadays would be *dissipative balancing* rather than *passive balancing*.

On the other hand, there is the method *active/nondissipative balancing* [11]. This alternative, drawing again on the example of SoC balancing, consists in the re-allocation of the energy of the unbalanced cells, while avoiding thermal dissipation solutions. This equilibrium is achieved by means of an active balancing system that redistributes the energy of the most charged cells to the weaker cells or auxiliary load circuits [33]. Yet, as discussed earlier, *dissipative* solutions nowadays already integrate active components and controls. On this premise, *nondissipative balancing* is a more appropriate name for these solutions.

To implement both methods of balancing series-connected cells, there are two aspects from the actuation moment perspective. The first option focuses on balancing once the operating parameter of the cell reaches the limit, while others have yet to do so. As an example, Figures 2.3a and 2.3b show what this phenomenon could look like for SoC balancing with *dissipative* and *nondissipative balancing*. The second alternative is based on performing balancing throughout the cell operation, as shown in Figure 2.3c. Although this solution can be implemented by *dissipative balancing*, the main option is to employ *nondissipative balancing* methods. Therefore, when selecting one of the two options, one should also consider the period required for the minimisation of any asymmetry.

A glance at the various techniques that have been studied reveals that the simplest and most popular technique relies on balancing the voltage at the terminals of the cells connected in series [32]. That said, this voltage value may vary due to the electrical resistance of both the system wiring and the cell itself. As a result, voltage balancing may not always be the most accurate indicator. An alternative to voltage balancing, which is also widely used, is SoC balancing with either *dissipative* or *nondissipative balancing*. Nevertheless, this option presents the challenge of accurately estimating the SoC of all the cells, beyond the complexity of the balancing circuit. Currently, developments that employ advanced Kalman Filters [34] are gaining relevance and may boost SoC estimation for balancing. Still, a variety of alternatives have been published in the literature that are not limited to voltage or SoC, examples such as Barreras et al. [35] show how multiple objectives can be taken into account when developing the balancing algorithm.

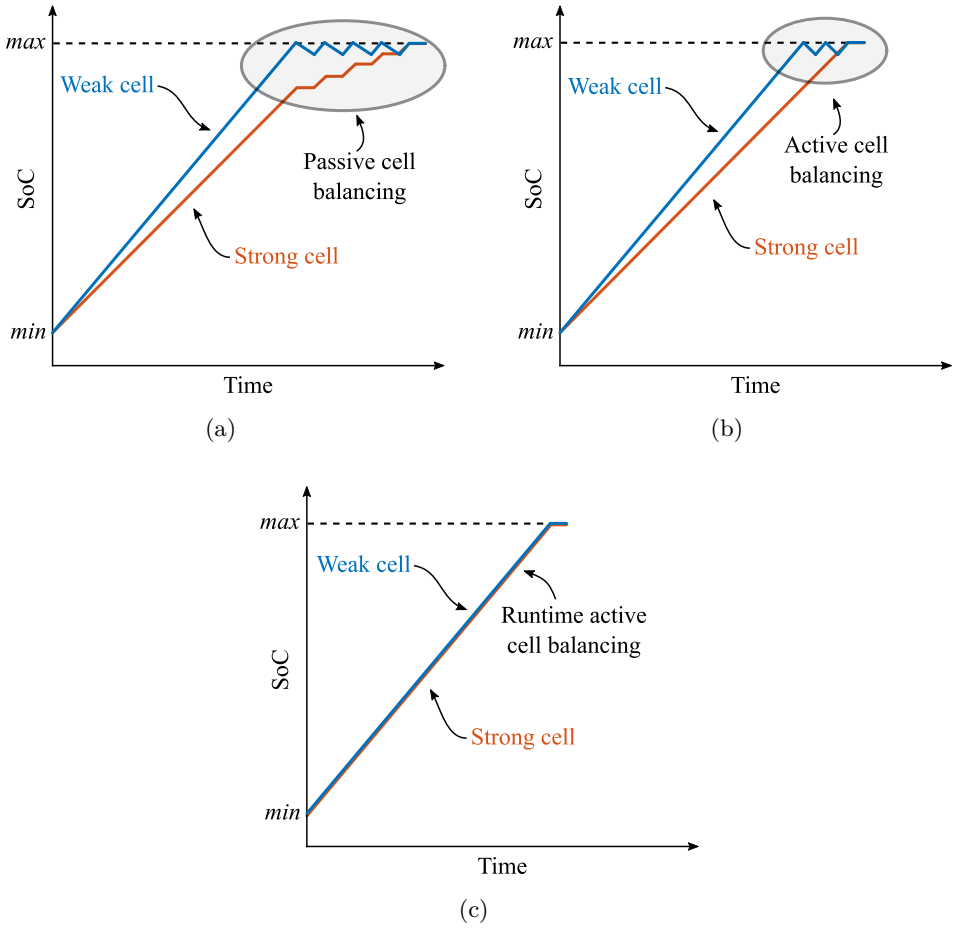

Figure 2.3: SoC balancing alternatives: a) *Dissipative balancing* at the end-of-charge, b) *Nondissipative balancing* at the end-of-charge, and c) *Nondissipative balancing* during operation [18].

2.1.1.2 *Cell balancing circuits*

For the implementation of balancing algorithms it is mandatory to have an equalisation circuit that is adapted to the requirements. These design demands can have a direct impact on the development of the balancing circuit. When it comes to dissipative circuits, the topology mostly adopted resembles Figure 2.4, where a controllable switch allows individual cells voltage and SoC management. Often, high value resistors are utilised to limit the overall amount of heat generated inside the battery-pack during balancing, which is generally performed at the end of the charge.

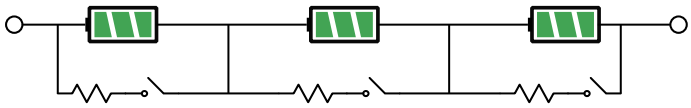

Figure 2.4: *Dissipative* cell balancing circuit. The excess energy is dissipated by the resistors.

For nondissipative balancing solutions, power converters are required for power reallocation. As less power is dissipated with these circuits, higher balancing efficiency and faster

balancing times are achieved at the expense of more complex hardware and software. When analysing the different alternatives, data evidences that the more sophisticated circuits provide a wider range of options. Based on the analysis carried out by Ghaeminezhad et al. [36], these circuits are divided into four main groups:

- **Adjacent-based configuration:** Energy is transferred between the adjacent cells and modules, and can be categorised as series-based [37], layer-based [38] and module-based cell-cell topologies [39]. Each of them is shown in Figures 2.5a, 2.5b and 2.5c respectively.

- **Nonadjacent-based configuration:** *Nondissipative balancing* circuits connect each cell or module with the whole battery-pack, and energy is transferred between them. The nonadjacent-based topology is divided into series-based [40] (Figure 2.5d) and module-based cell-pack [41] (Figure 2.5e).

- **Direct cell-cell topology:** Energy is reallocated from any cell to any other cell by employing an appropriate control system, regardless of whether the cells are adjacent or nonadjacent. The direct cell-cell topology is illustrated in Figure 2.5f [42].

- **Mixed topology:** Hierarchical balancing concept is introduced to achieve cell balancing either employing adjacent or nonadjacent topologies. For instance, the bottom layer balances the cells within each module, under the control of a slave BMS; the top layer is responsible for equalising the available capacity between the modules through the associated topology, under the control of a master BMS. This is depicted in Figure 2.5g [43].

In summary, while *nondissipative balancing* circuits enhance efficiency and leverages available energy, the advantages over *dissipative balancing* systems, which feature simpler hardware designs and lower costs, are rather marginal. On this ground, many commercial systems opt for *dissipative balancing* circuits given to their straightforward hardware configuration and cost-effectiveness.

2.1.2 New trends in battery systems

Given the above, in order to adapt the batteries to the characteristics of each application, it is necessary to consider their sizing by serialising and paralleling the cells. This is due to the fact that, as the number of cells in series that make up the battery increases, the probability of suffering from the weakest cell limitation is greater. In other words, the larger the dimensions of the BESS, the greater is the complexity of the solutions aimed at resolving the heterogeneity represented in Section 2.1.1. In this line, paralleling cells on smaller scales, or modules in larger scale applications, runs the risk of operating with different terminal voltage units, which can cause unwanted current flows, and, consequently, led to cell overcharging/discharging, efficiency reduction, and temperature rise.

In the last decade, modular or reconfigurable configurations have become increasingly popular and very advantageous in new BESSs designs. This is mainly due to the constraints imposed by the limitations of series and parallel connections of a single BESS. Indeed, these new alternatives allow for capacity expansion, improved fault redundancy and ease of maintenance, while ensuring uninterrupted operation of the BESS.

2.1.2.1 *Reconfigurability*

Traditionally, the different approaches to BESS design have converged on establishing a fixed architecture of both cell and module connections, featuring no flexibility of control over each element. A clear example of the latter is the cell-to-pack structure that dominates the electric transport industry. In view of traditional models' constraints, reconfigurable solutions are gaining ground, notably in the academic world.

Conventional balancing circuits and algorithms are limited to equilibrating the possible differences among the cells, as presented in Section 2.1.1. Instead, in the new reconfigurable battery systems, the flexibility of the circuitry allows for varying its characteristics, including the voltage and the available capacity. This versatility opens up a new line of research, in order to determine the control target and the type of algorithm to be implemented, with a view to improving the performance and lifetime of the BESS.

Enhanced flexibility, however, also poses challenges from a safety perspective. Conventional BESS designers focus primarily on pack-level reliability to prevent short circuits, malfunctions and abuse. With reconfigurable batteries, there are new challenges to overcome [44, 45]:

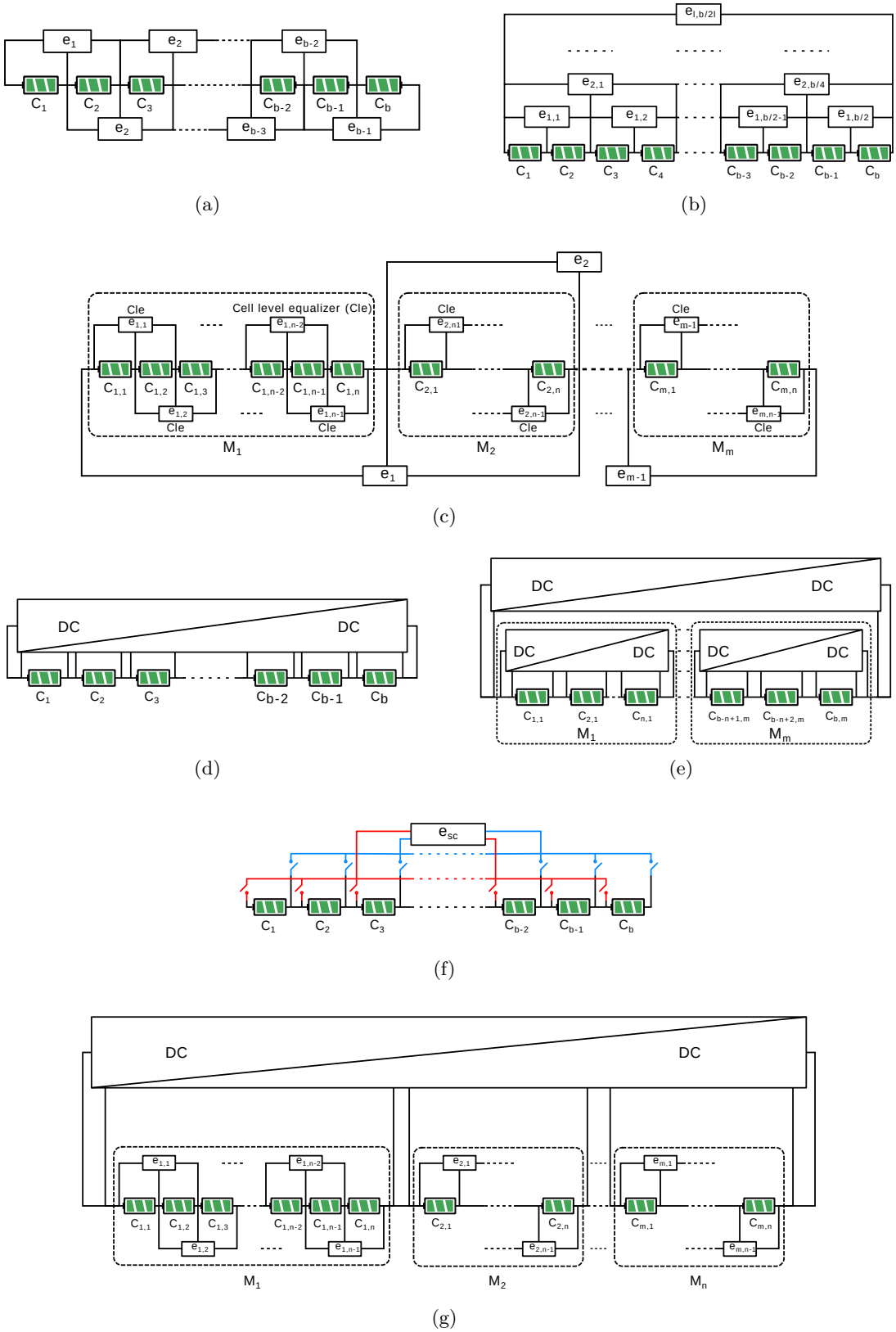

Figure 2.5: *Non-dissipative* cell balancing systems: a) Series-based adjacent cell-cell topology, b) Layer-based adjacent cell-cell topology, c) Module-based adjacent cell-cell topology, d) Series-based cell-pack topology, e) Module-based cell-pack topology, f) Direct cell-cell topology, and g) Mixed topology [36].

- **Circuit safety:** Short-circuiting is considered the most destructive issue concerning circuit safety. When traditional architectures are replaced by complex configurations with a large number of switches, these electronic devices become more error-prone, leading to short circuits. Consequently, destructive current circulation becomes more likely. In this context, while new-generation components have evolved to address this vulnerability, there is still a lack of large-scale reconfigurable system protection due to the inherent difficulty.

- **Thermal issues:** Thermal stress accelerates cell imbalance leading to increased degradation. On this premise, alongside the risk of conventional systems, regarding heat generation from cells and external components, reconfigurable architectures have to deal, as well, with a large number of switches that generate heat through power losses. Should the thermal sizing not be performed correctly or a failure during operation occurs, the battery can suffer from thermal runaway. As a result, these adaptive circuits are considered to be more vulnerable systems.

- **Efficient sensing:** To avoid any hazard, as is the case with traditional BESSs, large-scale reconfigurable battery-packs must be monitored carefully, periodically, and accurately [46]. That being said, implementing a more complex system requires a greater investment in system development. Failure to do so can lead to severe errors. In fact, integrating simpler and cheaper solutions may result in critical malfunctions. Moreover, with a system comprising more electronic components and increased communication channels, the likelihood of failure and the challenge of managing digital I/O also increases. A well-designed sensing circuit for a large scale reconfigurable battery system is supposed to jointly consider cost, circuit design issues, fault tolerance under various environments, as well as influences introduced by the high mount of noisy sensor measurement.

- **Passive components:** Selecting the right passive components throughout the design process is a major challenge that calls for an exhaustive understanding of, for instance, battery features, circuit characteristics and fault tolerance requirements. Further, in reconfigurable battery-pack designs, active and passive components including, switches, fuses, and pre-charge circuits have critical influence on system characteristics, namely, weight, cost, volume, and safety.

All these reconfigurable BESS features vary depending on the design typology chosen. These typologies are mainly classified by the number of switches that are integrated for

the connection of each cell. An example of this is illustrated in Figure 2.6, where the main configurations discussed in the literature are presented.

In light of Figure 2.6, diverse comparative frameworks emerge from the existing literature (Table 2.1). On the one hand, the number of switches employed by each topology must be noted. On the other hand, the type of inter-cell connection enabled by each configuration - serial, parallel and hybrid - must also be factored in. Moving into further comparisons, the complexity of manufacturing or fault tolerance must also be weighed up from a qualitative perspective.

Table 2.1: Reconfigurable architectures functional comparison [47].

	Switches per cell	Connection			Man. complex.	Fault tolerance
		Series	Parallel	Hybrid		
[48]	1	Y/N	N/Y	N	Low	Low
[49]	$1< x <2$	Y	N	N	Low	Low
[50]	2	Y	N	N	Low	Low
[51]	3	Y	Y	N	Medium	Medium
[52]	3	Y	Y	N	High	Strong
[53]	4	Y	Y	N	Medium	Strong
[54]	5	Y	Y	Y	Medium	Strong
[55]	6	Y	Y	Y	High	Strong

Amidst the process of adopting reconfigurable systems, the concept of reconfigurable modules has also been introduced in order to transfer the advantages from the cell level to the module level [56]. Both intra-module and inter-module alternatives have the potential to improve existing solutions, yet most of them require extensive research and experimental analysis in order to demonstrate their viability in real-world application.

2.1.2.2 *Modularity*

Current BESSs provide increasingly better performance and longer lifetimes with improved battery state estimation algorithms, battery prediction models and advanced control strategies. That said, contemporary battery-packs remain limited in capability to operate optimally each of the different modules. Few cell-to-cell imbalances within a module can be addressed by cell balancing solution, nevertheless module-to-module imbalance management still has great potential for improvement. Having identified this shortcoming, the design alternative aimed at controlling modules, which, while controlled independently, are all part of the same system that must supply the demand of the application, is becoming steadily more prominent.

This module type presents the following characteristics. Internally, it retains the same functions as the conventional ones, thus, preserves the tasks of measurement, estimation,

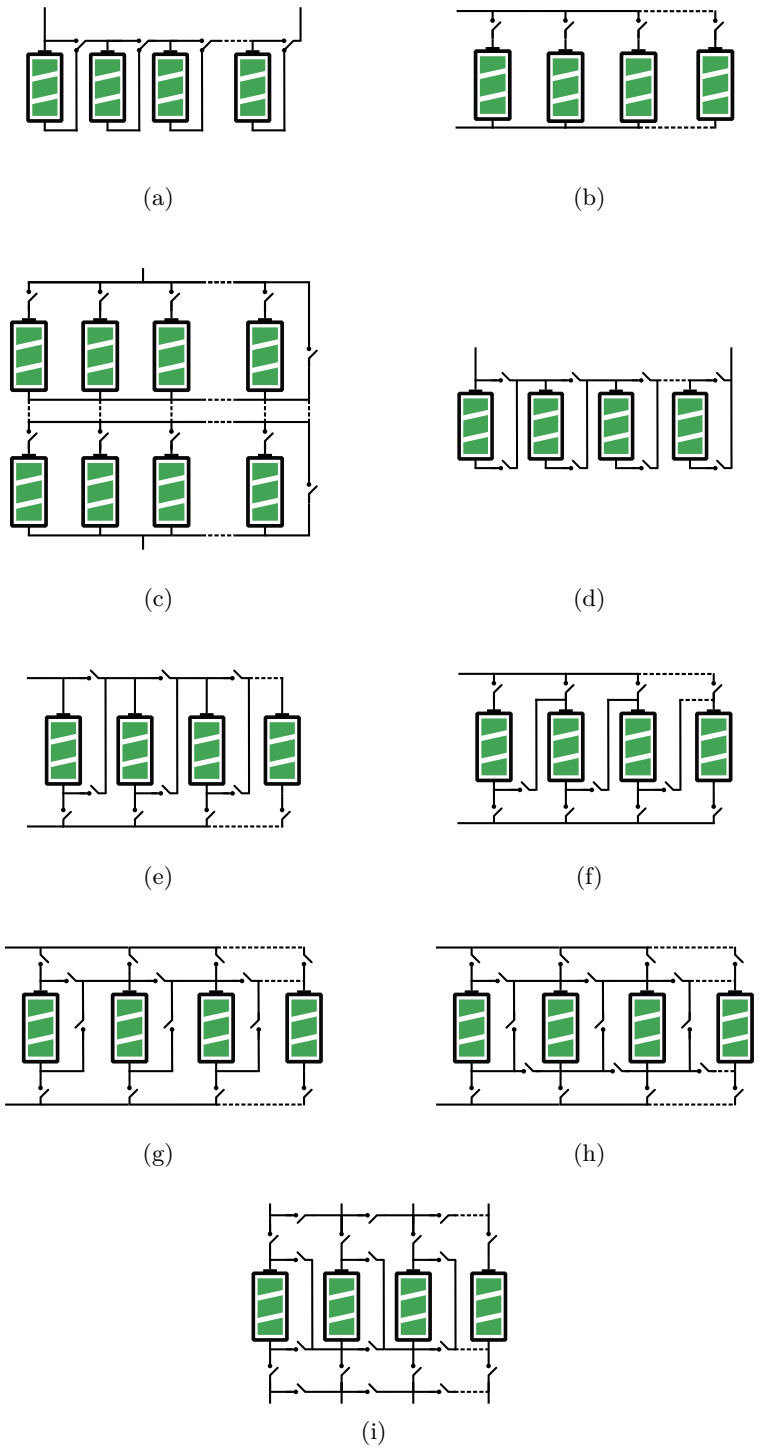

Figure 2.6: Reconfigurable cell connection configurations: a) Single-switch per cell in series, b) Single-switch per cell in parallel, c) Quasi-one switch per cell, d) Two switches per cell, e) Three switch per cell, f) Three switch per cell, g) Four switches per cell, h) Five switches per cell, and i) Six switches per cell.

prediction, balancing and safety. Unlike conventional module concept, instead of connecting them directly to each other, connects the different units via power converters. These converters, located at the output of each module, enable the option of regulating the operating power of each unit. Hence, by means of a control algorithm, it is possible to determine the power distribution between the modules, since they no longer have to operate with the same power setpoint. Such distribution enables the development of controls with different objectives, with a view to improving the performance of the BESS and to extend its lifetime. On these grounds, focusing the scope to fully DC systems shown in Figure 2.7, these are the different modular storage systems configurations:

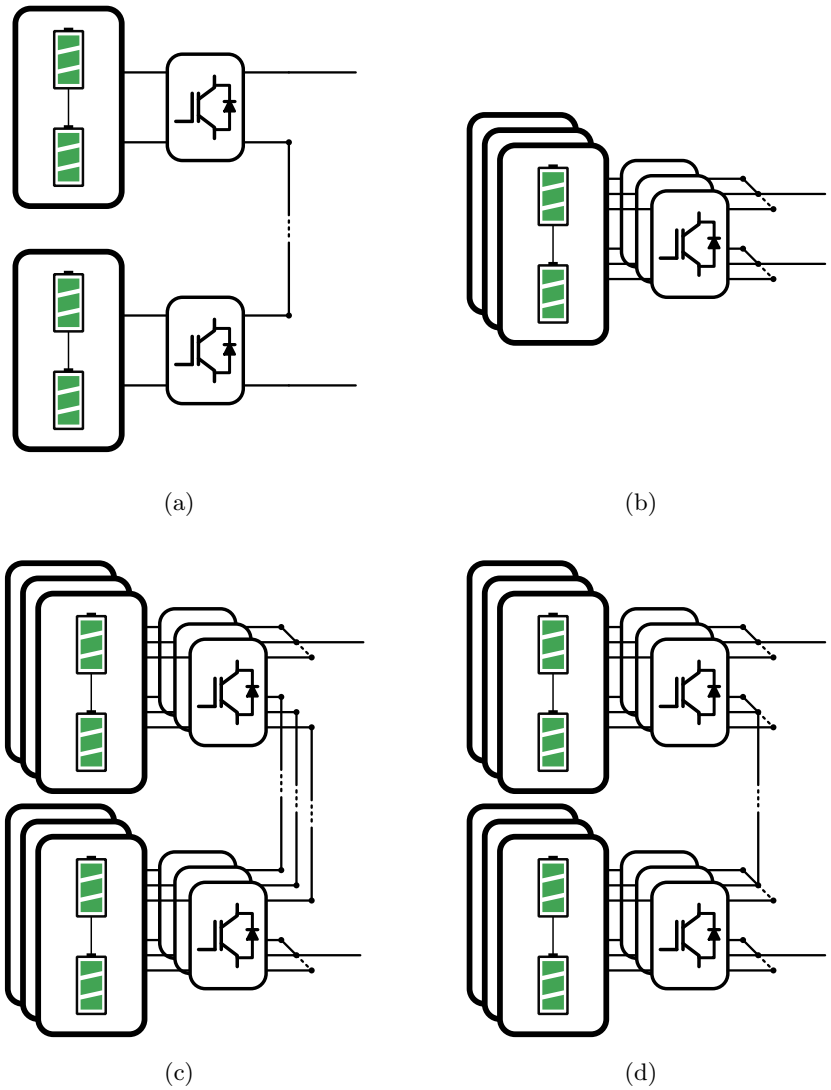

Figure 2.7: Modular BESS topologies: a) Series, b) Parallel, c) Series-parallel, and d) Parallel-series.

- **Series:** In series configuration, the modules are cascaded to achieve the application voltage. By being connected in series, the output current of all modules is identical

to each other. As a result, the power delivered by each module can be monitored by adjusting the output voltages at the module level.

The most important advantage of this configuration is its high voltage level capability, just serialising modules and avoiding complex high voltage amplification converters. Drawbacks revolve around the limited controllability of the system. Improved controllability calls for higher output voltage variability of the modules, which weakens the main contribution of this configuration. In the event of a failure, the faulty module must be bypassed to keep the system operational, while the other modules compensate for the voltage drop.

- **Parallel:** Parallel connection of modules involves coupling these directly to a common DC bus. With regard to current distribution, BESS current is alocated among every module, but not necessarily evenly. This provides the possibility to control the power supplied per module by means of the current flow.

  The parallel configuration offers high controllability to the BESS, where each module can operate at the selected power without control limitations. In addition, when the power required by the application is low and can be supplied with few modules, redundant units could self-diagnose by charging/discharging their power through remaining modules. If necessary, extra modules could easily be added to the system, while avoiding excessive initial oversizing. That being said, all these advantages come at the expense of a complicated DC-DC converter design if the application/battery voltage ratio demands a high amplification.

- **Parallel-Series:** In this topology, the modules are first connected in parallel, and then each set of parallel modules is serialised. With this topology, the system has to share the power between the modules based on two criteria: first, the power that each serialised set of modules has to supply in order to reach the voltage of the application; and, second, the power that each module in parallel must supply with a view to maintaining the balance of the system and meet the application's demand.

  The main advantage of the parallel-series configuration is that it allows higher voltages to be reached than the parallel architecture, while retaining relatively high control over the modules. Besides, the connection and disconnection of the CBMs is also direct, and can be performed by means of a single decoupling contactor. Still, without underestimating its strengths, it is important to note that the control of this

configuration can be of greater complexity, as there are two parameters to adjust: the series branch voltage and the parallel module current.

- **Series-Parallel:** This alternative prioritises the series modules connection to meet the application voltage, and, in turn, connects the serialised module sets in parallel to achieve the power demand. In so doing, each of the arms connected in parallel can provide a different output current. To control the output power of the individual modules in series, it is necessary to adjust their output voltages, keeping their sum equal to the bus voltage.

  Each parallel-connected arm can be controlled independently without limitations. As a result, it facilitates the integration of batteries of different technologies or power ratings. Within each parallelised arm, there are still control limitations, due to the series modules connection, which also reduces the redundancy and fault tolerance of the BESS.

In the literature, several examples delve into the design, development, and implementation of modular batteries. Concerning configurations that prioritise CBMs in series, a greater number of research studies have been conducted in academia. For instance, in 2018, Frost et al. [57] introduced a novel serialised battery management solution based on a completely decentralised strategy. Another serialised modular system was presented by Altaf et al. [58], where they utilised a model predictive control (MPC) to balance the SoC and temperature of different CBMs. As an example of in-field application, Cai et al. [59] implemented a grid-tied BESS of 2 MW/2 MWh used for electric energy time-gap shift in the local grid. Efficiency measurements of this system have indicated that one full-cycle of the whole BESS around the nominal operating point has an efficiency higher than 90%. Regarding parallel configuration, Moo et al. [60] experimentally analysed parallel CBMs, concluding the advantages posed by this design. Another notable example of in-field application is the M5BAT project [61], where a system of 6 MW/7.5 MWh comprising 10 CBMs with five different battery chemistries, including three Li-ion battery technologies and two different lead-acid batteries, were installed. This grid-tied battery is used to ensure frequency containment reserve (FCR) service with an average round-trip efficiency of 72.8% [62].

Drawing on the topologies described above, it is relevant noting on qualitative and quantitative analyses published in the literature. These include reliability, fault-tolerance, controllability, efficiency and scalability, among others. On these grounds, it is possible to

highlight the characteristics that generate the greatest interest, as mentioned by Ma et al. [63]:

- Efficiency can be enhanced by optimised modular design and control, by tailoring the BESS to specific application and avoiding low power/energy operating regions. Especially in series configurations characterised by designs that are not only more efficient, but also more cost-effective, than paralleling topologies.

- CBMs, via power converters, allow enhancing system performance by being able to apply more complex controls. Although serial configurations may exhibit greater consistency, rapidity and stability, the alternative of paralleling offers the greatest flexibility from a control point of view.

- From a reliability and fault-tolerance point of view, modular strategies have advantages, particularly the parallel configuration. This results from being able to control and isolate each module individually, minimising the impact on the rest of the system.

- Scalability and adaptability are also crucial factors of intelligent modular systems. Therefore, adaptability of the dimensions of the storage system is permitted by adding the strictly necessary CBM, avoiding oversizing, as well as facilitating the integration of hybrid solutions with even second-life batteries.

- The economic aspect represents a major challenge that is still to be studied in more detail. This requires not only an analysis of the initial investment, but also an examination of the modular configuration impact over lifetime. Additionally, the fact that the control has a direct impact on the final result when making any comparison is to be considered.

This section introduces the most relevant concepts on modular BESS. In this context, different modular topologies and their characteristics have been considered, and literature-based design examples have been included. Accordingly, it is concluded that the CBM configuration has the potential to outperform current alternatives. That being said, determining which of the modular topologies represents the best solution, either, parallel, serial or mixed, requires more detailed research for each application.

2.2 BATTERY MANAGEMENT

Regarding BESS battery management, reference must be made to criteria set for determining the current to be charged or discharged in a battery. This control is of utmost importance in view of its impact on the sizing of the storage system, which, in turn, conditions both its performance and the lifetime of the battery. Determining this current does, however, raise some challenges worth considering. To begin with, there are many variables to be weighed in optimising this battery management. On top of that, as the size of the storage system increases, so does the number of cells and, with it, the challenges to be overcomed for optimal functioning. Upon such difficulties, detailed information of operating models and the control objectives is critical in preventing oversimplifications that neglect major battery phenomena.

To solve above-mentioned challenges, and as part of the mentioned assessment, a hierarchical approach characterised by a layered control can be introduced. This top-down structure can be regarded to be similar to the one introduced by Ma et al. [63], or to a microgrid described by Unamuno et al. [64], where each level of control performs separate functions. Taking these studies as a reference, in one respect, the uppermost or external control of a BESS, which will be referred to as tertiary from here on, would exercise control at application/utility level. This control layer will determine when the BESS has to be charged/discharged and under which power setpoint. Conversely, the most internal control of the BESS serves the task of controlling the battery by analysing in detail the simplest unit of the battery, which is the cell. In so doing, this level of energy management, categorised as primary control, analyses the state of each cell and determines how every cell should operate in order to comply with the command received from higher level controls. In between the tertiary control (i.e. the most external control) and the primary control (i.e. the most internal control), stands the secondary control. This intermediate control's function is to determine the operating characteristics of the battery modules, comprising cell arrays/matrix, with a view to supplying the power setpoint established by the intermediate control. Building on these three control levels, the hierarchical arrangement, depicted in Figure 2.8, can be simplified for applications with a single or a few cells. Still, this becomes of particular relevance in medium-large sized storage systems where there is a large number of units.

By categorising the overall problematic into different levels, each tier addresses the differing needs of a storage system. As such, every layer can operate on the basis of

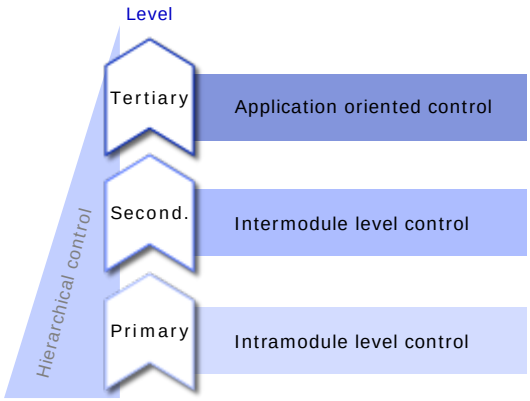

Figure 2.8: Hierarchical control structure for BESSs.

a single goal, or multiple control objectives, in order to bring the performance of the system closer to its optimum level. Exemplary of this premise are the several scientific studies published, which span from minimising cost by means of battery use [65, 66], to reducing battery degradation while complying with charging time targets [67, 68]. In this management endeavour, there is often a need to take into account various constraints, to secure the operating conditions of the BESS. Finally, depending on the complexity and requirements of each control level, there is a plethora of options for battery performance optimisation algorithms. The most widespread alternatives in this framework are the rule-based and heuristic approaches. That said, given the improved computational capacity of contemporary systems, mathematical optimisation based approaches, such as predictive or artificial intelligence (AI) based managements, are gaining traction.

2.2.1 Management strategy

In determining the control strategy, it is essential to define the objective of the algorithm, whether it is a solution for the primary, secondary or tertiary management layer. From this point of departure, the need arises to set, on the one hand, which control level is being worked on, and, on the other hand, which variables and parameters are necessary and available. Thus, the control will be adapted to the requirements of each objective, always meeting the needs of the application. In this task, given the wide range of options, it is indispensable to consider the different alternatives in terms of control algorithms. All this, analysed in more detail below, is summarised in Figure 2.9.

2.2.1.1 *Control variables*

In formulating a control strategy for a battery, it is necessary to identify the many variables and their implications, not only direct but also indirect (i.e. hard-constraint), on the fulfilment of the main control objective.

BATTERY SYSTEM VARIABLES

If we analyse the state variables of a battery, regardless of the elements or the application itself, measurable and non-measurable groups can be distinguished:

- **Measurable** states of a battery are those variables that can be measured quantitatively, by using a variety of techniques and instruments. These measurements provide key information about the battery to ensure safety and control strategies' implementation. The measurable states include: 1) voltage, 2) electrical current, 3) surface temperature, and 4) expansion pressure.
- **Non-measurable** states relate to battery's condition or behaviour that are difficult or impossible to quantify directly during operation by using traditional measurement techniques. These states often require inference or indirect observation through advanced battery modelling alternatives, such as PBMs. Some non-measurable states

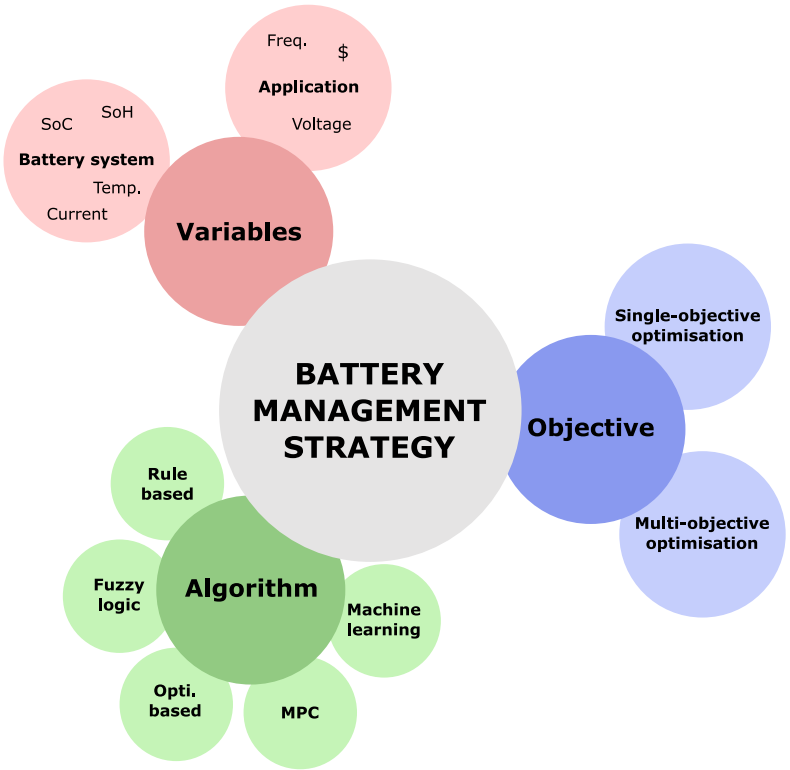

Figure 2.9: Battery management strategy summary.

may include: 1) SoC, 2) SoH, 3) internal lithium concentrations, 4) internal potentials, and 5) electrode capacities, among others.

APPLICATION ORIENTED VARIABLES

A battery has to fulfil a function, which differs depending on the application, yet is always reflected in the form of electrical power. As a result, it is not enough to address state variables of a cell or battery, it is also relevant looking at a higher level, especially when developing a primary control strategy for a BESS. Depending on the application, different system variables must be weighed up [69, 70]:

- **Frequency regulation:** Keep grid frequency within a certain range, by modulating the power output of the BESS in response to load/generation variations. This helps stabilise the grid and ensure system reliability by balancing in real-time supply and demand mismatch.
- **Voltage support:** BESS can supply or absorb reactive power to mitigate voltage fluctuations and maintain voltage within a specified range. The goal is to ensure grid stabilisation.
- **Power peak shaving:** Reducing peak power demand, by discharging the BESS during periods of peak demand, stabilises power generation from the main sources. In so doing, the cost of electricity is reduced, the efficiency of the grid is improved and the pressure on the grid infrastructure is decreased.
- **Energy arbitrage:** This determines the optimal charge and discharge setpoint of the BESS to benefit from differences in electricity generation intermittence and price variations. Hence, BESS is charged when electricity prices are low, or overgeneration occurs, and discharge when prices or loads are high, allowing users to save money and maximise revenue.
- **Islanded operation:** BESSs are required to meet the power demand in islanded areas with local generation sources, including renewable energy systems or diesel generators. Effective control ensures the stability and performance of islanded microgrids during both grid-connected and islanded modes of operation.

2.2.1.2 *Control objectives*

Given all these state variable alternatives, which can be considered as constraint or target, it is not straightforward to determine the best solution. This is illustrated by some

conflicting views regarding the best way to manage battery power. Some prioritise the use of a single target, while others, additionally, include constraints to limit other battery variables. That said, there are cases where, with or without constraints, several objectives are considered together [69].

- **Single-objective optimisation (SOO):** This optimisation problem involves optimising the BESS management by considering only one of the aforementioned variables in the objective function. In so doing, the optimal or sub-optimal solution improves the performance while satisfying constraints that may exist.

$$\begin{aligned} &\min f\left(x\right) = \min\left(f_1(x)\right) \\ &\text{subject to } x \in \boldsymbol{x} \end{aligned} \tag{2.1}$$

  As an examples of this type of control, Dorronsoro et al. [24] introduced a MPC, in this case, with the aim of minimising the cost of a BESS located in an EV charging station. The overall cost as well as the maximum peak-power are reduced with this control strategy.

- **Multi-objective optimisation (MOO):** This optimisation problem involves optimising a system or design by considering multiple objective variables or functions at the same time. Unlike SOO, MOO seeks to find a set of solutions that represent a trade-off between the competing objectives as shown in Equation 2.2, where *f(x)* refers to the objective, p is the amount of objective functions, and x and X are the feasible decisions and the feasible decisions space, respectively. In this optimisation process, a relevant factor when formulating these MOO problems is the need to adjust the impact of each factor in the cost function, by means of weighting factors.

$$\begin{aligned} &\min f\left(x\right) = \min\left(f_1(x), \ldots, f_p(x)\right) \\ &\text{subject to } x \in \boldsymbol{x} \end{aligned} \tag{2.2}$$

  As an example of these MOO problems, Ricardo et al. [17] introduce a multi-layer MPC based power management strategy, that, in comparison with the baseline - no control -, justifies the use of an MOO problem focused on the battery stress (current), ageing-rate and the temperature variations, with improvements of 28%, 7% and 57%, respectively. Pozzi et al. [71] propose a general cell balancing-aware nonlinear MPC scheme for the optimal charging based on a MOO problem. The results highlight

that this charging strategy outperforms other standard charging protocols (such as a CC-CV or a voltage-based procedure).

2.2.1.3 *Control algorithms*

In formulating the battery management strategy, in addition to detailing the necessary information on the previously introduced control variables and objectives, it is necessary to determine the type of control algorithm employed. This algorithm is based on a sequence of mathematical operations that allows setting the action to be performed to achieve intended outcomes. The most extended alternatives in the literature are presented below [69, 72]:

- **Rule-based control:** Relies on user predefined logic and thresholds to determine control actions based on the current measured/estimated battery system states. This control algorithm benefits from straightforward implementation, low computational complexity, and ease of interpretation. Nonetheless, this control can also be hampered by a lack of adaptability to changing operating conditions and a limited performance in complex environments.

- **Fuzzy-logic control:** Instead of rigid true/false distinctions, fuzzy logic deals with the gradual transition from true to false, and vice versa, enabling systems to handle ambiguity and vagueness in data and decision-making processes. This fuzzy logic control offers advantages in flexibility and robustness for BESSs. Still, it also poses challenges in terms of transparency, tuning complexity, and optimal charge/discharge management.

- **Optimisation-based control:** These control algorithms formulate control objectives as optimisation problems, aiming to find the optimal/sub-optimal battery operating conditions that satisfy constraints and objectives. This control alternative offers flexibility in handling complex objectives and constraints; this model is, indeed, capable of handling non-linear and dynamic systems. It also suffers, however, from a high computational complexity, as well as from inaccuracies in the battery model employed. A well-known risk is also obtaining a solution in a local optima.

- **Predictive control:** This is a control scheme where a model, in this case a battery model, is used for predicting the future behaviour of the system over finite prediction horizon. Based on these predictions, together with the present measured/estimated battery states, optimal control inputs are forecasted with regard to defined objective functions and subject to the system constraints. This optimisation process is repeated

once and over again, every certain time interval, to determine new control inputs. This MPC is suitable for systems with fast dynamics and variable operating conditions. Nonetheless, it is worth noting that computational complexity increases with longer prediction horizons, and tolerance calibration may be challenging.

- **Machine learning-based control:** This control involves the utilisation of algorithms and models to optimise the operation of BESS by leveraging historical and real-time data. Through techniques such as supervised learning, reinforcement learning, and deep learning, this control identifies optimal charging/discharging strategies to enhance the performance of the battery. It presents advantages in adaptability, optimisation, predictive maintenance, and scalability for BESSs. It also presents, however, challenges related to data dependency, complexity, interpretability, and overfitting.

2.2.2 Battery lifetime management

Batteries are medium-high-cost units, and as with any other industrial product, due to time and usage, their characteristics are altered. In the case of a BESS, it degrades throughout its operational lifespan until it reaches the end of its life. This implies that controlling the degradation of a battery is crucial to extend its lifetime and, in turn, minimise the economic impact of this system. In this endeavour, formulating optimal battery lifetime management solutions presents a substantial challenge given the complexity of battery ageing models.

The complexity of battery modelling lies in the difficulty of accurately estimating and predicting the internal chemical reactions of the battery. Because of this challenge, both the electro-thermal modelling of the cell/battery-pack assembly and the modelling of the battery degradation become an obstacle. Upon the struggling of understanding and representing the battery operation, control becomes an even tougher endeavor. To exercise this control, the manufacturer sets, already, a series of hard limits that determine the area in which the battery must operate, in terms of voltage, current, or temperature. This range is better known as the safe operating area (SOA). Many applications, however, beyond controlling the evolution of these three parameters set by the manufacturer, choose to further define an even more restrictive static SOA. This practice of limiting the operating window of the battery (example in Figure 2.10), often referred to as battery derating, has an impact on reducing battery performance.

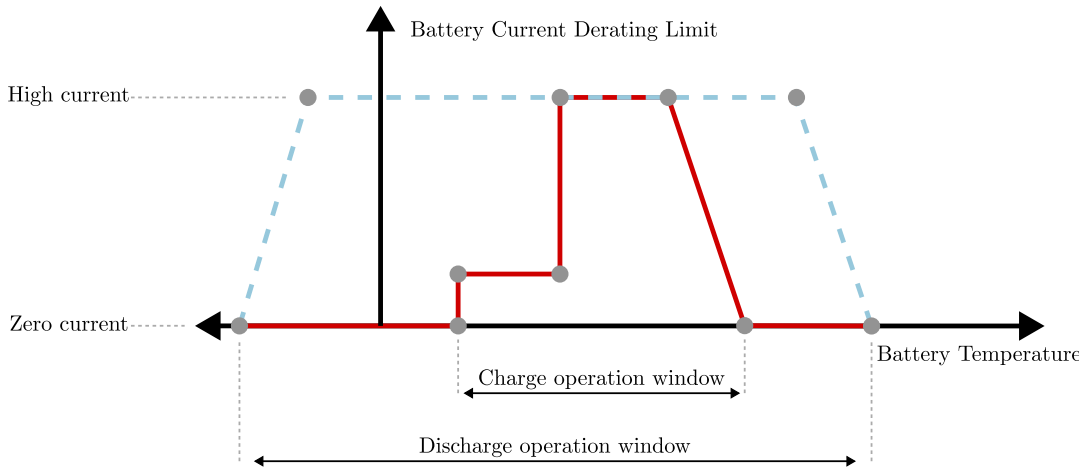

Figure 2.10: Temperature-based derating strategy example [73].

The concept of derating involves decreasing operating thermal and electrical stresses of components, which mitigates the rate of degradation and prolongs their expected lifetime [74]. Yet, these solutions generally set a constant/static SOA for the entire battery-pack, regardless of the fact that new and old units can generally withstand different operating conditions. On this premise, as cells age, the same scenario may result in heterogeneous ageing rates and mechanisms [19]. In other words, the battery calls upon a dynamic SOA that can modulate the operation, according to the ageing estimations and predictions at each point in time. In this sense, dynamic ageing-aware control systems improve performance as more accurate battery models/heuristics and more advanced control strategies are predicted. Accordingly, dynamic ageing-aware control systems improve performance as more accurate battery models/heuristics and more advanced control strategies are involved.

This approach opens up the possibility for new classifications of battery control strategies, as well as for a proposal of new control alternatives for improving battery performance. An example of the latter is the work of Ruan eta al. [13], paper in which they suggest a new way of classifying the different control strategies. In systematising this taxonomy, two parallel classifications of battery management strategies are defined as shown in Figure 2.11: on the one hand, static or dynamic derating; and on the other hand, model-based or heuristic method based controls. Each of the different alternatives are detailed below to indicate the advantages and disadvantages of the different options, with a view to identifying the choice with the greatest potential.

2.2.2.1 *Static derating*

In the context of static derating methods, the battery performance limiting constraint remains constant during its entire lifetime, regardless of the impact of battery ageing

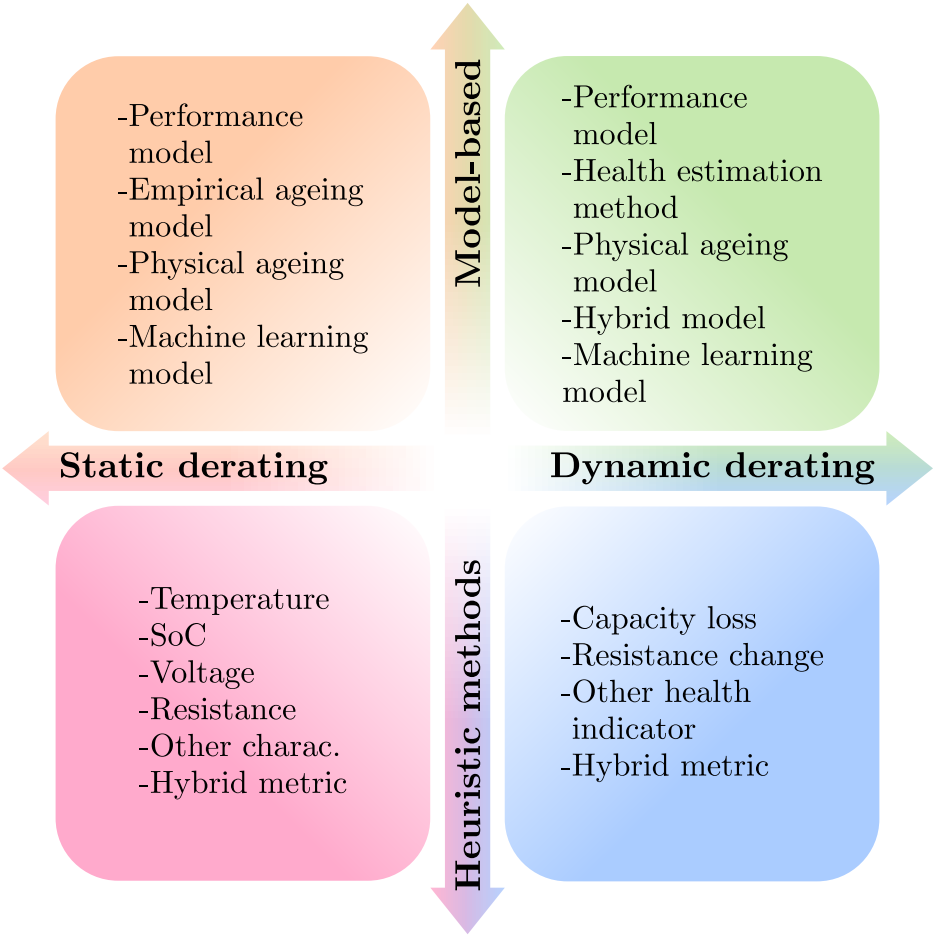

Figure 2.11: Battery ageing-aware derating categorisation (adapted from [13]).

phenomena. For this purpose, battery variables, such as current or voltage, are regulated during charging or discharging operations to ensure functioning within the SOA. These static limits can be related to temperature, SoC, electrical resistance or voltage for example.

All these static derating can be divided into different categories, depending on whether they are based on a heuristic approach or a model-based method:

HEURISTIC METHOD

A heuristic method refers to an approach to problem-solving which utilises a practical method that, albeit not "perfect," it is adequate for achieving a short-term goal or approximation. Considering that finding an optimal solution is often impractical, heuristic methods facilitate the expedited formulation of a satisfactory solution. Thus, when dealing with batteries, heuristic reduction methods refer to qualitative analysis based on experimental results to determine the ageing and safety characteristics of cells. There are different strategies based on heuristics that can be classified as follows:

- **Temperature-based derating:** The temperature of the batteries is limited to, first, minimise solid electrolyte interface (SEI) growth and Li deposition; and, second, to reduce the impact of temperature gradients. In light of the above, Patnaik et al. [75] presented a standard constant-current constant-voltage (CC-CV) with a constant temperature limitation. Through this methodology, the charging current is modulated to keep the battery temperature below a pre-set point.

- **SoC-based derating:** SoC and depth of discharge (DoD) management is relevant as well to minimise battery ageing during battery rest and operation states. Pertaining to this, Angenendt et al. [76] constrained the battery functioning at high SoC values in their simulation, extending battery lifetime by around 100%. Instead, Chahbaz et al. [77] pointed out that it is crucial to keep battery DoD below 50%, regardless the mean SoC, in order to minimise cell ageing.

- **Voltage-based derating:** Several investigations have analysed the impact of varying the operating voltage range, taking into account the limitation that this generates on the available energy and power. As an example of the above, Gao et al. [78] state that the constant-voltage (CV) process is limited to 4.1 V, constant throughout its lifetime, instead of 4.2 V. This value is aimed at enhancing the lifetime of the battery.

- **Resistance-based derating:** The resistance of the battery varies depending on variables such as the SoC, current, temperature and applied current. Contingent on these being set, identifying battery resistance is possible to modulate the operating current. As an example, Sebastian et al. [79] introduced a two-stage constant-current (CC) charging method, imposing a 1C current until electrical resistance is low enough to apply a 2C current. In so doing, battery lifetime is increased up to 44%.

- **Other derating strategies:** In addition to the previous strategies, there are also alternatives such as anode potential derating to regulate battery performance. In this regard, Liu et al. [80] developed a charging technique based on anode potential that approximately halves the charging time, while keeping battery ageing similar to the baseline.

MODEL-BASED METHOD

Model-based methods involve the implementation of mathematical or computational models to estimate and predict the patterns of systems, processes, or phenomena. In the realm of batteries, model-based solutions provide more accurate information compared to

methods that are, solely, reliant on heuristics approaches. This derating strategy enables a mathematical representation of battery behaviour, facilitating the consideration of the batteries' states and the establishment of consistent thresholds for derated operation. The different alternatives identified in the literature can be categorised as follows:

- **Empirical model-based derating:** Experimental test data is widely used in literature to develop empirical ageing model. In resorting to these tests, they intend to represent the ageing behaviour of the cell. An example of this is the work done by Schimpe et al. [73], in which an ageing rate constraint is determined, by means of sensitivity analysis, with the aim of derating battery operation. Building on this logic, over the first year, battery lifetime increases up to 76.17% at expenses of a 9.36% lower energy output.

- **Physical model-based derating:** This kind of model describes the internal chemical and electrochemical reactions that represent the performance of the battery for derating purposes. On this point, Yin et al. [81] analysed different constant constraints, including ion concentrations, SoC and side reaction rate, to determine the charging protocol of a cell. The results, based on a battery-in-the-loop system, demonstrate a reduction of the charging time of about 40%, while maintaining the same battery ageing rate suggested by the manufacturer.

- **Machine learning model-based derating:** With the rise of AI, more and more solutions related to machine learning (ML) are being proposed. In relation to this, Bibinsha et al. [82] introduced a ML based capacity loss prediction system for SoC derating, enabling a life extension of around 2% according to simulations.

- **Performance model-based derating:** This kind of models aim to modulate the charging or discharging current of the battery based on any user-defined battery model. As for this, Ya et al. [83] presented an electro-thermal model based charging strategy to optimise temperature increase and charging current. Results show an improvement of 17.9% and 9.5%, respectively.

2.2.2.2 *Dynamic derating*

When it comes to dynamic derating methods, constraints limiting battery performance are updated throughout the battery's lifetime, as conditions and operating parameters evolve in real time. In this vein, during the charging or discharging process, battery variables, such as current or voltage, are regulated to ensure operation within the variable SOA.

Instead, in static derating the SOA does not evolve. These adaptive limits can be related to temperature, SoC, electrical resistance or voltage for example.

HEURISTIC METHOD

- **Capacity-loss based derating:** This type of model regulates the battery current, in line with the predicted capacity loss, and thus, regulates the health of the cell. An example of the latter is the work carried out by Koleti et al. [84], where they present a CC-CV-CC charging strategy that regulates the CV voltage, therefore, extending the useful life of the battery up to a 75%.
- **Resistance change-based derating:** As mentioned above, resistance-based solutions modulate the battery current, in accordance with the change in electrical resistance. For instance, in the work of Sieg et al. [85], authors aim regulating the current, by factoring resistance variation, as the cell ages.
- **Other indicators based deratings:** Other metrics, namely, battery health or even hybrid indicators, are susceptible to being implemented for heuristics based dynamic derating strategies. Touching upon this, Koleti et al. [86] developed a control strategy that strives to detect the Li plating, in order to update CV constraint. Through this strategy, these scholars are able to extend the service life by up to 45% compared to the baseline.

MODEL-BASED METHOD

- **Health estimation-based derating:** Such control alternatives intend to derate battery current based on its health estimation. As an example, Lee et al. [87] adaptively modulate the charging current during batteries' lifetime, according to voltage variation and capacity loss correlation.
- **Performance estimation-based derating:** By way of illustration, Guo et al. [88] employed an ageing dependant lumped equivalent-circuit model (ECM), with a view to update the battery charging voltage. In so doing, battery lifetime can increase up to 290%.
- **Physical ageing model-based derating:** An example of this kind of control is the one carried out by Mandli et al. [89], where not only the charging time, but also

the SEI growth, is taken into account. These alternatives seek to consider physical parameters of the batteries to improve the performance and lifetime of the battery.

- **Other model-based derating:** Other types of controls, such as hybrid-derating, are considered in this derating strategy group. As for this, Su et al. [90] introduced a new approach that involves a performance model, a physical ageing model and a ML, with the purpose of updating the battery charging current, which can, in turn, enable to charge batteries faster while decreasing the capacity fade.

2.2.2.3 *Comparison of derating methods*

This wide variety of alternative battery operation derating is a further indication of the difficulty of optimally controlling a BESS. Upon this challenge, selecting the best option for each usage scenario requires a more comprehensive study. This assessment must take into consideration the data and models available for the development, along with the objectives of the battery itself and the function to perform in the application. In order to facilitate the understanding of the above, a brief comparison is presented below.

On the one hand, the main characteristics, i.e. advantages and disadvantages, of heuristic and model-based methods are summarised. The former seeks the trade-off between optimal performance and computational complexity, by means of low-complexity solutions. Although the latter uses a more complex model, it retains a reasonable accuracy in order to find an optimal or sub-optimal operating condition. The Table 2.2 introduces greater details on these two options.

Table 2.2: Brief comparative between heuristic and model-based methods [91].

Method approach	Advantages	Drawbacks
Heuristic algorithm	· Low computational complexity. · Low data requirements	· Unable to get even sub-optimal solutions. · Rules selected carefuly
Model-based algorithm	· System represented more accurately. · Global optimal or sub-optimal results.	· Dedicated model design for each case. · Case-by-case control adaptation. · Higher computational complexity.

On the other hand, it is worth looking at the advantages and disadvantages of static and dynamic derating. The first option is commonly based on simplifications intended to limit the steady degradation of the battery's lifespan. Despite this strength, the fact remains that such solutions result in overly generalised alternatives. Dynamic derating, which is the second option, offers improved performance, compared to former's, as a result of its lifetime

adaptability. In spite of the preceding, dynamic solutions call for more sophisticated control algorithms and monitoring systems to continuously update the operating limits in response to varying conditions.

In view of the above, an optimal or near-optimal result requires the use of derating strategies that adapt dynamically, while directly considering the information generated with a model that represents the battery performance. At the expense of computational load, greater accuracy in battery performance is key to obtaining results that allow batteries to be fully exploited.

2.2.3 Battery management architecture

In developing any of the control algorithms introduced earlier in this chapter, it is mandatory to consider the most appropriate type of control architecture for each management level shown in Figure 2.12. There are three main design alternatives that currently exist from a decision-making governance standpoint: centralised, decentralised and distributed control [92]. Each of these choices, explained in greater detail throughout this section, are developments that have been gradually adopted from the computer-science industry. All of them are present in Figure 2.12.

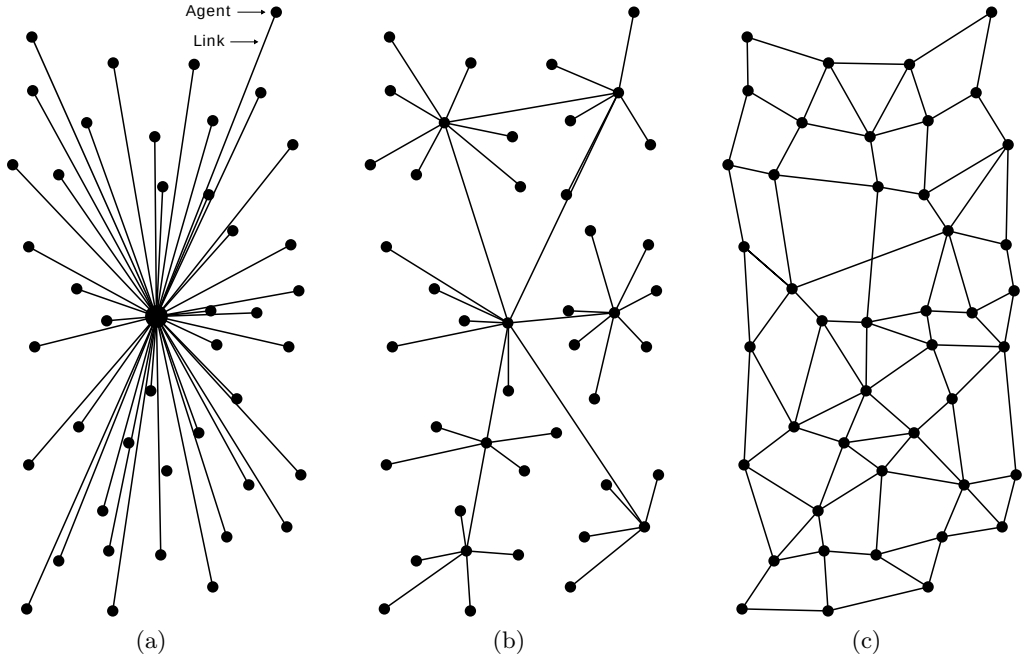

Figure 2.12: Control system architecture: a) centralised, b) decentralised, and c) distributed cite.

2.2.3.1 *Centralised*

In a centralised approach, each agent autonomously communicates and interacts directly with a central operator. This central hub should be capable to monitor, collect, and analyse real-time data, as well as determine suitable control signals to all units, while saving event records in a log file. Figure 2.12.a illustrates the general concept of the communication framework within a power system. This is the most widely used control architecture for BESS management [93–95], and these are its main characteristics:

- High traceability and controllability.
- Heavy computation burden.
- Not easy to expand.
- High single-point failure risk.
- Not plug-and-play functionalities.
- High level of connectivity to interact with all the agents.

2.2.3.2 *Decentralised*

In a decentralised control paradigm, such as the one shown in Figure 2.12.b, individual agents or clusters of agents operate autonomously or under the guidance of designated leaders. Decision-making processes rely on local data measurements, including voltage and frequency readings, with a finite number of inter-agent connections. Consequently, decentralised control methodologies demand minimal connectivity since they primarily depend on locally measured parameter values [96]. The main features are the ones listed below:

- Do not require a high level of connectivity.
- Robustness against a single point failure.
- Less computational load issues.
- Higher level of privacy and protection.
- Global optimisation, stability, or reliability of the entire system cannot be assured.

2.2.3.3 *Distributed*

In contrast to systems governed by decentralised methodologies, wherein agents rely on local measurements, systems employing distributed control methods enable agents to exchange information with neighbouring units as illustrated in Figure 2.12.c. In other words, within systems employing distributed methodologies, agents do not only use local measurements, but also share the capability to transmit and receive necessary data. Hence, such control systems can attain global optimisation, reliability, and stability akin to centralised control methods [97, 98]. This kind of control architectures present the following characteristics:

- Easy to expand and support scalability.
- Computational cost is distributed among multi-agents.
- System will not shutdown by a single point of failure.
- Not affected by the dynamic topology.
- Supports a plug-and-play characteristics.
- The most complex solution between the three options.

2.3 RESEARCH PROPOSAL

2.3.1 Summary of the overview

To address the main challenges outlined in this chapter, a number of research areas have been identified that merit further study, with a view to maximising the potential of BESS.

First, improvements from a conventional hardware design point of view are to be noted. The conventional battery architecture approach has enabled the development of simpler products, whilst preserving their functionality and marketability. In this process, the adoption of electrochemical Li-ion batteries has been driven forward. Despite significant advances in these new alternatives, it is important not to overlook the fact that their greater efficiency also brings with it greater complexity. Challenged by the study of these intricacies, new reconfigurable solutions with great potential, due to the high controllability at the cell level or even at the module level that they offer, have not been slow to emerge.

Notwithstanding the quantitative but also qualitative advantages introduced by these options, scaling such alternatives, at least at the cell level, significantly increases the number of components and, once again, the complexity of product development.

In a context such as this, of medium and large systems, where a battery-pack is based on a set of modules, the transition to CBM-based systems presents an indisputable potential (in this research only DC systems are considered). These controllable modular batteries present a higher degree of control at the system level, which opens new doors for power sharing, sizing and fault tolerance design strategies of BESSs. When designing these modular batteries, there are several configuration alternatives to consider, including parallel, series and their combinations, each with its advantages and disadvantages. Among these options, prioritising the parallelisation of modules whenever possible can be key, mainly because of the flexibility it provides when it comes to developing the control. All in all, the ultimate goal is, as noted above, to improve results both quantitatively and qualitatively.

Second, when it comes to battery management controls, the solution is not straightforward. Its complexity lies in several aspects:

- Knowledge of how the battery works is essential for a better understanding of how to control it. No matter how much work has been done, this is a field that still calls for further innovation.
- The type of application and dimensions of the BESS are also essential in formulating the control strategy.
- The choice among the different types of algorithms for the development of the control is also a challenge, due to the difficulty of determining which of the alternatives offers the optimal result.

In light of the above, the system approach at module scale requires special attention. In this context, control is not considered from an application point of view, nor from an individual cell point of view. When dealing with modules, some alternatives prioritise the balancing of measurable-state variables, while others choose to manage the modules for the balancing of non-measurable variables, such as SoC or SoH. In all of these cases, the aim is to achieve optimal performance. Most alternatives, however, do not contemplate the option of operating the modules, on the basis of their coupled electro-thermal and ageing models, in order to meet the control objective, even if this means generating greater imbalances between the modules.

In parallel, there are control algorithms beyond the widespread rule-based approach that allow a better exploitation of the potential of batteries, for instance, by using an MPC, which takes advantage of the information provided by models and the predictive capability of some systems or applications. This is an example of how the use of "accurate" battery models and more advanced control algorithms can dynamically adapt to any scenario and thus get more out of battery life. On top of this, when it comes to the choice of control architecture, decentralised or distributed control architecture has advantages over centralised control architecture. That said, for the development of a new control concept, the centralised alternative is preferable as it is more practical in terms of decision making, considering the access it provides to all system information.

Through this analysis, a gap has been identified that presents a great potential related to CBMs for medium-large systems, as well as to the control algorithm necessary for their development. Yet, to formulate the best control alternative, there are many competing options to compare in finding a solution that enables enhanced battery utilisation. In fulfilment of this objective, this analysis seeks to identify the control alternative that allows the greatest profit from a performance and lifetime point of view.

2.3.2 Research question

In view of each of the sections analysed and the conclusions obtained throughout Chapter 2, it is concluded that existing approaches do not fully exploit the potential of the BESS, since a) from a structural point of view, CBM presents multiple technical improvements that justify its adoption, and, b) as regards the management strategy, improvements can be considered from a standpoint of new models and battery variables that are either objectives of the control, or new control algorithms. Building on the research potential presented by these conclusions, the following research question arises, along with four further sub-questions that remain unexplored:

How can the power demand be shared among multiple controllable battery modules in a BESS, with a view to enhance system performance and extend battery lifespan?

1. *Is it possible and beneficial to use a coupled electro-thermal and ageing battery model in the control algorithm?*

When proposing a control algorithm, it is feasible to dynamically consider the impact of each control command on the system. The use of a coupled electro-thermal and ageing battery model presents the opportunity to make any control decision upon all the information that has a bearing on the battery.

2. *Can the control algorithms that predict the operation of a modular BESS be used to determine the optimal mode of operation?*

   Control algorithms such as MPC allow the use of models, namely, the battery model, to search for the optimal operating point. These solutions enable a decision making that adapts to both present and future demand, always seeking to minimise the defined objective function.

3. *Is it possible to formulate a SOO to control the modules or is it necessary to use a MOO?*

   When dealing with BESSs, there are several variables that can be used as control targets. As the number of objectives increases, it, however, often becomes necessary to analyse the appropriate weighting factors. Therefore, an adequate SOO is very useful in facilitating the formulation of the control algorithm.

4. *If the new control algorithm is compared to the baseline, is the former capable of improving the latter's performance?*

   Once the control algorithm has been developed, it is essential to make a comparison with another control alternative, which can be considered as a baseline. In so doing, it is possible to determine whether the new solution is an upgrade over the existing one.

Chapter 3

BATTERY SYSTEM MODELLING

In studying and developing a system for the control of a BESS, it is reasonable to consider a number of different cell models. When selecting these models, it is worth noting that just as a highly accurate but a complex model may not be useful, an oversimplified model may, as well, yield results that are not sufficiently representative of the system's operation. As a consequence, both the results and the conclusions drawn may not be optimal for BESS management. With this in mind, different modelling alternatives and the choice made are briefly mentioned at the beginning of this chapter, followed by a detailed presentation of the cell and the module model used.

Given the increasing uptake and application of batteries, their utility has gone beyond any basic use in their early days. With the rise of multiple potential applications, areas such as modelling, control and sizing have become progressively more complex. This is reflected in today's BESS design process, which considers the performance of the battery from an electrical, thermal, mechanical, and degradation point of view. For engineers to be able to carry out such developments, however, knowledge of how to model each of these aspects of a BESS is required. Upon this modelling task, three main modelling streams are identified in the literature and are summarised below:

- **ECMs:** These models are the simplest and, at the same time, the most widespread approach to represent the operation of a cell or battery [10]. They rely on common electronic components to create an electrical-circuit that approximates the behaviour of the real cell in voltage and temperature, under different operating currents. These models allow the cell to be kept in the safe operating range, while being simple and robust in the implementation. The major challenge these present is that they do not provide much of the internal physical information, which, in turn, implies that they may require a large amount of experimental testing to accurately represent the operation of the cell or battery [99]. This is especially evident in designs where the evolution and impact of the degradation is to be considered.

- **PBMs:** Physico-chemical models attempt to represent the internal phenomena of the cell, with a view to going beyond such a generalised behavioural representation as that of ECMs. A greater degree of detail of the cell's operation, however, can affect the complexity of the model and therefore its usefulness. As an example, a micro-scale model is unfeasible to apply behavioural modelling purposes. Further advances are yet being made in continuum scale techniques, for instance, with the pseudo-two dimensional (P2D) model and model order reduction techniques, as well as with parametrisation methods to obtain the internal data of the cell. In so doing, the potential of PBMs, in comparison to current solutions, is beginning to be realised [11, 12, 100].

- **Data-driven models:** Information concerning battery behaviour and characteristics is becoming increasingly accessible, primarily through open-access sources and advancements in measurement techniques [101]. This data availability is driving interest in using AI solutions to improve BESS performance. Lombardo et al. [9] presented a review in order to analyse the potential of AI in the field of batteries. This research

underlines the potential of data-driven models beginning with the "Application to Materials Design and Synthesis" and concluding with "Application to Battery Cell Diagnosis and Prognosis", via areas such as "Materials and Electrode Architecture Characterisation". Although this is currently a new field of study, it is regarded as having great potential to boost the uptake of BESS.

These modelling strategies provide valuable information for understanding operation at the individual cell level. Nevertheless, in working with a system based on multiple units, it is necessary to determine a method or strategy that allows the operation of a set of cells to be represented as well. This is due to the fact that, for various reasons, namely divergences in the cells, given the manufacturing process or thermal gradients within a module, the degradation of the cells takes different forms, as mentioned in Chapter 2. This increased heterogeneity, ultimately, conditions the performance of the system as a consequence of the weakest cell. Therefore, beyond cell modelling, it also becomes essential to determine how to represent or manage the system at the module level, in order to optimally control and operate the BESS.

In spite of the above, in the realm of modelling BESSs, the scope transcends the comprehension of the system's dynamics; it demands the integration of economic considerations. While the emphasis may traditionally be focused on technological and academic advancements, the economic viability of such solutions is indispensable for promoting sustainable business models associated with BESSs. Consequently, the incorporation of an economic cost model becomes imperative. This model facilitates the assessment of indicators like capital expenditure (CAPEX) and operating expenditure (OPEX), which are pivotal in evaluating product profitability and overall feasibility [102]. Moreover, such modelling introduces a novel control objective, thereby enriching the formulation of BESS management algorithms.

Throughout this chapter it is thus introduced, first, in detail, the cell model selected from the literature, with its coupled electro-thermal and battery ageing model; second, the module model to be considered, as well as the parameters and variables that are necessary to determine the initialisation of the system; and, finally, the cost model of the system to analyse the behaviour of the BESS from an economical point of view.

3.1 CELL MODELLING

In this research we have chosen to use a cell model based on an ECM. This option is currently the most widespread in research and industry, as evidenced by the wide variety of studies compiled, for example, in the review on degradation modelling carried out by Mayemba et al. [103]. That said, having a model-based control strategy as the objective of this research, it is important to know that the selected control algorithm can be adapted to other cell models to minimise the same objective. When it comes to ECMs, there are a wide variety of examples available in the literature, each of them different in the strategy of modelling the electrical, thermal or degradation performance of the cell; or in the cell chemistry selected at the time of modelling. Among the different options in the literature, it has been decided to use the electro-thermal and degradation cell model developed by Schimpe et al. [104].

In making the choice of the degradation model, in light of the vast array of options presented in the literature, a wide range of characteristics are to be considered:

- **Accuracy, precision & validation:** It is imperative to assess the accuracy and precision of each model in predicting battery ageing. For this purpose, the cell model must be validated against experimental data or real-world performance to ensure reliability of predictions. The model of Schimpe et al. [104], shows, for instance, an ageing prediction error below 1% of the original cell capacity and a maximum relative error for the capacity loss that is below 21%.

- **Model complexity & applicability:** It is worth looking at the complexity of the model and whether it aligns with the available data and computational resources. In this particular case, despite being a non-linear non-convex model, since it has been used to formulate other control solutions in the past [73, 105], it is considered that it can be functional to provide an answer to the research question.

- **Time resolution:** It shall be assess whether the model provides the temporal resolution required for the corresponding application. Some models may provide ageing predictions at different time scales (e.g., hourly, daily, monthly). In this scenario, both the electro-thermal and the degradation models can be adapted to different simulation and prediction step-times.

- **Availability of model for implementation:** It is relevant to consider whether the model is available as an open-source software, commercial software, or implemented

in a specific simulation environment. In this regard, accessible software tools facilitate model integration and implementation into existing workflows. In this instance, the model of Schimpe et al. [104] provides all the necessary electro-thermal and degradation data for its implementation, yet occasionally the models published in open source do not facilitate the necessary data completely.

- **Long-Term Predictions:** To weight the capability of the model to make long-term predictions of battery ageing over the entire lifespan, from a coupled electro-thermal and capacity loss point of view, is critical. Long-term predictions are crucial for assessing the lifetime performance and optimising maintenance strategies. In this research, the degradation model has been experimentally validated with data obtained for up to 348 days, a period not sufficient to understand its operation over its entire lifetime, which is common in battery modelling, but sufficient to formulate a control strategy that takes degradation into account.

In the following, the most relevant characteristics of the model are introduced. The general parameters of the datasheet of this commercial cell $LiFePO_4$ (Sony US26650FTC1), are illustrated in Table 3.1. This table includes a number of comments specified in the modelling work of Schimpe et al. [104]. In greater detail, the subsequent sections introduce the electric, thermal and battery degradation models separately.

3.1.1 Electrical model

This electrical model is intended to faithfully represent the voltage between the cell terminals following the schematic presented in Figure 3.1. For this purpose, three parameters need to be considered: 1) the open-circuit voltage (OCV) of the cell, 2) the electrical impedance to predict the impact of the current on the voltage, and 3) the influence of hysteresis on the cell voltage. That said, for the development of this research, it has been assumed that the dominant phenomena to represent the voltage are the first two, since neglecting the impact of the hysteresis is, indeed, a widespread practice in the literature [17, 35]. This being so, it is possible to formulate the Equation 3.1 to represent the voltage between the positive and negative terminals.

$$v_{\text{cell}} = v_{\text{ocv}}\left(q_{\text{cell}}\right) + R_{\text{cell}}\left(q_{\text{cell}}, T_{\text{cell}}, u\right) \cdot u \tag{3.1}$$

Table 3.1: Datasheet parameters of the cell Sony US26650FTC1 [104].

Parameter	Value	Notes
Nominal voltage	3.2 V	
Nominal capacity	3000 mA	Rated capacity is 2850 mAh, but tested capacity at BoL is 3000 mAh.
Charge voltage	3.6 + 0.05 V	3.6 V is used in this study.
Discharge voltage	2 V	2.5 V is used in this study
Continuous maximum charge current	2.85 A	Maximum current is determined as 1C. Then, as the nominal capacity at BoL is 3000 mAh the current is set at 3 A.
Continuous maximum discharge current	20 A	
Temperature range charge	0 to 45 ºC	In this study discharge temperature is considered because it is a wider range.
Temperature range discharge	-20 to 60 ºC	This is the range used for the analysis.

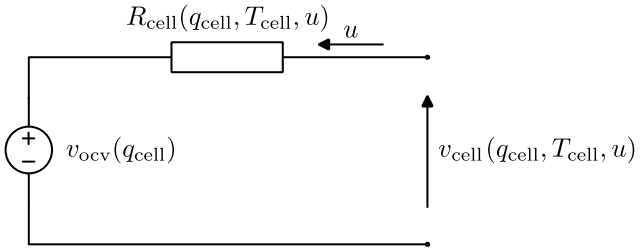

Figure 3.1: Representation of the used ECM.

In this Equation 3.1, the v_{ocv} is the OCV of the cell, while the R_{cell} is the electrical resistance in series and u is the control variable, which is the electrical current in this case. To prevent damage to the battery cells, it is necessary to limit voltage between the two terminals:

$$\underline{v_{\text{cell}}} \leq v_{\text{cell}} \leq \overline{v_{\text{cell}}} \begin{cases} \overline{v_{\text{cell}}} = 3.6\text{V} \\ \underline{v_{\text{cell}}} = 2.8\text{V} \end{cases} \tag{3.2}$$

where $\overline{v_{\text{cell}}}$ and $\underline{v_{\text{cell}}}$ are voltage limits.

To determine the value of v_{ocv} Equation 3.3 is defined. This polynomial is used to represent the cell OCV based on the SoC. For this purpose, a tuning has been performed so

that the experimental data shown in [106] (at C/50 and a temperature of 25 °C) are approximated by two exponential expressions $[\sigma_1; \sigma_2; \sigma_3; \sigma_4] = [3.2116; 0.0473; -0.7487; -36.1274]$. Both the experimental data and the data corresponding to Equation 3.3, as well as its error, are presented in Figure 3.2.

$$v_{\text{ocv}} = \sigma_1 \cdot \exp^{q_{\text{cell}} \cdot \sigma_2} + \sigma_3 \cdot \exp^{q_{\text{cell}} \cdot \sigma_4} \tag{3.3}$$

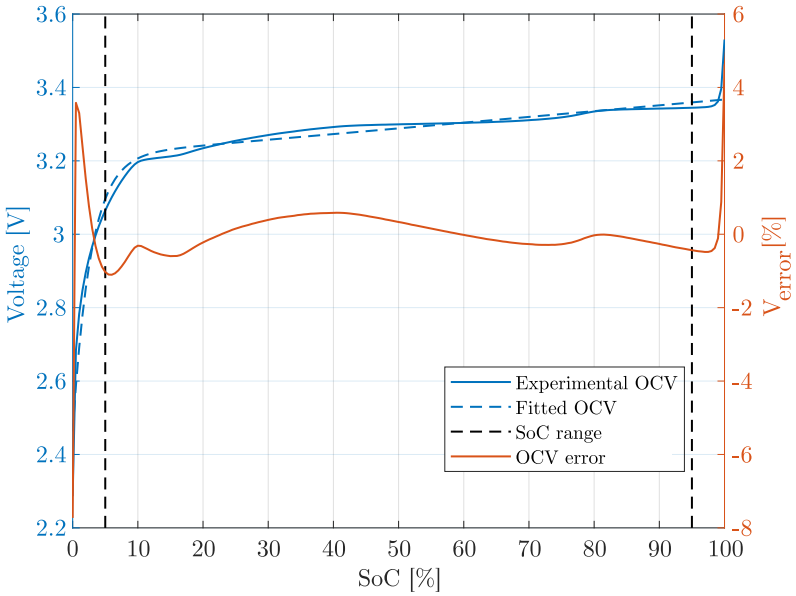

Figure 3.2: OCV data: experimental curve, fitted curve and tuning error. Full range tuning maximum relative error is 7.73%, while RMS error is 24 mV. Within the operation SoC range the maximum relative error equals 1.1%, and the RMS error is 12.7 mV.

As for the electrical resistance (R_{cell}), its modelling is considered to depend on three main factors mentioned by Schimpe et al. [106]: the temperature, the SoC and the current (charge or discharge). For this study, their experimental data are fitted to obtain two polynomials, $f_{R_{\text{ch}}}$ and $f_{R_{\text{dch}}}$: one for the charge resistance and one for the discharge, both visible in Figures 3.3a and 3.3b. In Appendix A details about both polynomials, and the adaptations that have been made to facilitate the use of these non-continuous functions in the control, are available.

$$R_{\text{cell}} = \begin{cases} R_{\text{cell}} = f_{R_{\text{ch}}}(q_{\text{cell}}, T_{\text{cell}}) & \text{if} \quad u \geq 0 \\ R_{\text{cell}} = f_{R_{\text{dch}}}(q_{\text{cell}}, T_{\text{cell}}) & \text{if} \quad u < 0 \end{cases} \tag{3.4}$$

To predict the change in SoC, represented as $\dot{q}_{\text{cell}}$, the current operated by the cell and its nominal capacity (Q_{cell}) are taken into account. This calculation, represented in

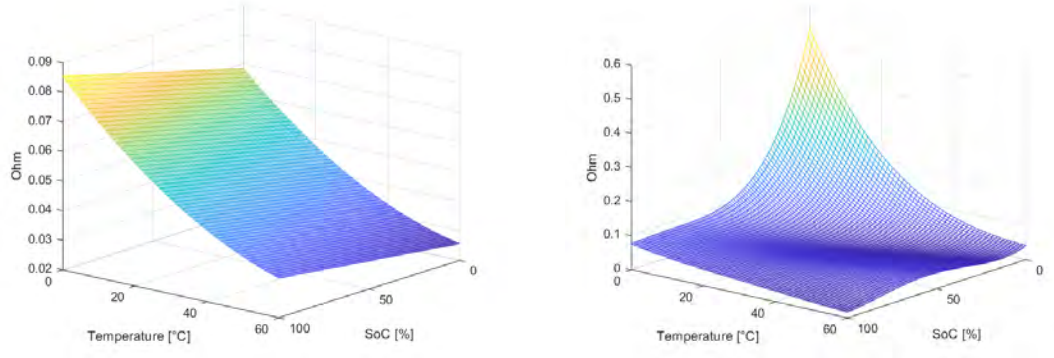

(a) (b)

Figure 3.3: Electrical resistance of the cell: a) during charge, and b) during discharge.

Equation 3.5, can also be calculated taking into account the impact of capacity loss (Q_{Loss}), in order to consider the impact of degradation.

$$\dot{q}_{\text{cell}} = \frac{u}{Q_{\text{cell}} - Q_{\text{Loss}}} \tag{3.5}$$

Due to safety reasons related to over-charge and over-discharge situations, the functional SoC range is limited:

$$\underline{q_{\text{cell}}} \leq q_{\text{cell}} \leq \overline{q_{\text{cell}}} \begin{cases} \overline{q_{\text{cell}}} = 95\% \\ \underline{q_{\text{cell}}} = 5\% \end{cases} \tag{3.6}$$

where $\overline{q_{\text{cell}}}$ and $\underline{q_{\text{cell}}}$ are maximum and minimum q limits.

Finally, as for the electrical model, the operating power (P_{cell}) of each cell is determined by the Equation 3.7, which is dependent on the cell terminal voltage and the electrical current.

$$P_{\text{cell}} = v_{\text{cell}}(q_{\text{cell}}, T_{\text{cell}}, u) \cdot u \tag{3.7}$$

3.1.2 Thermal model

As important as the electrical model of the cell is the model that represents, in a reliable way, the thermal behaviour of each unit. Taking article [106] as a reference, Equation 3.8 is formulated to predict the temperature change at each instant.

$$\dot{T}_{\text{cell}} = \frac{1}{C_{\text{th,cell}}} \cdot \left[h_t \left(T_{\text{amb}} - T_{\text{cell}}\right) + P_{\text{losses,cell}}\right] \tag{3.8}$$

The maximum ($\overline{T_{\text{cell}}}$) and minimum ($\underline{T_{\text{cell}}}$) temperature constraints for the battery operation are set as:

$$\underline{T_{\text{cell}}} \leq T_{\text{cell}} \leq \overline{T_{\text{cell}}} \begin{cases} \overline{T_{\text{cell}}} = 60°\text{C} \\ \underline{T_{\text{cell}}} = -20°\text{C} \end{cases} \tag{3.9}$$

By having a thermal model implemented as a 0D lumped thermal capacity, it is necessary to calculate the heat capacity $C_{th,\text{cell}}$ using Equation 3.10. Its calculation calls for considering the mass of the cell m, which is equal to 85 g, and the specific heat of the cell $C_{p,\text{cell}}$, which is equivalent to 838 J/(kg K).

$$C_{th,\text{cell}} = m_{\text{cell}} \cdot c_{p,\text{cell}} \tag{3.10}$$

In order to predict the temperature evolution, it is also relevant to have knowledge of the heat generated by the internal reactions of the cell. In this research, it is assumed that the dominant phenomenon in generating this heat is related to the Joule effect, with power losses (P_{losses}) being dependent on the electrical resistance and the electrical current, as shown in Equation 3.11.

$$P_{\text{losses,cell}} = R_{\text{cell}}(q_{\text{cell}}, T_{\text{cell}}, u) \cdot u^2 \tag{3.11}$$

3.1.3 Ageing model

The degradation model formulated by Schimpe et al. [104] is a semi-empirical capacity loss model with a reduced internal set of cell data. Its formulation accounts for the degradation caused by the energy storage and the capacity loss, as a consequence of battery cycling. In so doing, it resorts to an initial experimental analysis in which the cells are tested at different temperatures, SoCs and C-rate values, in order to then fit the ageing model of the Equation 3.12. This proposed ageing model for determining the total cell capacity loss, denoted as Q_{Loss}, integrates the cumulative effects of four distinct stress factors contributing to capacity loss, elaborated upon in greater detail within this section. By this mean, it is also feasible to predict battery's SoH variation following Equation 3.13.

$$\begin{aligned} Q_{\text{Loss}}\ (q_{\text{cell}}, T_{\text{cell}}, I_{\text{Ch}}, Q_{\text{Tot}}\ , Q_{\text{Ch}}, t) =& k_{\text{Cal}}(q_{\text{cell}}, T_{\text{cell}}) \cdot \sqrt{t} \\ &+ k_{\text{Cyc,High T}}\ (T_{\text{cell}}) \cdot \sqrt{Q_{\text{Tot}}} \\ &+ k_{\text{Cyc,Low T}}\ (T_{\text{cell}}, I_{\text{Ch}}) \cdot \sqrt{Q_{\text{Ch}}} \\ &+ k_{\text{Cyc,Low T High SoC}}\,(q_{\text{cell}}, T_{\text{cell}}, I_{\text{Ch}}) \cdot Q_{\text{Ch}} \end{aligned} \tag{3.12}$$

$$SoH = \frac{(Q_{\text{cell}} - Q_{\text{Loss}})}{Q_{\text{cell}}} \tag{3.13}$$

Regarding the accuracy of this cell ageing model and its parametrisation, according to Schimpe et al. [104], the validation results are in good agreement with the predicted values. Following a validation process of 348 days at a temperature between 10 y 45 °C, the error of the model is below 1% of its nominal capacity at the beginning of the lifetime, while the maximum relative error for capacity loss is below 21%.

3.1.3.1 *Calendar ageing*

The phenomenon of calendar ageing in batteries involves the progressive reduction of cyclable lithium, due to the expansion of the SEI layer at the anode, which can permanently entrap lithium. Nonetheless, as the thickness of the SEI layer increases, leading to capacity loss, the growth rate decreases owing to the self-inhibited slowing of the reaction. According to Schimpe et al. [104], following the examples on the literature, this phenomenon can be described with square-root dependence on time (t). So as to assess in the impact of SoC and temperature on this ageing mechanism, the stress factor k_{Cal} is defined. In this light, the calendar ageing can be calculated as follows:

$$Q_{\text{Cal}} = k_{\text{Cal}}(q_{\text{cell}}, T_{\text{cell}}) \cdot \sqrt{t} \tag{3.14}$$

To determine the value of the stress factor, and thus the impact of temperature and SoC on capacity loss, it is assumed that there is no correlation between the two variables (see Equation 3.15). Hence, the dependence on temperature is modelled through the Arrhenius equation, while SoC is modelled through a reformulated Tafel equation. The value of the stress factor linked to calendar ageing is, therefore, calculated using the Equation 3.16, and Figure 3.4a shows its different values. All necessary parameters are listed in Table 3.2.

$$k_{\text{Cal}}(q_{\text{cell}}, T_{\text{cell}}) = k_{\text{Cal,Ref}} \cdot f(q_{\text{cell}}) \cdot f(T_{\text{cell}}) \tag{3.15}$$

$$k_{\mathrm{Cal}}(q_{\mathrm{cell}}, T_{\mathrm{cell}}) = k_{\mathrm{Cal,Ref}} \cdot \exp\left[\frac{-E_{\mathrm{a,Cal}}}{R_{\mathrm{g}}}\left(\frac{1}{T_{\mathrm{cell}}} - \frac{1}{T_{\mathrm{Ref}}}\right)\right] \cdot \left(\exp\left[\frac{\alpha \cdot \mathrm{F}}{R_{\mathrm{g}}}\left(\frac{U_{\mathrm{a,Ref}} - U_{\mathrm{a}}(q_{\mathrm{cell}})}{T_{\mathrm{Ref}}}\right)\right] + k_0\right) \tag{3.16}$$

3.1.3.2 *Cycling ageing*

In the analysis and modelling of the degradation caused by cycling of the cells, Schimpe et al. [104] identify three dominant ageing mechanisms: cycling the battery at high temperatures, charging the battery at low temperatures and powering the battery at high SoC with low operating temperatures. Building upon the prior assumption that all ageing mechanisms can be assessed through superposition, each of the three mechanisms are individually modelled.

- **High temperature ($Q_{\mathrm{L,Cyc,HighT}}$):** The degradation from cycling the cell at high temperature is captured by Equation 3.17. This degradation mechanism is accentuated with higher capacity throughput Q_{Tot}, both charge and discharge, as well as higher operating temperatures. The impact of these higher temperatures is reflected in the calculation of the stress factor $k_{\mathrm{L,Cyc,HighT}}$ of Equation 3.18. The parameters for its calculation are available in Table 3.2, while Figure 3.4b illustrates graphically the impact of temperature on the value of $k_{\mathrm{Cyc,HighT}}$.

$$Q_{\mathrm{Cyc,HighT}} = k_{\mathrm{Cyc,HighT}}(T_{\mathrm{cell}}) \cdot \sqrt{Q_{\mathrm{Tot}}} \tag{3.17}$$

$$k_{\mathrm{Cyc,HighT}}(T_{\mathrm{cell}}) = k_{\mathrm{Cyc,HighT,Ref}} \cdot \exp\left[\frac{-E_{\mathrm{a,Cyc,HighT}}}{R_{\mathrm{g}}}\left(\frac{1}{T_{\mathrm{cell}}} - \frac{1}{T_{\mathrm{Ref}}}\right)\right] \tag{3.18}$$

- **Low temperature ($Q_{\mathrm{Cyc,LowT}}$):** In contrast to the high temperature, the loss of capacity during cycling at low temperatures accounts for the impact of the C-rate. Each of these variables is applied by means of independent exponential experiments. It should also be noted that, in this case, the charge throughput is considered only in charge direction Q_{Ch}. Equations 3.19 and 3.20 show in detail how to calculate the value of the capacity loss and stress factor based on the parameters defined depicts, all things considered, the various operating values of $k_{\mathrm{Cyc,LowT}}$.

$$Q_{\mathrm{Cyc,LowT}} = k_{\mathrm{Cyc,LowT}}\ (T, I_{\mathrm{Ch}}) \cdot \sqrt{Q_{\mathrm{Ch}}} \tag{3.19}$$

$$k_{\mathrm{Cyc,LowT}}\left(T_{\mathrm{cell}}, I_{\mathrm{Ch}}\right) = k_{\mathrm{Cyc,LowT,Ref}} \cdot \exp\left[\frac{E_{\mathrm{a,Cyc,LowT}}}{R_{\mathrm{g}}}\left(\frac{1}{T_{\mathrm{cell}}} - \frac{1}{T_{\mathrm{Ref}}}\right)\right] \cdot \exp\left[\beta_{\mathrm{LowT}}\frac{I_{\mathrm{Ch}} - I_{\mathrm{Ch,Ref}}}{C_0}\right] \tag{3.20}$$

- **Low temperature & high SoC ($Q_{\mathrm{Cyc,LowT\&HighSoC}}$):** The capacity loss caused by the degradation mechanism at low temperatures and high SoCs at different currents is taken into account by Equation 3.21. In this regard, the impact of the charge throughput Q_{Ch} is based on a linear relation.

$$Q_{\mathrm{Cyc,LowT\&HighSoC}} = k_{\mathrm{Cyc,LowT\&HighSoC}}\left(q_{\mathrm{cell}}, T_{\mathrm{cell}}, I_{\mathrm{Ch}}\right) \cdot Q_{\mathrm{Ch}} \tag{3.21}$$

To calculate the value of the stress factor $k_{\mathrm{Cyc,LowT\&HighSoC}}$, the influence of temperature and current is considered independently, as with the SoC. If, however, the value of q is not above the value of $k_{\mathrm{Cyc,LowT\&HighSoC}}$ defined in Table 3.2, the value of $k_{\mathrm{Cyc,LowT\&HighSoC}}$ will be equal to zero. Figure 3.4d shows, as such, the different values of the stress factor depending on the operating conditions.

$$\begin{aligned} &k_{\mathrm{Cyc,LowT\&HighSoC}}\left(q_{\mathrm{cell}}, T_{\mathrm{cell}}, I_{\mathrm{Ch}}\right) \\ &= k_{\mathrm{Cyc,LowT\&HighSoC,Ref}} \cdot \exp\left[\frac{E_{\mathrm{a,Cyc,LowT\&HighSoC}}}{R_{\mathrm{g}}}\left(\frac{1}{T_{\mathrm{cell}}} - \frac{1}{T_{\mathrm{Ref}}}\right)\right] \\ &\quad \cdot \exp\left[\beta_{\mathrm{LowT\&HighSoC}} \cdot \frac{I_{\mathrm{Ch}} - I_{\mathrm{Ch,Ref}}}{C_0}\right] \\ &\quad \cdot \left(\frac{\mathrm{sgn}\left(q_{\mathrm{cell}} - q_{\mathrm{cell,Ref}}\right) + 1}{2}\right) \end{aligned} \tag{3.22}$$

To formulate this degradation model, averaged experimental conditions are considered for the calculation of the stress factors. Yet, in a real application where batteries are installed, variables such as SoC or temperature vary. This can result in a big challenge since the degradation model cannot be applied dynamically in order to predict its evolution. There are examples in the literature, such as the ones based of Rainflow or full equivalent cycles (FECs) strategy for ageing prediction [107, 108]. The alternative suggested by Schimpe et al. [104] is to use the approach proposed by Thomas et al. [109], based on a rate-based integral approach. So, following Equation 3.23, it is possible to calculate the capacity loss at each step-time, being τ the time variable and φ the charge throughput Q of operation.

$$
\begin{aligned}
q_{Loss} = & \int k_{\mathrm{Cal}}(q_{\mathrm{cell}}, T_{\mathrm{cell}}) \cdot \left(2\tau^{0.5}\right)^{-1} d\tau \\
& + \int k_{\mathrm{Cyc,HiqhT}}(T_{\mathrm{cell}}) \cdot \left(2\varphi_{\mathrm{Tot}}^{0.5}\right)^{-1} d\varphi_{\mathrm{Tot}} \\
& + \int k_{\mathrm{Cyc,LowT}}\left(T_{\mathrm{cell}}, I_{\mathrm{Ch}}\right) \cdot \left(2\varphi_{\mathrm{Ch}}^{0.5}\right)^{-1} d\varphi_{\mathrm{Ch}} \\
& + \int k_{\mathrm{Cyc,LowT\&High\,SoC}}\left(q_{\mathrm{cell}}, T_{\mathrm{cell}}, I_{\mathrm{Ch}}\right) d\varphi_{\mathrm{Ch}}
\end{aligned}
\tag{3.23}
$$

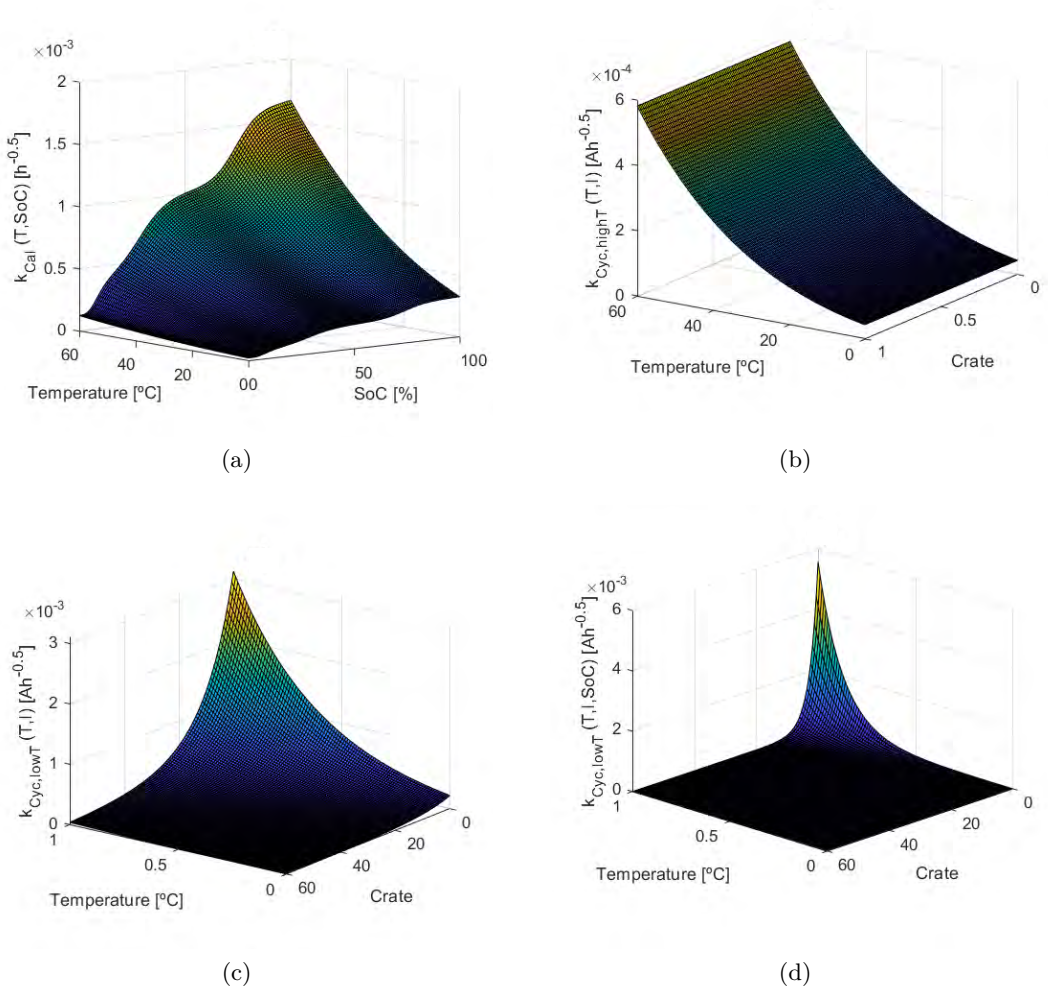

Figure 3.4: Evolution of the ageing stress factors under different operating conditions: a) Calendar ageing stress factor (Unit: $\mathrm{h}^{-0.5}$), b) Cycling ageing stress term due to charge/discharge at different temperatures (Unit: $\mathrm{Ah}^{-0.5}$), c) Cycling ageing stress factor at different charging currents and temperature conditions (Unit: $\mathrm{Ah}^{-0.5}$), and d) Cycling stress factor at high SoC values when operating at different charging current and temperature conditions (Unit: Ah^{-1}) [104].

Table 3.2: Battery ageing model parameters [104].

Model Parameter	Value	Note
$k_{\text{Cal,Ref}}$	$3.69 \cdot 10^{-4} \cdot \text{h}^{-0.5}$	$T = 25°C, q = 50\%$
$k_{\text{Cyc,HighT,Ref}}$	$1.46 \cdot 10^{-4} \cdot \text{Ah}^{-0.5}$	$T = 25°C, I = 1C$
$k_{\text{Cyc,LowT,Ref}}$	$4.01 \cdot 10^{-4} \cdot \text{Ah}^{-0.5}$	$T = 25°C, I_{\text{Ch}} = 1C$
$k_{\text{Cyc,LowT\&HighSoC,Ref}}$	$2.03 \cdot 10^{-6}\text{Ah}^{-1}$	$T = 25°C, I_{\text{Ch}} = 1C$
$E_{\text{a,Cal}}$	$2.06 \cdot 10^{4}\text{J/mol}$	$q = 100\%$
$E_{\text{a,Cyc,HighT}}$	$3.27 \cdot 10‘4\text{J/mol}$	$I = 1\text{C}$
$E_{\text{a,Cyc,LowT}}$	$5.55 \cdot 10^{4}\text{J/mol}$	$I_{Ch} = 1\text{C}$
$E_{\text{a,Cyc,LowT\&HighSoC}}$	$2.33 \cdot 10^{5}\text{J/mol}$	$I_{Ch} = 1\text{C}$
α	$3.84 \cdot 10^{-1}$	
β_{LowT}	2.64 h	
$\beta_{\text{LowT\&HighSoC}}$	7.84 h	
T_{Ref}	298.15 K	
$I_{\text{Ch,Ref}}$	3A	
$U_{\text{a,Ref}}$	$1.23 \cdot 10^{-1}\text{V}$	q = 50%
k_0	$1.42 \cdot 10^{-1}$	
U_{a}	$U_{\text{a}}(\text{q})$	[110]
F	96485 C/mol	
R_{g}	8.314 J/(mol K)	
$\text{SoC}_{\text{limit}}$	82%	

3.2 MODULAR BATTERY MODELLING

In most applications where a single cell falls short, it is necessary to design modules that incorporate cells connected in series to increase the voltage level and parallel cells, to, in turn, increase the stored capacity. If all these cells have exactly the same initial states/parameters and have a completely symmetrical circuit, it is sufficient to analyse the operation of a single cell. Nevertheless, in the development of a BESS, none of these conditions are met.

As introduced in Chapter 2, initial states and internal parameters' deviation is a common practice in cell manufacturing. This heterogeneity is further increased by the system layout, which generally does not degrade every cell in the same way, due to mainly SoC and temperature issues. This implies that, for optimal management of the storage system, it is advisable to consider the operating characteristics of each cell individually. Otherwise, the weakest cell may end up conditioning the operation of a considerably larger system.

To overcome cell to cell differences, a cell balancing circuit is generally used in conjunction with a primary layer or intra-module level control algorithm. In this task it is estimated, not only that the modules have these balancing solutions integrated, but also that they act fast enough so that the challenge of the weakest cell is not critical when applying any secondary or tertiary control layer. In this manner, it is deemed an option to apply a simplification where the system operation is represented, by analysing the operation of a single cell and, subsequently, scaling, based on the number of cells in series and parallel [73, 105, 106].

Keeping this simplification in mind, it is possible to formulate the Equation 3.24 for the calculation of the module voltage v_{BM}, and the Equation 3.25 for the current u_{BM}. It is thereby possible to calculate the power P_{BM} by means of Equation 3.26. For its calculation it is required to know the number of cells in series (M_s) and in parallel (M_p).

$$v_{\mathrm{BM}} = \sum_{m_s=1}^{M_s} v_{\mathrm{cell},m_s}\left(q_{\mathrm{cell}}, T_{\mathrm{cell}}, u\right) \tag{3.24}$$

$$u_{\mathrm{BM}} = \sum_{m_p=1}^{M_p} u_{m_p} \tag{3.25}$$

$$P_{\mathrm{BM}} = v_{\mathrm{BM}} \cdot u_{\mathrm{BM}} = \sum_{m_s=1}^{M_s} v_{\mathrm{cell},m}\left(q_{\mathrm{cell},}, T_{\mathrm{cell},}, u\right) \cdot \sum_{m_p=1}^{M_p} u_{m_p} \tag{3.26}$$

In the case of SoC and temperature, the dynamics at cell level and module level are considered to be equal, as shown in Equations 3.27 and 3.28.

$$\dot{q}_{\mathrm{BM}} = \dot{q}_{\mathrm{cell}} \tag{3.27}$$

$$\dot{T}_{\mathrm{BM}} = \dot{T}_{\mathrm{cell}} \tag{3.28}$$

Finally, with Equation 3.29, it is possible to calculate the total degradation accumulated by the module, by multiplying the capacity loss of a cell with the number of cells in series and in parallel.

$$Q_{\mathrm{Loss,BM}} = \sum_{m_s=1}^{M_s} \sum_{m_p=1}^{M_p} Q_{\mathrm{Loss}_{ms,mp}} \tag{3.29}$$

3.3 BATTERY COST MODELLING

There are many papers in the literature that have suggested looking into the correlation between battery degradation and the economic aspect, in order to maximise benefits. Upon different proposals, it is possible to make a classification with three main alternatives [111]:

1. At times, the cost of the storage system is determined in a way that allows to optimally exploit the ratio between benefit and degradation of the battery. In such cases, a multi-criterion problem scalarisation is required [112], so as to tune a penalty/weighting factors that enables the battery operation to be regulated.

2. The cost of operating the battery $\mathbb{C}_{\mathrm{SoH}}^{\mathrm{ageing}}$ is set by predicting or estimating the degradation. To do so, as per Equation 3.30, it is also necessary to determine the specific battery cost c_{BM}, the nominal energy E_{BoL} at BoL in Wh, and the available capacity limit that defines the EoL of the cell [113, 114]. The value of Q_{cell} at EoL ($Q_{\mathrm{cell,EoL}}$), depending on the kind of application, can be set at different levels, such as 80% or 60% of the nominal capacity value [115]. Regarding the value of c_{BM}, as shown in Figure 3.5, it is common to assign the value of the initial investment or battery replacement ($\$_{\mathrm{BM,total}}$), including some additional cost ($\$_{\mathrm{Additional}}$), such as maintenance.

$$\mathbb{C}_{\text{SoH}}^{\text{ageing}} = \frac{c_{\text{BM}} * E_{\text{BoL}}}{\text{Q}_{\text{cell}} - \text{Q}_{\text{cell,EoL}}} \tag{3.30}$$

$$c_{\text{BM}} = \$_{\text{BM,total}} + \$_{\text{Additional}} \tag{3.31}$$

3. The cost of operating the battery, in this case, is predicted by the number of FEC expected until SoH reaches EoL (FEC_{EoL}). Thus, following the Equation 3.32, and with the values c_{BM} and E_{BoL}, it is possible to predict the operating cost of the BESS [116, 117].

$$\mathbb{C}_{\text{FEC}}^{\text{ageing}} = \frac{c_{\text{BM}} * E_{\text{BoL}}}{FEC_{\text{EoL}}} \tag{3.32}$$

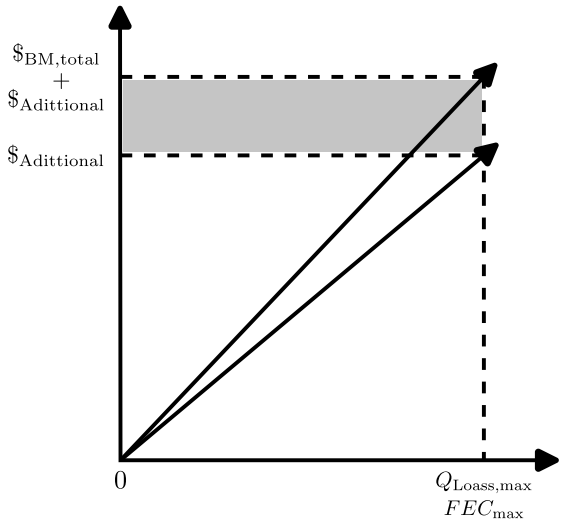

Figure 3.5: Battery cost modelling illustration.

Among these three options, having a model that considers battery degradation and not FECs, the possible alternatives are limited to the first and the second options. That said, the first alternative requires a sensitivity analysis that may involve a large number of simulations in search of the best cost factor. Instead, when dealing with commercial BESS, by having the CAPEX defined and sometimes the OPEX as well, it is possible to consider the cost subject to battery degradation in order to optimise battery performance. Accordingly, to model the cost of the battery storage system, the second alternative is considered. Thus, as it will be explained in the following chapters, a SOO problem can be formulated for battery system management.

Chapter 4

MODEL PREDICTIVE CONTROL FOR CONVENTIONAL BATTERY SYSTEMS

In formulating a control strategy for a BESS, multiple alternatives have been considered in the existing literature. Still, as indicated in Chapter 2, there remains a wide range of research areas open to optimisation of battery management algorithms. Upon this window for action, prior to formulating an energy management algorithm for a modular BESS, the management of a single module, based on the selected cell model, calls for an analysis of an ageing-aware MPC functionality. The objective of the cost function of this control is to minimise the total economic cost. In this task, a grid-connected residential application with a PV installation scenario is chosen.

As introduced throughout Section 2.2, there is a wide range of options when it comes to the control strategies for BESS. In order to respond to the research proposal for battery performance prediction, this study has opted to develop an energy management algorithm based on an MPC. This alternative is a computer-based control algorithm employed in engineering and industrial applications, with a view to optimise the performance of dynamic systems. Unlike conventional controls, most of which operate on the ground of rule-based algorithms, the MPC employs a look-ahead strategy, aimed at computing the best sequence of inputs, so as to achieve the target output in an optimal way. Thus, when dealing with a dynamic system that needs to constantly adapt to a variable reference, according to the new operating states predicted by the control, the operating setpoint is optimised to give the best possible response [118].

The operation of the MPC involves several key steps. First, a mathematical model of the system's dynamics is needed, in this case, implementable in discrete-time. This model is thereafter used to predict the future evolution of the system, over a predefined finite-length moving window (N_p). At each step, MPC calculates the optimal control inputs by solving an optimisation problem that minimises a cost function, generally composed of terms representing performance objectives and constraints. Accordingly, the calculated control inputs are applied to the system, and the process repeats once the control horizon (N_c) is over, as shown in Figure 4.1.

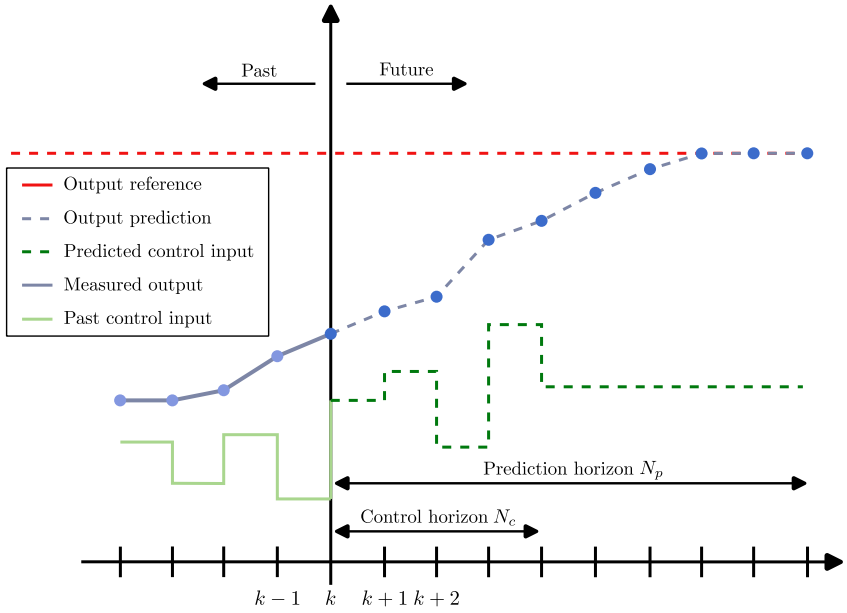

Figure 4.1: MPC illustration (adapted from [119]).

This form of predictive control is a well-known solution in the engineering environment, and it is gradually revealing its usefulness in the area of batteries [120]. By way of illustration,

De Castro et al. [17] suggest the use of an ECM based two-layer MPC, with the aim of achieving cell balancing, by controlling the thermal and SoC imbalances, the power losses, as well as the ageing stress factors. Another example is the work conducted by Kawakita de Souza et al. [121], in this research MPC is utilised to account for the evolution of time and temperature during the charging process, enabling this procedure to be completed in 500 seconds. MPC is also gaining presence in the PBM environment [120]. For instance, the research of Zhou et al. [122] proposes to employ MPC to reduce degradation mechanisms, such as lithium plating or SEI growth. With these MPC functionalities and the research questions in mind, while factoring the selected battery model, in the following section a control strategy for battery ageing-aware management is formulated, by means of non-linear MPC.

In formulating the battery management strategy, in line with the research question posed, the form of the cost function to be minimised by the MPC must also be taken into account. This entails considering whether it is possible to define the problem as a SOO, or if a MOO should be used instead. Addressing this dichotomy, the literature provides examples for both cases. In the case of SOOs, Ronghua et al. [123] have proposed a battery ageing-aware and temperature-aware predictive energy management strategy for parallel hybrid EVs, with a cost function that focuses only on the minimisation of the economic cost related to the ESS. In fact, the practice of using the economic cost has been contemplated by several other authors when formulating SOO problem [24, 124]. East et al. [125] follow the same strategy of considering a SOO, albeit for the sole purpose of optimising energy use in the hybrid system while minimising degradation. Complementing prior sources, there are several authors who, faced with the difficulty of formulating a SOO problem, at times suggest a MOO problem. As an example of this, Kordabad et al. [126] developed a MPC, based on Reinforcement Learning, that focuses on optimising the economic objective cost including low and high SoC values impact. In the academic paper by De Castro et al. [17] a MOO is also formulated when considering the impact of different battery stress factors on the same cost function. A third example could be that of Le Floch et al. [127], where they include the time-varying grid price, as well as the voltage deviation penalisation in the cost function. Moreover, Wang et al. [126] also pose a MOO by taking into account the impact on the cost function of the charging time, energy loss, and temperature rise. Although all the examples indicate that both options are functional, the choice of one of the options must be made in order to perform the control problem formulation correctly. Upon this selection, in this case the SOO is considered to be a more interesting and straightforward

alternative to answer the research question, given that an economic cost model is available to represent the impact of the operation of each of the agents that participate in the system, which, in turn, translates into the non-need to scale a multi-criteria problem.

4.1 CONTROL PROBLEM FORMULATION

With the optimal battery management in mind, a tertiary level ageing-aware control strategy is formulated via an economical non-linear MPC [128]. This strategy is built on both, the model representing the electrical and thermal characteristics of the battery, as well as on the degradation and economic cost presented in Chapter 3. Additionally, in this formulation, the model of the remaining system, a residential dwelling, is included to represent the cost of its functioning. This allows the battery operation to be regulated while minimising the overall running cost.

To do this, the first step is to specify the case-study at hand. On this instance, it is a BESS located in a residential dwelling, for the purpose of supplying the house's energy demand with the support of the grid and a PV system. The system operates as follows: the PV system supplies power whenever possible (positive P_{PV} during generation); meanwhile, the battery P_{BM} (positive for charging, negative for discharging) and the grid P_{Grid} (positive when energy surplus, negative to feed the load) are committed to managing that solar power optimally P_{PV}, while supplying the household's energy consumption P_{Load} (negative to represent demand). This is shown in Equation 4.1.

$$0 = P_{\mathrm{PV}}[k] + P_{\mathrm{Load}}[k] - P_{\mathrm{Grid}}[k] - P_{\mathrm{BM}}[k] \tag{4.1}$$

To develop the target algorithm, the next step is to have a system model for predicting the states, as represented in discrete-time form in Equation 4.2. In so doing, $\boldsymbol{x}$ represents the states of several system parameters, including the electrical, thermal and ageing characteristics of the cell, as well as the ones related to the case-study. All these states, based on the battery model from Chapter 3 and case-study data from Section 4.2.1, are shown in Equation 4.3. In this context it is pertinent to mention that index k refers to the discrete-time representation.

$$\boldsymbol{x}[k+1] = \boldsymbol{x}[k] + \Delta\boldsymbol{x}[k] \tag{4.2}$$

$$\boldsymbol{x} = \left[q_{\text{cell}}; v_{\text{cell}}; T_{\text{cell}}; P_{\text{cell}}; \mathbb{C}_{\text{SoH}}^{\text{ageing}}; Q_{\text{Loss,BM}}; \varphi_{\text{Ch}}; \varphi_{\text{Tot}}; T_{\text{amb}}; P_{\text{PV}}; P_{\text{Grid}}; P_{\text{Load}}; \mathbb{C}_{\text{Grid}}; \alpha; \beta \right] \tag{4.3}$$

Once battery ageing is predicted, following Equation 4.4, it is necessary to convey this capacity loss value to an economic cost $\boldsymbol{J}_{\text{BM}}$, which enables the optimisation of the system performance.

$$\boldsymbol{J}_{\text{BM}}[k] = f_{\text{cost}}(\mathbb{C}_{\text{SoH}}^{\text{ageing}}[k], Q_{\text{Loss,BM}}[k]) = \mathbb{C}_{\text{SoH}}^{\text{ageing}}[k] \cdot Q_{\text{Loss,BM}}[k] \tag{4.4}$$

Considering the states of the remaining system, represented in Equation 4.3, the economic value of operating the rest of the system ($\boldsymbol{J}_{\text{supply}}$) is predicted, as denoted in Equation 4.5. Using the case-study of this article as reference, τ denotes the discrete time-step, while $\mathbb{C}_{\text{supply}}$ and P_{supply} represent the grid energy cost $\mathbb{C}_{\text{Grid}}$ and the grid power P_{Grid} respectively.

$$\boldsymbol{J}_{\text{supply}}[k] = f_{\text{supply}}(\mathbb{C}_{\text{supply}}[k], P_{\text{supply}}[k]) = \mathbb{C}_{\text{Grid}}[k] \cdot P_{\text{Grid}}[k] \cdot \tau \tag{4.5}$$

To conclude, having defined the cost prediction models, as well as the different weighting factors α and β (for the battery and for the grid, respectively), the general quadratic cost function to be minimised is formulated as a single-objective problem, as depicted in Equation 4.6a.

$$\min J(u[k]) = \sum_{k=0}^{N_p} \left(\boldsymbol{J}_{\text{BM}}^T[k] \alpha^2[k] \boldsymbol{J}_{\text{BM}}[k] + \boldsymbol{J}_{\text{supply}}^T[k] \beta^2[k] \boldsymbol{J}_{\text{supply}}[k] \right) \tag{4.6a}$$

$$s.t. \quad \underline{\boldsymbol{x}} \leq \boldsymbol{x}[k] \leq \overline{\boldsymbol{x}} \tag{4.6b}$$

Building on this general formulation for the optimal energy management of the BESS, and accounting for the fact that it is a BESS located in a residential dwelling, as introduced in Section 4.2.1, it has been deemed relevant to formulate three variants of the cost-function with a view to determining which of them has the best results and the highest potential.

4.1.1 Baseline model predictive control

This control strategy is a model-based dynamic derating strategy that takes account of the electrical and thermal operation of the cell, yet it does not take degradation into consideration. Thus, by simplifying the Equation 4.6a to scenarios where the battery is operated within its SOA, excluding the calculation of its capacity loss and, therefore, its cost ($\boldsymbol{J}_{BM}^{T} = 0$), the goal is to minimise the cost of using energy from the grid with the Equation 4.7.

$$\min J(u[k]) = \sum_{k=0}^{N_p} \left(\boldsymbol{J}_{\text{supply}}^{T}[k] \boldsymbol{J}_{\text{supply}}[k] \right) \tag{4.7}$$

4.1.2 Static model predictive control

This is a model-based dynamic derating strategy that sets the operating conditions depending on the cost function defined in Equation 4.8. In so doing, the battery ageing, and, in turn, the battery cost, are computed at every optimisation for their minimisation. In this regard, the objective function is derived from Equation 4.6a assuming $\alpha = \beta = 1$. Such assumption is made in order to keep the ratio of the battery and grid cost constant.

$$\min J(u[k]) = \sum_{k=0}^{N_p} \left(\boldsymbol{J}_{\text{BM}}^{T}[k] \boldsymbol{J}_{\text{BM}}[k] + \boldsymbol{J}_{\text{supply}}^{T}[k] \boldsymbol{J}_{\text{supply}}[k] \right) \tag{4.8}$$

4.1.3 Adaptive model predictive control

This is, as well, a model-based dynamic derating strategy that sets the operating conditions contingent on the cost function defined in Equation 4.9. This cost function, however, introduces adaptive α and β values, assuming that $\alpha = \beta$ is always fulfilled.

$$\min J(u[k]) = \sum_{k=01}^{N_p} \left(\boldsymbol{J}_{\text{BM}}^{T}[k] \alpha_k \boldsymbol{J}_{\text{BM}}[k] + \boldsymbol{J}_{\text{supply}}^{T}[k] \beta_k \boldsymbol{J}_{\text{supply}}[k] \right) \tag{4.9}$$

For a better understanding of the rationale and the value of this adaptive cost function, a closer look at the battery ageing model is required (see Equation 3.23). As the battery ages, the range of values of ageing factors $k_{\text{Cyc,HighT}}$, $k_{\text{Cyc,LowT}}$, k_{Cal}, and $k_{\text{LowT,HighSoC}}$ do not change. That being said, due to the sub-linear nature of the term $\int \left(2x^{0.5}\right)^{-1} dx$, where

x can be τ, φ_{Ch} and φ_{Tot}, the change in capacity loss for every step-time decreases as the cell ages. On this ground, the economic impact in the cost function changes by orders of magnitude. This is shown in Figure 4.2, where integration term values are calculated assuming initial values after 100% efficient full charge and discharge cycles and a step-time of 900 seconds. For the analysis, charge φ_{Ch} and discharge φ_{Tot} throughput values are taking nominal capacity as reference: 5%, 15% and 25%. These ageing terms change significantly over time, and the difference in this magnitude will directly impact the value of the cost function for their respective capacity loss terms. In consequence, this can cause conflicts with the fixed tolerance value of the solver for the BoL conditions, since the capacity loss, and hence, economic cost values can fall below the set tolerance of the solver. In this scenario, the solver may struggle to optimise the global cost of the system.

In light of the above, the problem to be solved is scaled according to the parameter that will exhibit the largest magnitude change. Based on Figure 4.2, it is concluded that in Equation 4.10 τ is the most limiting factor for the optimisation, always factoring the initial assumptions. As such, by following Equation 4.11 it is possible to determine the adaptive value of α and β,

$$\begin{aligned}\alpha[k] = \beta[k] =& \lambda_1 \cdot \max\left(\frac{\left(\frac{\tau}{3600}\right)^{0.5}}{\left(\frac{t[k]+\tau}{3600}\right)^{0.5} - \left(\frac{t[k]}{3600}\right)^{0.5}}, \frac{{\Delta\varphi_{\mathrm{Ch}}}^{0.5}}{(\varphi_{\mathrm{Ch}}[k] + \Delta\varphi_{\mathrm{Ch}})^{0.5} - \varphi_{\mathrm{Ch}}[k]^{0.5}}, \right. \\ & \left. \frac{{\Delta\varphi_{\mathrm{Tot}}}^{0.5}}{(\varphi_{\mathrm{Tot}}[k] + \Delta\varphi_{\mathrm{Tot}})^{0.5} - \varphi_{\mathrm{Tot}}[k]^{0.5}} \right)\end{aligned} \tag{4.10}$$

$$\alpha_k = \beta_k = \lambda_1 * \frac{\left(\frac{\tau}{3600}\right)^{0.5}}{\left(\frac{t[k]+\tau}{3600}\right)^{0.5} - \left(\frac{t[k]}{3600}\right)^{0.5}} \tag{4.11}$$

where the value λ_1, equal to 9, is a variable that adds some flexibility in adjusting the MPC, with a view to improving the cost function scaling and the control accuracy of the optimisation formulated in Equation 4.9. These values are updated only at the beginning of every optimisation for two reasons: on the one hand, since their variation over the prediction horizon is not considered to be critical; and, on the other hand, as, should the value of α and β vary over the course of the optimisation, each economic cost would be adapted to a different scale.

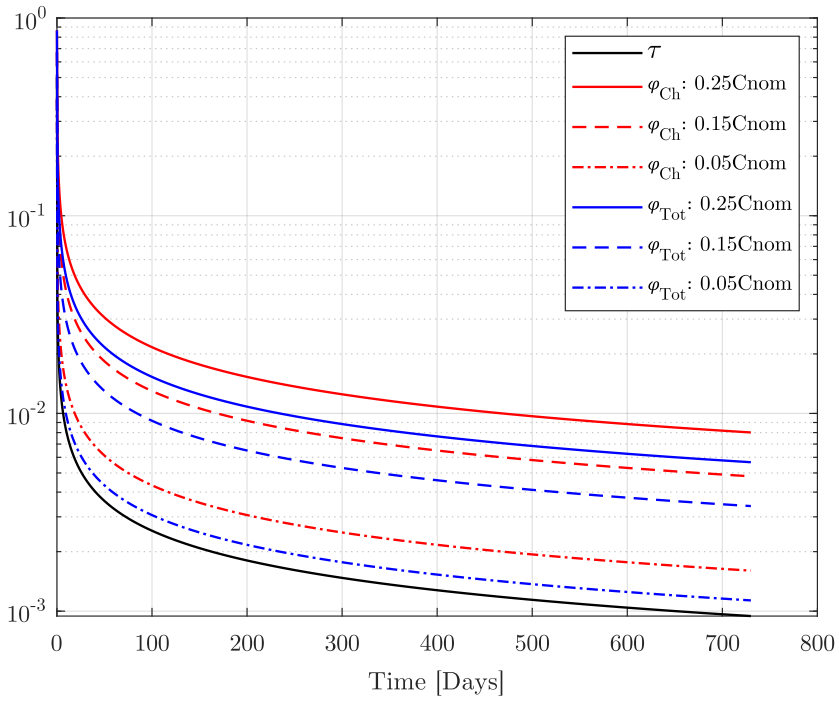

Figure 4.2: Sub-linear nature of the term $\int \left(2x^{0.5}\right)^{-1} dx$, where x can be τ, φ_{Ch} and φ_{Tot}. Capacity loss rate for every step-time decreases as the cell ages.

4.2 SIMULATION SETUP

4.2.1 Case-study data

In this context, the selected case-study, introduced in Section 4.1, is about a BESS located in a residential dwelling, for the purpose of supplying the house's energy demand, with the support of both, the grid and a PV system. To evaluate the performance of the previously formulated control strategies, based on a MPC, it is mandatory, first, to identify the system variables that can be classified as predictable and, second, to determine the input data that represents their evolution. There are four variables that can be anticipated in this case-study, and the profiles used for each one of them are shown in Figure 4.3:

- **Household power demand(P_{Load}):** A daily profile representing the monthly average (month: October) is calculated on the basis of [129]. An annual energy demand of 5000 kWh [130] is, likewise, defined.

- **Solar power (P_{PV}):** Data on radiation is extracted from [131], in order to generate a daily profile representing the monthly average (location: Sacramento, CA, USA). The power peak of the installation is 10kW [73].

- **Ambient temperature (T_{amb}):** A daily profile representing the average for the month is generated based on the data from [131].
- **Grid cost ($\mathbb{C}_{\text{Grid}}$):** Based on the monthly average, a daily profile is created, taking as a reference data obtained from [132].

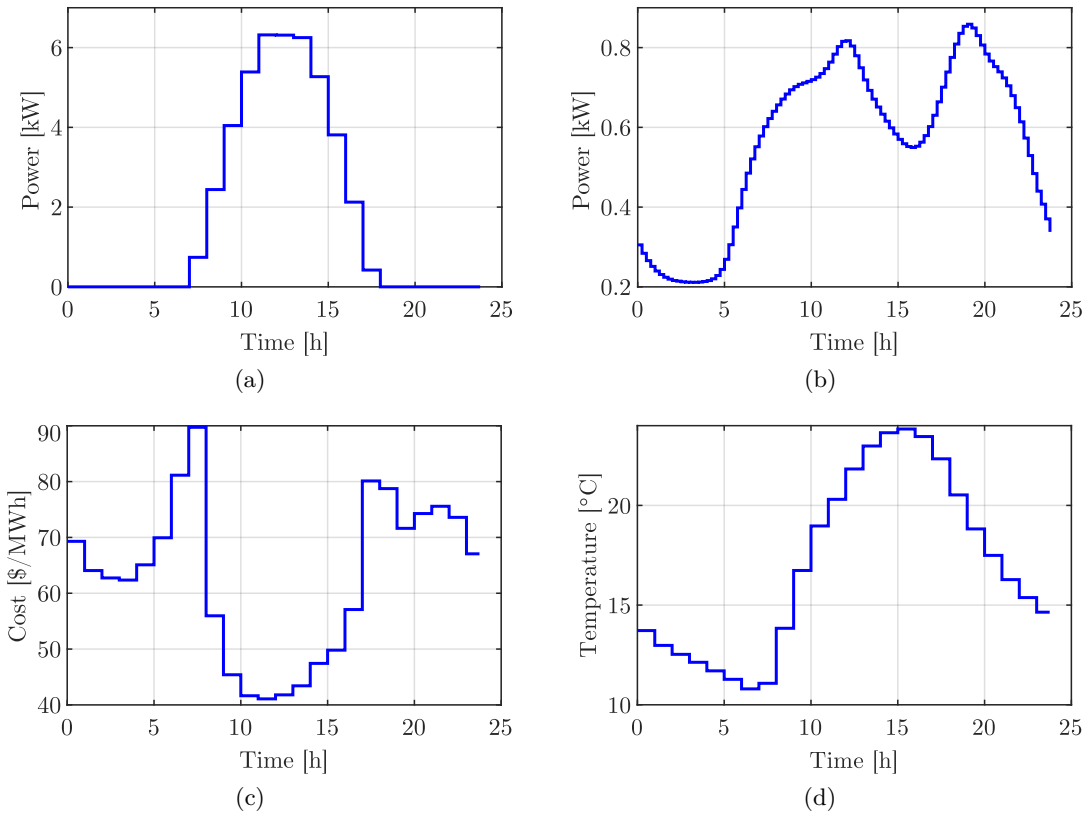

Figure 4.3: Predictable input data for the household scenario.

4.2.2 Battery parameter initialisation

Additionally to the previously introduced case-study related predictable input data, a series of parameters related to the battery are called upon. With reference to the presented cell and module model in the Chapter 3, and following the example in [73], a 2.5 kWh battery is considered for this analysis, with a 16P16S cell configuration. Regarding the economic cost model of the BESS, the initial investment is assumed to be of 700 $ (350 $/kWh, this is a general approach that has been determined for this research) [133–135] and the EoL is expected to be achieved when the nominal capacity of the cell is below 60% of its BoL value. On top of this data set, five assumptions have been made for the initialisation of the battery in each simulation:

- **Assumption 1:** When modelling the battery, it is undertaken that all cells operate in the same way, without heterogeneities.
- **Assumption 2:** An initial SoH value of 1 is presumed for the initialisation of every simulation.
- **Assumption 3:** To initialise the tests at different points in the life of the battery, it is assumed the criterion of one full charge and discharge cycle per day with an efficiency of 100%. Accordingly, the data used for the ageing rate initialisation of the different simulations are shown in the Table 4.1.
- **Assumption 4:** The initial battery temperature is set to equal the initial ambient temperature.
- **Assumption 5:** The initialisation of the SoC has a direct impact on the final cost, which is relevant when analysing a real system. However, by considering the same initialisation point for all simulations, it is useful to better analyse the decision making and operating dynamics of the MPC.

Table 4.1: Battery initialisation parameters at different lifetime stages.

Parameters	Day 1	Week 1	Month 1	Month 6	Year 1	Year 2
Ah_{Ch} [Ah]	3	21	90	480	1080	2160
Ah_{Tot} [Ah]	6	42	180	960	2160	4320
time [h]	24	168	720	4320	8640	17280
SoC [-]	0.5	0.5	0.5	0.5	0.5	0.5
SoH [-]	1	1	1	1	1	1

Having previously introduced the input data related to the case-study and having determined the initial conditions, as well as the assumptions, the next section defines the characteristics of the MPC algorithm.

4.2.3 Control settings

Once the optimisation problem has been formulated and the data for the case-study analysis has been presented, the next step is to determine the characteristics of the control system in order to determine the optimal operation of the BESS. In this instance, as it is a non-linear and non-convex optimisation problem due to the characteristics of the cell model,

it is opted to resort to the solver interior point optimisation (IPOPT) using YALMIP (a toolbox for modelling and optimisations in MATLAB®) [20]. In addition to the solver, more control characteristics are needed to be determined for optimisation. Regarding these factors, it is worth noting that the MPC is a complex algorithm that generally requires heuristic knowledge for its tuning. In this scenario, the step-time of the system has been set to 15 minutes, taking into account both the battery dynamics and the predicted data related to the case-study in Section 4.2.1. In order to determine the prediction horizon, both 8 and 16 steps (2 and 4 hours, respectively) have been considered to be of interest, in view of the dynamics of the application. Finally, as it regards the operation of the control system, a series of extra data are shown in Table 4.2 (framed within an iterative experimentation approach).

Table 4.2: Optimisation problem settings for the residential dwelling scenario.

Parameters	Value
Optimisation solver	IPOPT
Prediction horizon (N_p)	8 and 16
Optimisation step time	15 minutes
Initial guess	Yes
Maximum iterations	1e4
Maximum CPU time	3 minutes
Optimal solver tolerance	1e-12
Acceptable solver tolerance	1e-10
CPU	AMD Ryzen 7 7800X3D 4.2 GHz
RAM	32.0 GB

4.3 RESULTS AND DISCUSSION

In this section, the performance of the three MPC strategies introduced in Section 4.1 is evaluated in a residential PV + BESS scenario. The performance is compared not only from a operation dynamics point of view, but also from the overall operation indicators at the end of the 24 hours cycle. In addition, an RCP system is used to analyse the performance of the best of the three options in order to make a first experimental feasibility approach.

4.3.1 Simulation analysis

This section presents the results obtained in the simulations. This analysis has considered the three control strategies: static MPC, adaptive MPC and baseline MPC. As this is a complex comparison, the study is divided into two parts: first, the results of static MPC and baseline MPC are displayed and compared with those of adaptive MPC, from a dynamics point of view; and, second, results obtained at the end of each 24-hour simulation are examined under different battery life conditions and various prediction horizons.

4.3.1.1 *Battery system dynamics*

The design of a control strategy calls upon an analysis of the system's dynamics throughout its operation. In so doing, the impact of one or another control setpoint on the BESS can be contrasted, even with prior heuristic knowledge. The objective is to understand the strengths and weaknesses of each of the three cost functions to be minimised. To this end, findings obtained are dissected across various life aspects and with different cost functions: day 1 and year 1; static MPC vs adaptive MPC, as well as, baseline MPC vs adaptive MPC.

First, Figures 4.4 and 4.5 depict the comparison of static MPC vs adaptive MPC, considering the battery life at day 1 and year 1. In these figures, results are shown during a 24-hour simulation, for the case of a prediction horizon of 8 steps. Under these premises, the following operating phases and dynamics can be observed:

1. When the battery has stored energy and its use is more economical than the grid, the discharge of the BESS is prioritised. This phenomenon occurs in static MPC and adaptive MPC.

2. If the control deems unnecessary the energy stored in the battery for the operation along the prediction horizon, it may determine to discharge it to the grid. This phenomenon occurs in the static MPC and adaptive MPC.

3. Upon a critical increase in the cost of the grid in the near future, it is observed that the system may choose to charge the battery from the grid for subsequent discharge. This phenomenon is more dominant in the adaptive MPC than in the static MPC.

4. During periods in which the battery is discharged and is not foreseen to be needed, the most economical option is the non-use of the BESS, keeping it at the minimum SoC. This is only appreciable in the adaptive MPC.

5. When the system foresees a future consumption of the household, and the use of the battery, together with the PV system, is found to be a more economical option, it is opted to charge the BESS; always in accordance with the forecasted need along the prediction horizon. This is more accurately met in the adaptive MPC.

Having reviewed the alternatives and concluded that the adaptive MPC has better dynamics than the static MPC, the next step is to compare the best of these two options with the dynamics of the baseline MPC. These results are visible in Figures 4.6 and 4.7, also at the scale of a single cell during a 24-hour simulation, for the case of an 8-step prediction horizon. When performing this analysis, the comparison of the previously mentioned dynamics is remarkably analogous. Therefore, it is safe to argue that, based on these results, the adaptive MPC is a better choice than the baseline MPC.

Considering the preceding, a system based on the adaptive MPC presents dynamics that, first, end up in better overall results, and second, fit more accurately the theoretical behaviour that the complete system should display. As an example of the adaptability of this control, Figure 4.8 shows the evolution of the adaptive factor of Equation 4.11, not only for lifetimes of day 1 and year 1, but also for other scenarios that are contemplated in Table 4.1.

Finally, regardless of which of the options provides better results, it is interesting and advisable to analyse the evolution of the solver diagnostics. This allows to find out if the optimisation process has been carried out correctly (diagnostic equals 0) or if there has been some kind of error during the optimisation process, for instance, a maximum number of iterations (diagnostic is 3) or a time limit (diagnostic is -1). For further details about diagnostic errors see Appendix B. In the results presented in Figures 4.9 and 4.10, it becomes apparent that, although the adaptive MPC is the best performing control algorithm from an economic point of view, the solver suffers more with the adaptive MPC than with the static MPC or the baseline MPC. This means that the adaptive factor improves the results while making it more difficult for the solver to optimise the performance of the BESS correctly.

4.3.1.2 *Analysis at end of the cycle*

Beyond displaying the operating dynamics of each of the three controls (baseline, static and adaptive), the different performance indicators at the end of the cycle are also to be analysed and compared. Especially the economic cost, which is the sole objective of the

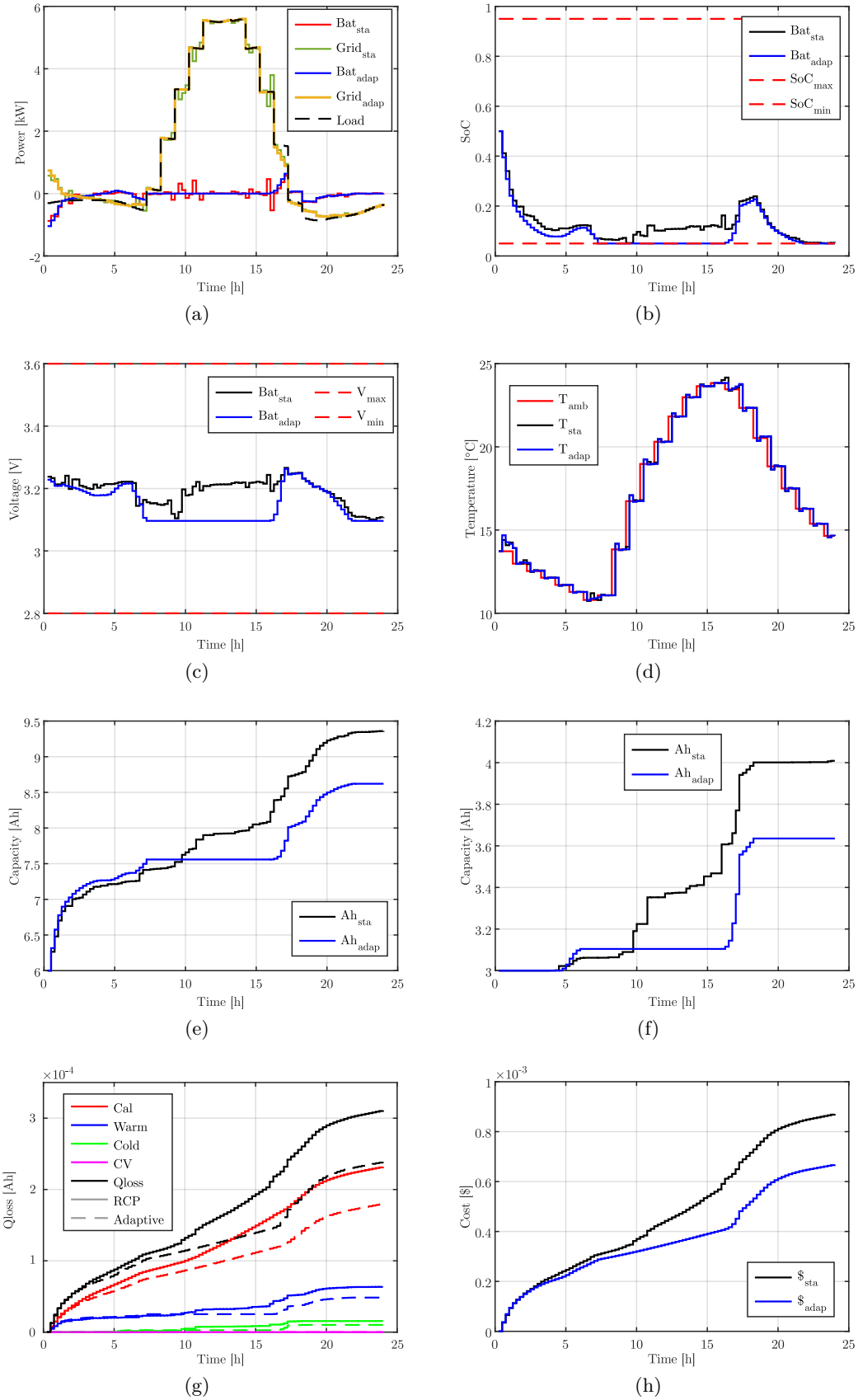

Figure 4.4: Static MPC vs adaptive MPC, at the first day with 2 hours of prediction horizon (N_p=8); a) Power profile, b) State of Charge, c) Voltage, d) Temperature, e) Overall capacity, f) Charged capacity, g) Capacity loss, and h) Cell operation cost.

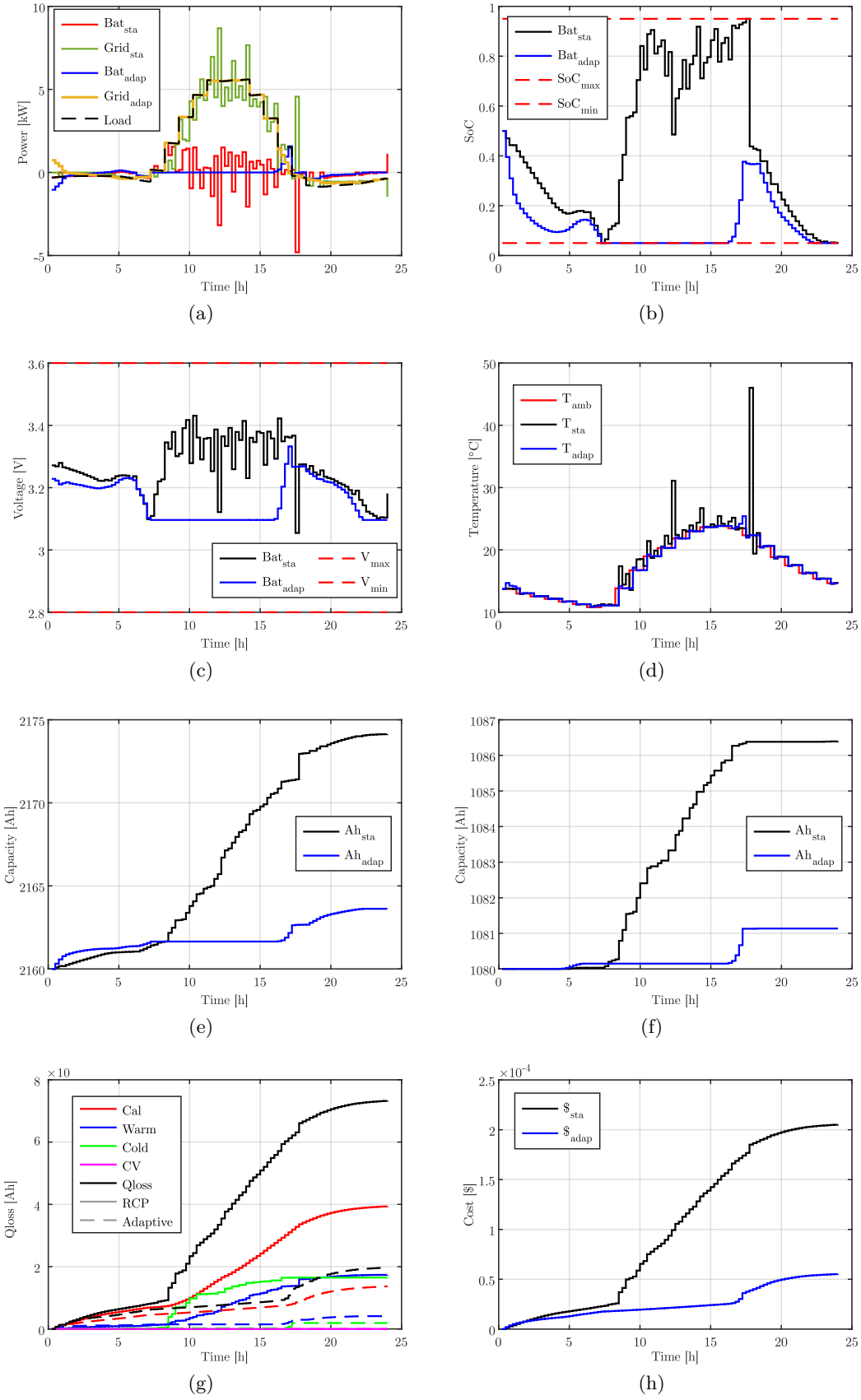

Figure 4.5: Static MPC vs adaptive MPC, at the first year with 2 hours of prediction horizon (N_p=8); a) Power profile, b) State of Charge, c) Voltage, d) Temperature, e) Overall capacity, f) Charged capacity, g) Capacity loss, and h) Cell operation cost.

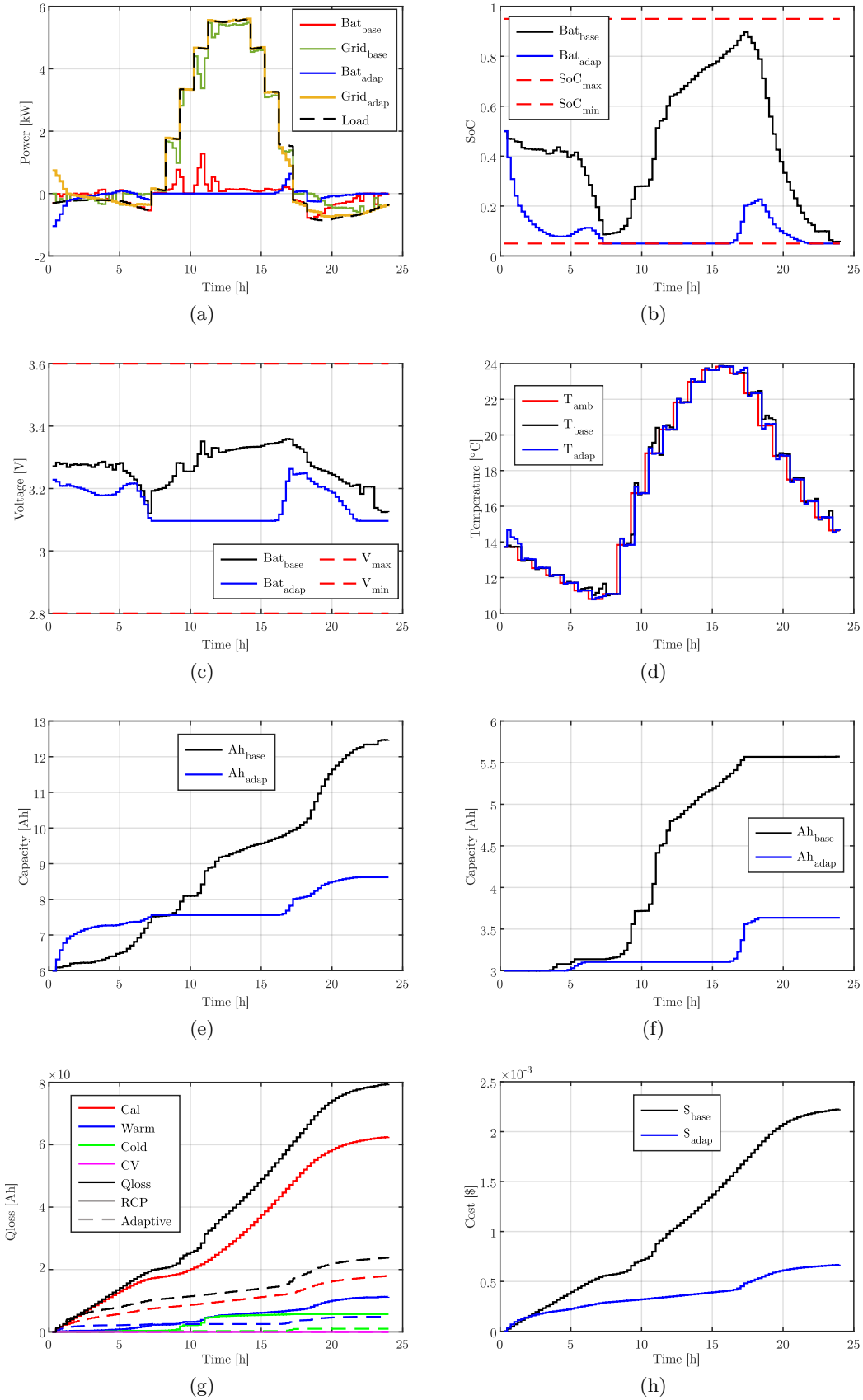

Figure 4.6: Baseline MPC vs adaptive MPC, at the first day with 2 hours of prediction horizon (N_p=8); a) Power profile, b) State of Charge, c) Voltage, d) Temperature, e) Overall capacity, f) Charged capacity, g) Capacity loss, and h) Cell operation cost.

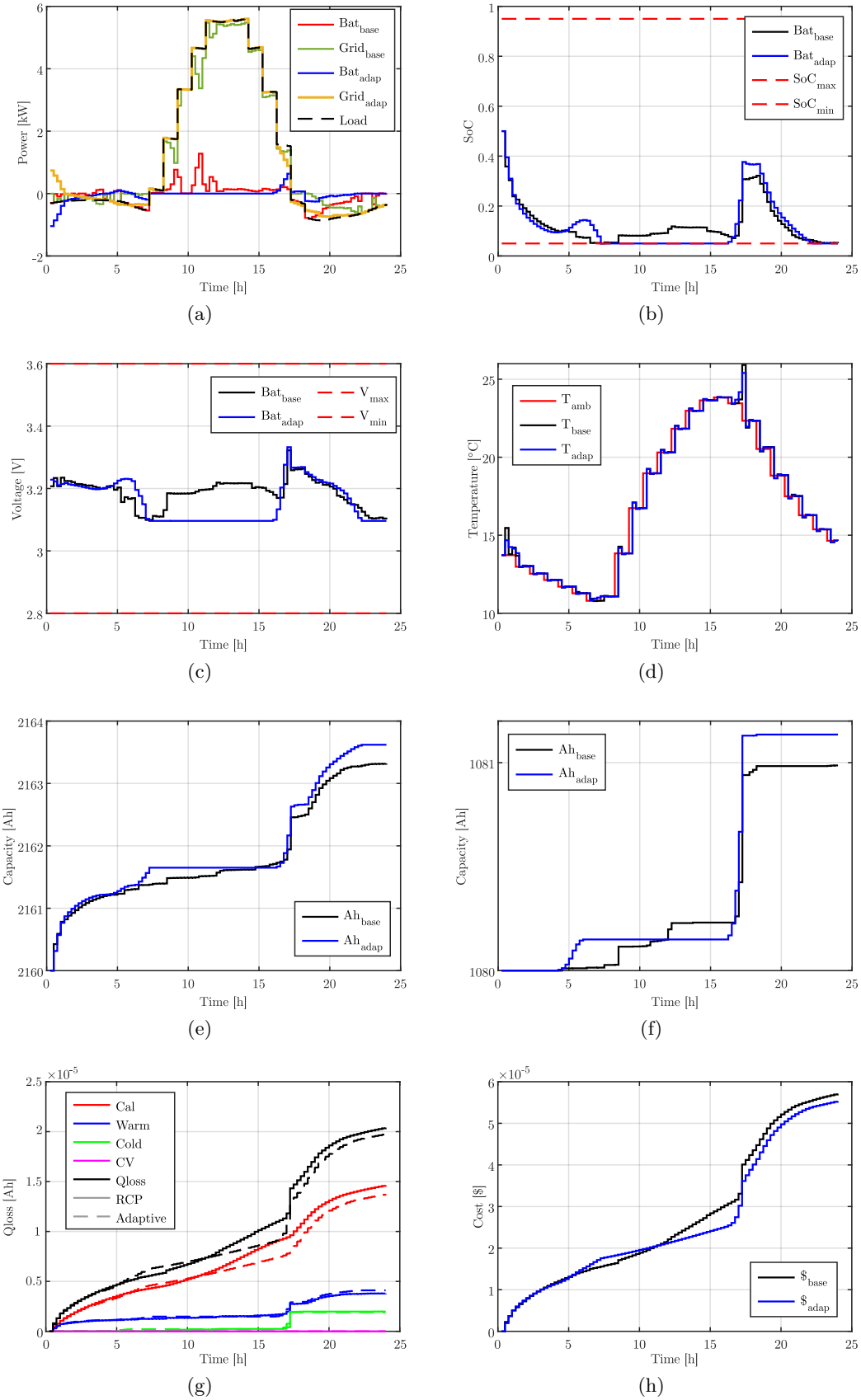

Figure 4.7: Baseline MPC vs adaptive MPC, at the first year with 2 hours of prediction horizon (N_p=8); a) Power profile, b) State of Charge, c) Voltage, d) Temperature, e) Overall capacity, f) Charged capacity, g) Capacity loss, and h) Cell operation cost.

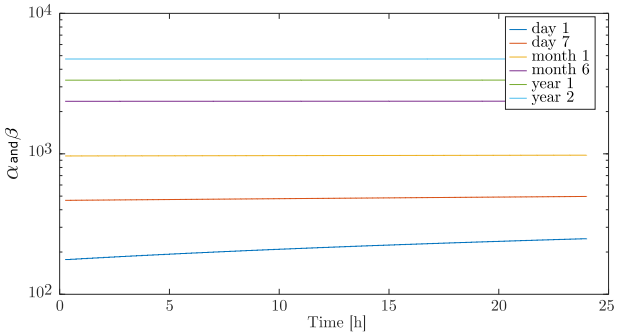

Figure 4.8: Adaptive factor α and β evolution over 24h simulation at different ageing scenarios for N_p=8.

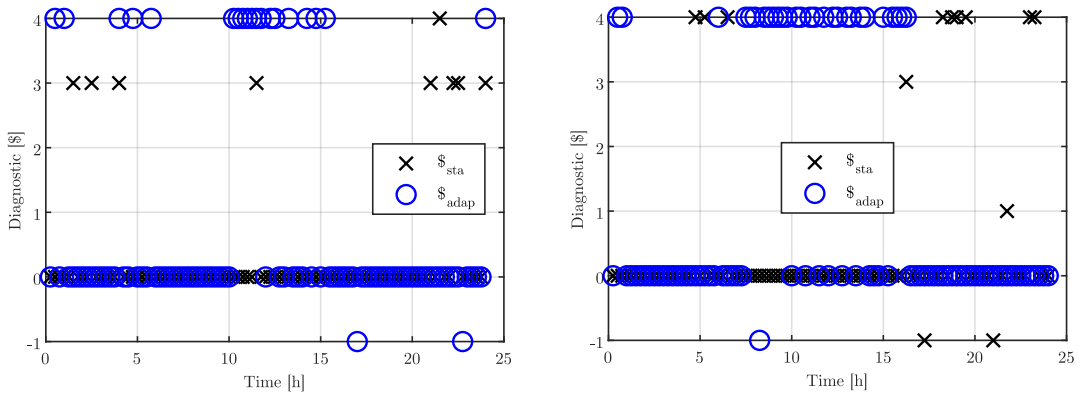

Figure 4.9: Adaptive MPC vs static MPC simulation solver optimisation diagnostic comparison (N_p=8); a) Day 1, and b) Year 1.

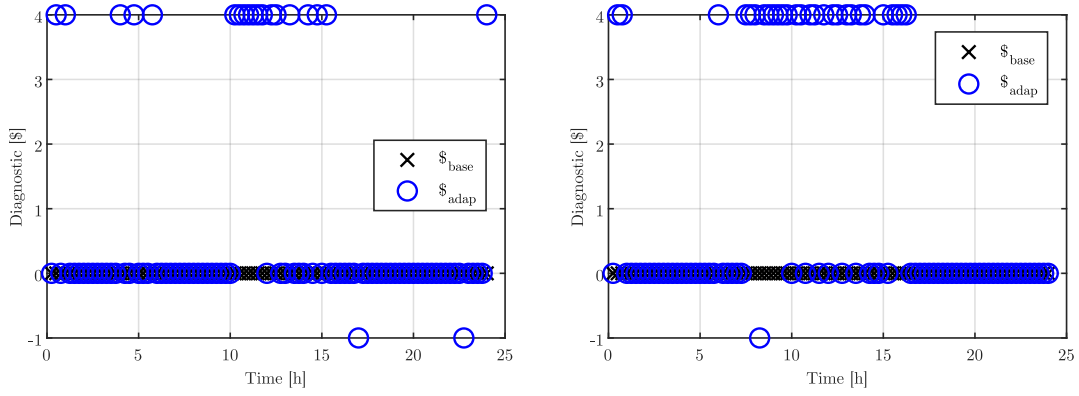

Figure 4.10: Adaptive MPC vs baseline MPC simulation solver optimisation diagnostic comparison (N_p=8); a) Day 1, and b) Year 1.

cost function and, accordingly, the main key performance indicator (KPI) of the results obtained.

On the one hand, Figures 4.11 and 4.12 show results obtained from the point of view of capacity loss and economic cost, at the different battery life stages (see Table 4.1). Analysing first the degradation results, unlike in the adaptive MPC vs baseline MPC scenario, when comparing the static MPC with the adaptive MPC, it is observed that the latter option presents a lower capacity loss in all cases. In the former comparison, the degradation at the BoL is lower with the adaptive MPC, yet as the battery ages, this difference decreases until it reaches similar degradation values. Upon closer examination of the results from a cost point of view, however, the improvement of adaptive CPM is indisputable (with the exception of year 2, at which point the oscillating dynamics of the static MPC end up favouring the economic cost "unintentionally"). As to this, early in life, the price is reduced in the comparison of static MPC and baseline MPC by 9.08% and 42.58%, respectively. Cross-checking results one year on, the approximate maximum period for which the cell ageing model has been validated, the reduction is still 5.88% and 4.95%.

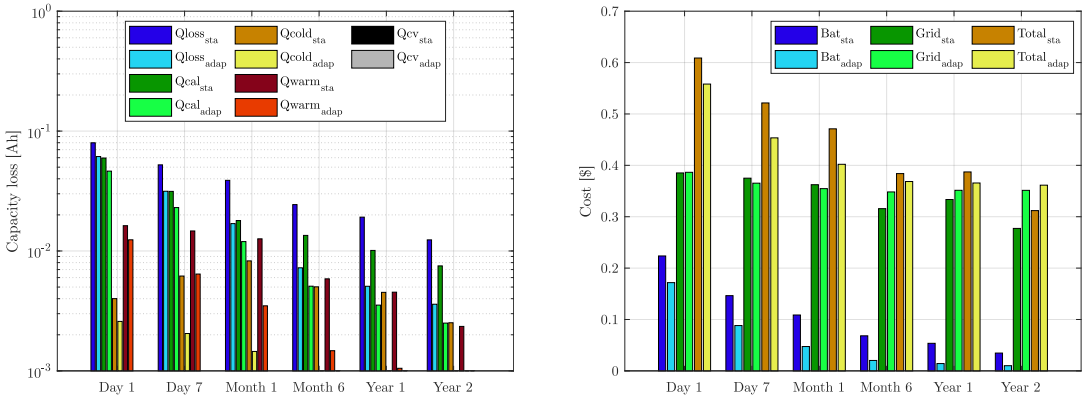

Figure 4.11: Static MPC vs adaptive MPC at the end of the 24 hours at different ageing levels (N_p=8): a) Capacity loss factors, and b) System operation economic cost.

On the other hand, in analysing the results, it is relevant to understand how the choice of prediction horizon affects outcomes, especially the cost. This stems from the fact that a longer prediction horizon grants access to a greater amount of information for the optimisation, which generally increases the stability of the system, albeit it also raises the computational complexity of the optimisation. For ease of understanding, results of this comparison, for an N_p equal to 8 and 16, are presented in Table 4.3. This table shows the results at the end of each simulation and at three points in battery lifetime (Day 1, Month 1, and Year 1):

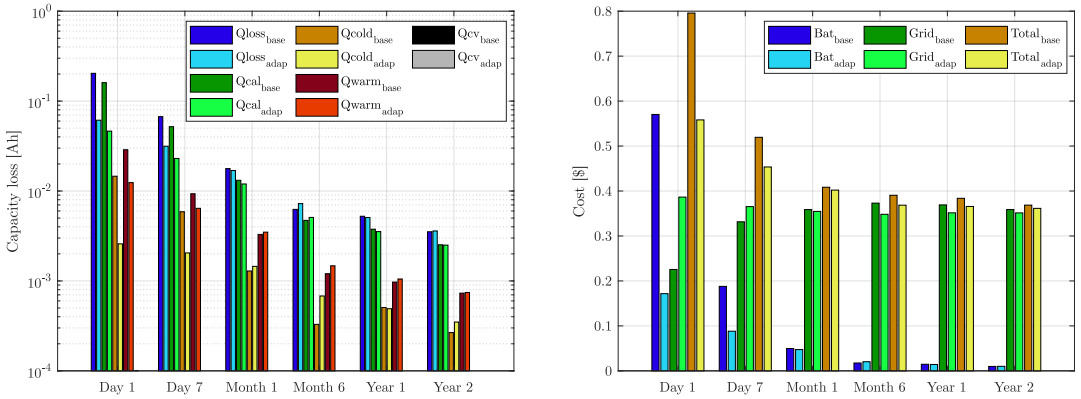

(a) (b)

Figure 4.12: Baseline MPC vs adaptive MPC at the end of the 24 hours at different ageing levels (N_p=8): a) Capacity loss factors, and b) System operation economic cost.

- **Day 1:** In both cases the amount of charged and total operated Ah by the adaptive MPC is lower than the operated by static MPC and the baseline MPC. Meanwhile, from the overall cost point of view, even with a N_p=16, the adaptive MPC results show an improvement of 21.64% and 45.12%. Data also demonstrate that the system performance dynamics for N_p equal to 8 are not fully consistent for an N_p of 16, because the latter exhibits a 5.38% higher overall cost values when comparing the results obtained with both adaptive MPCs. This only happens in this specific scenario due to solver diagnostic related issues.

- **Month 1:** In both cases the amount of charged and total operated Ah by the adaptive MPC is between the static MPC and the baseline MPC. Meanwhile, from the overall cost point of view, even with a N_p=16, the adaptive MPC results show an improvement of 37.33% and 12.58%. Data also proves that the system performance dynamics for N_p equal to 8 are consistent for an N_p of 16, but in this case, the latter exhibits a 19.08% lower total cost values when comparing the results obtained with both adaptive MPCs.

- **Year 1:** In both cases the amount of charged and total operated Ah by the adaptive MPC is between the static MPC and the baseline MPC. In the minetime, from the overall cost point of view, even with a N_p=16, the adaptive MPC results show an improvement of 6.83% and 29.92%. Data also confirms that the system performance dynamics for N_p equal to 8 are consistent for an N_p of 16, while the latter option exhibits a 27.88% lower total cost values when comparing the results obtained with both adaptive MPCs.

Considering the above, results of the Table 4.3 reveal that as the battery life progresses, the ageing-rate suffered by the cells decreases, and, therefore, a greater use of the battery, with a higher prediction horizon, and by means of an adaptive MPC, facilitates the minimisation of the overall cost.

4.3.2 Rapid control prototyping analysis

Results displayed so far are limited to the analysis performed by simulations where the adaptive MPC exhibits the best characteristics. Based on these findings, a further analysis of both the dynamics and the performance results, at the end of the studied period, is deemed to merit discussion. By means of the data obtained in the laboratory, a comparison with the results obtained previously is sought, so as to analyse the applicability of this control strategy in a real-time system. Having said that, it is relevant to mention that the development of an experimental platform, completely faithful to the described case-study, is out of the scope of this thesis. As an alternative, the development of an RCP system has been suggested. The main advantage of this RCP is the ability to develop, test, and debug control algorithms in a real hardware and real-time environment, allowing for more accurate and faster validation of the controller design before its final implementation in the case-study system [136, 137]. A detailed description of the setup and operation of this experimental platform is given in Appendix C.

To perform the aforementioned experimental analysis of the adaptive MPC, aiming to compare them with the results previously obtained, the different lifetimes shown in Table 4.1 are considered (Day 1, Month 1, Month 6, and Year 1), with the particularity of focusing on the only case of $N_p = 8$.

4.3.2.1 *Battery system dynamics*

Via the analysis of the adaptive MPC in the RCP system, an assessment and comparison of the dynamics of the battery operation, during the simulation period of 24 hours, has been conducted. These results are shown in Figures 4.13 and 4.14 for the ageing conditions of the first day and the first year, respectively.

A glance at these results reveals that the simulation and RCP results follow almost identical dynamics. So much so that the charging, discharging and rest periods are repeated in both cases. Once the correct operation of the RCP system has been determined, and the replicability of the results obtained in simulation, in an experimental environment, has

Table 4.3: Analysis of the energy management at different battery lifetimes with two prediction windows: N_p=8 and N_p=16.

		Day 1					
		N=8			N=16		
		Static	Adaptive	Baseline	Static	Adaptive	Baseline
Capacity [Ah]	Charged	258.25	162.65	658.49	505.98	314.05	737.54
	Total	860.08	670.91	1657.4	1347.04	973.71	1769.3
ageing [Ah]	Calendar	0.0596	0.0464	0.1603	0.1106	0.0661	0.1437
	Cold	0.004	0.0026	0.0146	0.0103	0.0054	0.0192
	Warm	0.0163	0.0124	0.0288	0.0241	0.0182	0.0324
	High SoC	0	0	0	0	0	0
	Total	0.0799	0.0613	0.2037	0.1451	0.0898	0.1952
Cost [$]	Battery	0.2236	0.1717	0.5703	0.40602	0.2514	0.5466
	Grid	0.3852	0.3865	0.2256	0.3092	0.3368	0.307
	Total	0.6089	0.5582	0.7959	0.7154	0.5882	0.8536

		Month 1					
		N=8			N=16		
		Static	Adaptive	Baseline	Static	Adaptive	Baseline
Capacity [Ah]	Charged	1076.6	275.28	254.66	1072.2	589.26	524.57
	Total	2379	896.17	853.48	2484	1524.1	1388.9
ageing [Ah]	Calendar	0.0179	0.012	0.0132	0.025	0.0207	0.0209
	Cold	0.0083	0.0015	0.0013	0.0087	0.0036	0.0028
	Warm	0.0126	0.0035	0.033	0.0142	0.0067	0.0057
	High SoC	0	0	0	0	0	0
	Total	0.0388	0.0169	0.0177	0.0479	0.0309	0.0293
Cost [$]	Battery	0.1087	0.0474	0.0497	0.1342	0.0867	0.0821
	Grid	0.3623	0.3547	0.3587	0.3216	0.2387	0.2842
	Total	0.4711	0.402	0.4084	0.4468	0.3253	0.3663

		Year 1					
		N=8			N=16		
		Static	Adaptive	Baseline	Static	Adaptive	Baseline
Capacity [Ah]	Charged	1637.4	290.61	252.53	1711.8	671.2	540.41
	Total	3618.5	926.82	849.84	3731.04	1687.9	1418.5
ageing [Ah]	Calendar	0.0101	0.0035	0.0038	0.0113	0.0061	0.0048
	Cold	0.0045	0.0005	0.0005	0.0048	0.0014	0.0012
	Warm	0.0045	0.0011	0.0009	0.0045	0.0021	0.0017
	High SoC	0	0	0	0	0	0
	Total	0.0192	0.0051	0.0052	0.0206	0.0096	0.0078
Cost [$]	Battery	0.0536	0.014	0.0147	0.0577	0.0268	0.0218
	Grid	0.3335	0.3514	0.3691	0.224	0.2369	0.3208
	Total	0.3872	0.3657	0.3838	0.2817	0.2637	0.3418

been assessed, a more detailed analysis can be carried out. The objective is to identify any differences related to the most faithful model to the real cell and its real-time operation in the RCP system. This research has found that, as expected, variables such as cell voltage, SoC or temperature in real-time do not vary as drastically as in a simulation with a step-time of 15 minutes. It is also interesting to note that the results presented in Figure 4.14 show the consequence of having simplified cell voltage models in the control algorithm, what ultimately has a direct impact on the power demand of the grid, and therefore, in the overall cost.

Finally, Figure 4.15 presents a comparison of the solver diagnostics obtained throughout both analyses. While the optimisation struggles in the simulations during the periods where PV overgeneration occurs, the real-time results show a completely different response. In this RCP system the solver is capable of getting an optimal solution in most of the cases.

4.3.2.2 *Analysis at the end of the cycle*

Beyond the analysis of the dynamics, the impact of possible performance differences on the optimisation objective, at the end of the analysis period, has to also be analysed. For this purpose, Figures 4.16a and 4.16b depict the sum of the capacity loss of all cells and the corresponding economical cost for both, the BESS and the grid. From these figures it can be noticed that, as a consequence of the slight variation in real-time, there are differences for all the ageing conditions. In terms of cost, in either case, the RCP system shows higher total costs than the adaptive MPC simulation, mainly because of the voltage prediction error. All these differences, however, do not exceed an average variation of 3.69% for the overall capacity loss and 2.81% for the total cost of operating the system.

4.4 SUMMARY AND CONCLUSIONS

The main objective of this chapter was to formulate the control problem by presenting three alternatives aimed at minimising the cost function - the economic cost - using the MPC. To this end, this chapter began by analysing the three alternatives, with the goal of determining which one presents the best result and, consequently, the greatest potential for this case-study. Next, the best of the three alternatives has been analysed on an experimental platform, by means of an RCP system, in order to assess the viability of the selected control algorithm in a real environment. This testing enabled conclusions to be

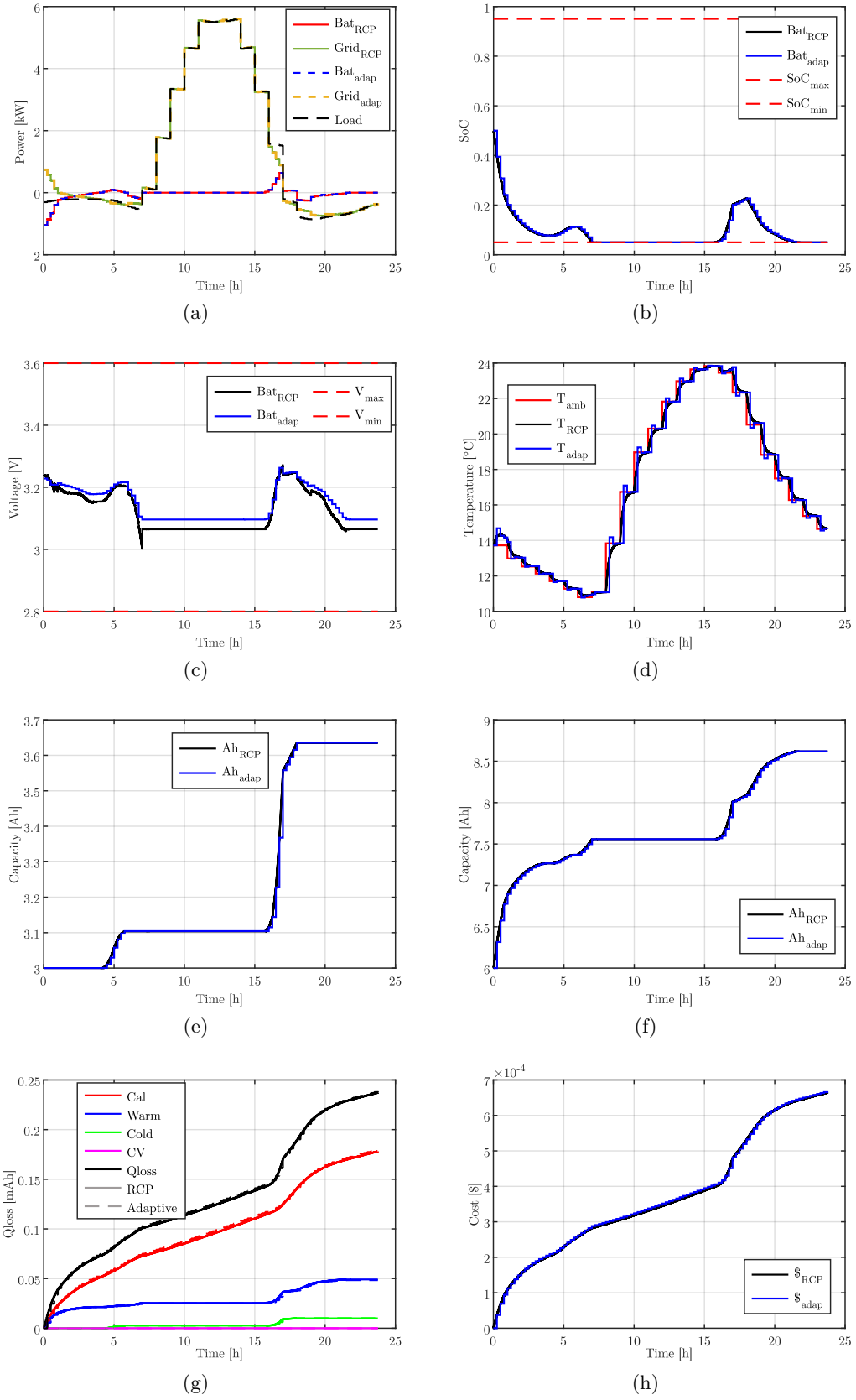

Figure 4.13: Simulation vs RCP system comparative at the first day and with 2 hours of prediction horizon (N_p=8); a) Power profile of the battery module, b) State of Charge, c) Voltage of the cell, d) Temperature, e) Overall capacity of the cell, f) Charged capacity of the cell, g) Capacity loss of the cell, and h) Cell operation cost.

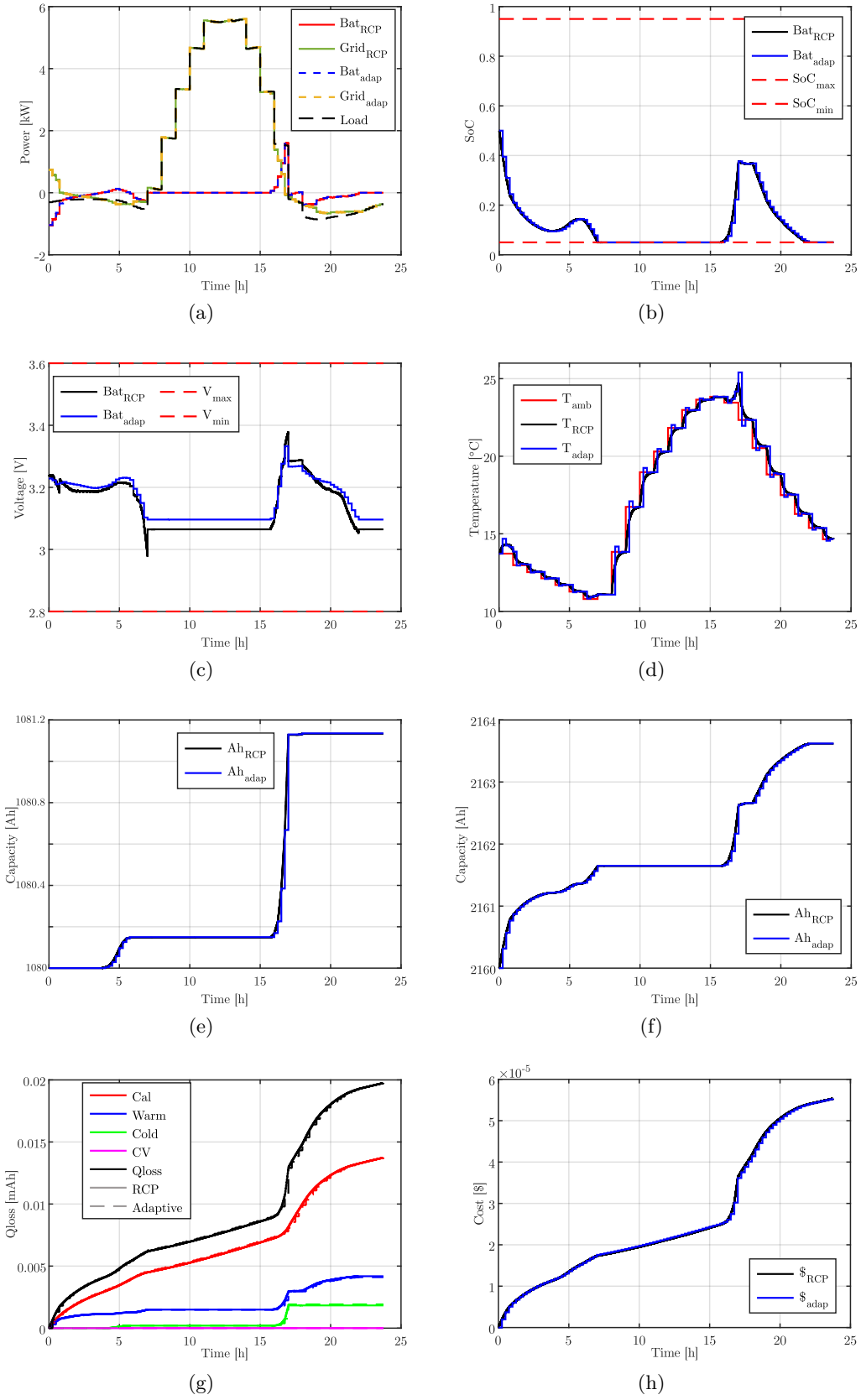

Figure 4.14: Simulation vs RCP system comparative after the first year and with 2 hours of prediction horizon (N_p=8); a) Power profile of the battery module, b) State of Charge, c) Voltage of the cell, d) Temperature, e) Overall capacity of the cell, f) Charged capacity of the cell, g) Capacity loss of the cell, and h) Cell operation cost.

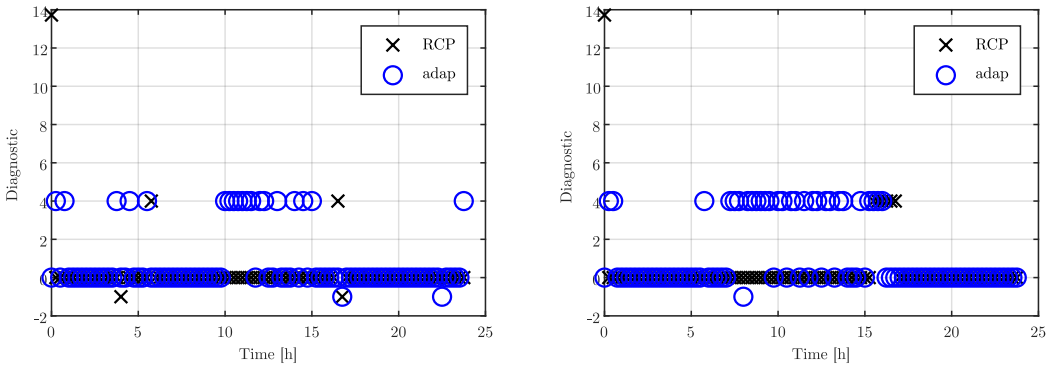

(a) (b)

Figure 4.15: Simulation vs RCP system solver optimisation diagnostics comparison for N_p=8: a) Day 1, and b) Year 1.

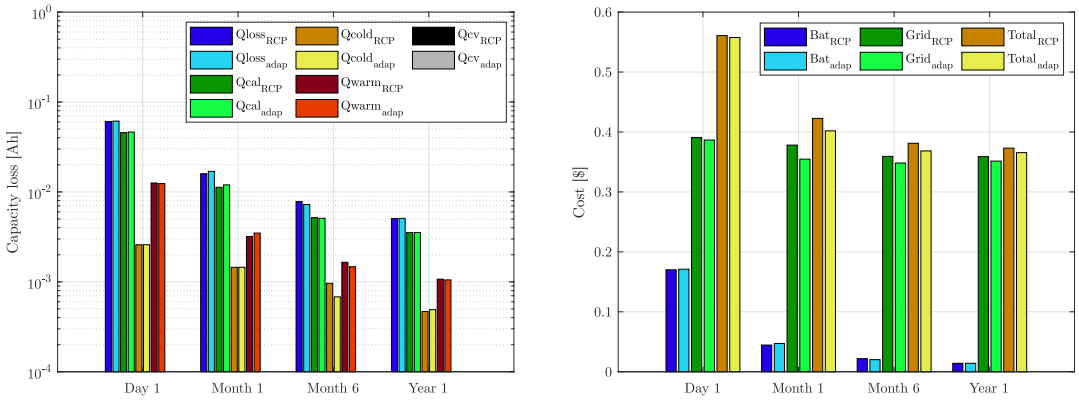

(a) (b)

Figure 4.16: Adaptive MPC vs RCP MPC at the end of the 24 hours at different ageing levels (N_p=8): a) Capacity loss mechanisms, and b) System operation economic cost.

drawn with a view to developing the control algorithm focused on the modular BESS in Chapter 5.

Based on an analysis of the dynamics and the cost function objective, the comparison among the baseline MPC, the static MPC and the adaptive MPC, at the end of the simulation, reveals that the third option is the best choice. This third option presents the best results, mainly due to its stability during the 24 hours simulation. Ultimately, the adaptability of the scale of the cost function to be minimised allows the solver to find a more suitable current setpoint for the operation of the BESS. Especially during periods where the operating cost is lower than usual (low battery ageing rate or no grid cost), and, therefore, the solver is not able to find the appropriate setpoint for the baseline MPC or the static MPC. Bearing this in mind, one might think that resorting to more demanding tolerance values could be an alternative to provide stability to that region of the system. Nevertheless, this is not accurate. In fact, it would have the opposite impact in other operating regions where the scale of the cost would be too high to run the optimisation. In addition to the impact of the solver, when analysing the repercussion of varying the prediction horizon, it has been found that, in the proposed case-study, increasing the prediction horizon can be a way of reducing the economic cost. Still, as few scenarios were considered, the prediction window requires a more in-depth research. Building on the results discussed, it has been concluded that the best control strategy, which is to be analysed in the RCP system, is the adaptive MPC.

The implementation of the adaptive MPC in the experimental environment has proven that previous simulation results are consistent even in a real-time system. This means that, despite differences in the dynamics of the distinct variables, such as voltage or power, due to simplifications made during modelling, the final results obtained in this real-time analysis support the earlier findings on the usefulness of the adaptive MPC.

Finally, in relation to the control for the modular BESS, it is possible to conclude that such a strategy can take advantage of the adaptive MPC basis, after having analysed its performance. The scalability of the cost function will remain relevant in a system with several modules operating at different ageing rates. On top of that, the differences identified between the predicted battery states and those measured in the real-time system can pave the way for a better approach to the power sharing strategy. Accordingly, instead of determining a constant operating current, determining a power distribution ratio would facilitate adapting to any unforeseen phenomena or disturbances.

Chapter 5

MODEL PREDICTIVE CONTROL FOR MODULAR BATTERY SYSTEMS

The control of a modular BESS has traditionally built on low complexity level controls, relying mainly on power-sharing strategies based largely on heuristic methods. Nevertheless, examples such as the one in Chapter 4 illustrate that employing electro-thermal battery models in multi-agent systems can be functional and useful. Therefore, leveraging this knowledge, this section formulates a control strategy that allows to control a modular BESS. For this purpose, an ageing-aware MPC is formulated, where multiple agents now refer to the different modules that make up the BESS. To complete the analysis of this control, a comparison is made with an alternative control strategy in the literature, upon making the power distribution according to the nominal capacity of the module.

When it comes to developing a medium to large BESS, as described in Section 2.1.2.2, battery modules are assembled and then connected in series and parallel to fit the application characteristics. In considering these modular configurations, the literature has already reviewed a wide range of options for managing internal cell-to-cell differentials by designing an intra-module cell balancing system. Yet, when it comes to an inter-module management that operates as a secondary control layer, existing scholarly contributions have fallen short in analysing its great potential for improvement. By developing CBMs that allow the operating power of each module to be regulated independently, a new opportunity opens up to investigate new power-sharing strategies that could optimise system performance, while taking advantage of the qualitative benefits of such topologies.

Several authors have already identified the shortcoming of traditional modular systems and begun to propose forms of leveraging the potential of integrating CBMs in a BESS. One of the most widespread solution is based on applying a strategy, such as the one analysed by Mühlbauer et al. [138], where the power-sharing factor ratio is determined to be equal to the ratio between the capacity of each module and the entire BESS. Another example is the research of Frost et al. [19], in which the operation of the different modules is regulated on the basis of the SoC, with a decentralised control. The experimental findings from the intelligent battery demonstrate a 46% increase in the available capacity (from 97 Wh to 142 Wh) when using active loading/charging. Despite their additions to the field, these two approaches consider the operation of the battery only from a capacity point of view, disregarding the thermal behaviour of the battery. An example that presents a shift from aforementioned proposals is the study published by Altaf et al. [139], in which they introduce an MPC that aims not only to balance the SoC, but also the temperature of the different modules. By doing so, they achieve promising results for module degradation management, even with a single step MPC. Building in the preceding, yet endeavouring to gain greater control over the capacity loss of each of the modules, Rehman et al. [18] aim to equalise the SoH of all the CBMs, by modifying their operable SoC range according to their SoH or accessible capacity. As a result, the modular system can extend the lifetime of a battery pack by up to 40%.

Upon reviewing relevant contributions in the literature, it is evident that there is a lack of scholarly attention on the coupled electro-thermal and ageing model, as a means to minimise the capacity loss and the economic cost of a modular BESS, by resorting to a predictive control strategy. Exploring this gap in the academic research, throughout this chapter the control problem is formulated in order to improve the performance of each

CBM, and its analysis is conducted by running simulations. These simulation results are also compared with an example from the literature, which is considered in this case as a baseline, grounded on capacity-aware energy management [138, 140]. For the development of this research, the knowledge obtained previously in Chapter 4 is applied, by virtue of its importance to consolidate the insights on both the battery model and the MPC. Furthermore, results gathered are compared with the capacity-aware management in the literature.

5.1 CONTROL PROBLEM FORMULATION

Aiming to answer the main research question, while leveraging the knowledge acquired in Chapter 4, this section presents the proposed control algorithm to perform power-sharing in a modular BESS. This strategy is grounded on the model characterising the electrical and thermal features of the battery, together with its degradation and economic cost, which enables the formulation of an MPC algorithm to further improve the performance of the modular BESS.

First, however, in order to understand the operating bases of a control algorithm that is intended to manage several modules, regardless of their topology, it is necessary to refer to Equation 5.1a. This shows how the operating power of the entire battery P_{BESS} is distributed among the different modules, based on the power sharing factors, $\phi_{\text{BM},[m_s,m_p]}$, defined by the energy management algorithm. This allows determining the operating power of each module, $P_{\text{BM},[m_s,m_p]}$. When the sum of the $\phi_{\text{BM},[m_s,m_p]}$ is not equal to 1, this indicates that the module is not supplying all the power demanded by the application. In this analysis M_s and M_p refer to the amount of modules in series and parallel, while subindex m_s and m_p are used to identify each of the different agents.

$$P_{\text{BM},[m_s,m_p]}[k] = \phi_{\text{BM}[m_s,m_p]}[k] \cdot P_{\text{BESS}}[k] \tag{5.1a}$$

$$s.t. \quad \sum_{m_s=1}^{M_s} \sum_{m_p=1}^{M_p} \phi_{\text{BM},[m_s,m_p]}[k] = 1 \tag{5.1b}$$

That being said, Equation 5.1a does not account for any type of constraint related to the different modular structure topologies presented in Section 2.1.2.2. CMB parallelisation is beneficial from a controllability point of view, however, it is known that serialising is necessary for certain high voltage applications. Thus, combined topologies should be

acknowledged by the designed control system. Accordingly, it is necessary to factor the operating constraint (Equation 5.2) established by the application voltage, where the sum of the voltage V_{BESS} of each serialised module set V_{m_s}, must be equal to the application voltage V_{system}.

$$V_{\text{system}}[k] = V_{\text{BESS}}[k] = \sum_{m_s=1}^{M_s} V_{\text{BM},m_s}[k] \tag{5.2}$$

In the following, on the one hand, an example of energy management for modular batteries, better known as "capacity-aware control", is presented; and, on the other hand, the adaptive MPC is introduced, enabling the optimisation of the operation of the modular BESS.

5.1.1 Capacity-aware control

This is a control strategy already reviewed in the literature [138,140], that is characterised by focusing its operation on identifying the nominal capacity of each of the modules. Subsequently, by means of the capacity ratio of each module with respect to that of the modular BESS shown in Equation 5.3, and considering any constraints that may be required, a power sharing strategy can be formulated for determining the value of ϕ, presented in Equation 5.1a.

$$\phi_{\text{BM},[m_s,m_p]}[k] = \frac{C_{\text{nom},[m_s,m_j]}[k]}{\sum_{m_s=1}^{M_s}\sum_{m_p=1}^{M_p} C_{\text{nom},[m_s,m_p]}[k]} \tag{5.3}$$

5.1.2 Adaptive model predictive control

In proposing the adaptive MPC that allows the optimal operation of a modular BESS, the analysis previously conducted in Section 4.1 has been the baseline. In light of this research, and accounting for u_{BM} the electrical current of each module, $\boldsymbol{J}_{\text{BM}}$ the economic cost of operating every module, and α the adaptive scaling factor, a quadratic cost function has been formulated, as shown in Equation 5.4. By means of this cost function it is possible to use an MPC to determine the optimal operating condition of each module.

$$\min J(u[k]) = \sum_{k=0}^{N_p}\sum_{m_s=1}^{M_s}\sum_{m_p=1}^{M_p} \boldsymbol{J}^T_{\text{BM},[m_s,m_p]}[k] \cdot \alpha^2_{[m_s,m_p]}[k] \cdot \boldsymbol{J}_{\text{BM},[m_s,m_p]}[k] \tag{5.4}$$

Still, this control algorithm sets the operating current of each module, when the Equation 5.1a requires power sharing ratios for each of the units. Therefore, it is mandatory to apply the Equation 5.5 to the results obtained on the basis of Equation 5.4.

$$\phi_{\mathrm{BM},[m_s,m_p]}[k] = \frac{v_{\mathrm{BM},[m_s,m_p]}[k] u_{\mathrm{BM}[m_s,m_p]}[k]}{\sum_{m_s=1}^{M_s} \sum_{m_p=1}^{M_p} v_{\mathrm{BM},[m_s,m_p]}[k] u_{\mathrm{BM},[m_s,m_p]}[k]} \tag{5.5}$$

Finally, Equation 5.6a allows the calculation of the scaling factor α of this cost function. The calculation of this term is based on Equation 4.10 and all related knowledge. For this case, however, as it is not a single battery unit, more factors are to be taken into account.

First, having several battery units, it is necessary to calculate the evolution of the factors γ_1, γ_2 and γ_3. This allows the scaling factor for each of the modules to be identified. When applying these values in the cost function of the Equation 5.4, though, as they have different values, the problem would not scale proportionally for each module.

Second, in using a single equal scaling value for all modules, if this is too high or too low, it can cause the use of α to end up being counterproductive. A high value may be useful for older modules but may negatively impact a newer module overscaling it, and vice versa. In fact, scaling the problem based on a newer module may generate oscillations in the operation of older modules, as explained in Chapter 4.

Three, other considerations to note are the values set for the τ, φ_{Ch} and φ_{Tot} in Equations 5.6b, 5.6c and 5.6d. As for τ, its value is determined by the discrete time-step of the case-study. Nevertheless, φ_{Ch} and φ_{Tot} are two factors that must be set on the basis of the approximate capacity variation that is intended, or expected, to be observed by the controller in each optimisation. In this case, the value of both factors is defined to be equal to 1% of the nominal capacity.

With these three factors considered, the Equation 5.6a is formulated for the calculation of α, where, using average values ($\overline{\gamma}_1$, $\overline{\gamma}_2$, and $\overline{\gamma}_3$), a balance between the different γ of the modules is sought.

$$\alpha_{[m_s,m_p]}[k] = \lambda_2[k] \cdot \max\left(\overline{\gamma}_{1,[m_s,m_p]}[k], \overline{\gamma}_{2,[m_s,m_p]}[k], \overline{\gamma}_{3,[m_s,m_p]}[k]\right) \tag{5.6a}$$

$$\gamma_{1,[m_s,m_p]}[k] = \frac{\left(\frac{\tau}{3600}\right)^{0.5}}{\left(\frac{t_{[m_s,m_p]}+\tau}{3600}\right)^{0.5} - \left(\frac{t_{[m_s,m_p]}}{3600}\right)^{0.5}[k]} \tag{5.6b}$$

$$\gamma_{2,[m_s,m_p]}[k] = \frac{{\Delta\varphi_{\mathrm{Ch}}}^{0.5}}{\left(\varphi_{\mathrm{Ch},[m_s,m_p]}[k] + \Delta\varphi_{\mathrm{Ch}}\right)^{0.5} - \varphi_{\mathrm{Ch},[m_s,m_p]}[k]^{0.5}} \tag{5.6c}$$

$$\gamma_{3,[m_s,m_p]}[k] = \frac{\Delta\varphi_{\text{Tot}}{}^{0.5}}{\left(\varphi_{\text{Tot},[m_s,m_p]}[k] + \Delta\varphi_{\text{Tot}}\right)^{0.5} - \varphi_{\text{Tot},[m_s,m_p]}[k]^{0.5}} \tag{5.6d}$$

$$\lambda_2[k] = \gamma_4^{1+\tanh\left(10\cdot\left(15-\overline{T}_{\text{amb},[m_s,m_p]}[k]\right)\right)} \tag{5.6e}$$

The calculation of α also includes a fourth term to be taken into account, λ_2. This term, initially introduced as an extra control tuning factor, determined through heuristic knowledge and a series of tests in simulation, has evolved to the form of the Equation 5.6e. Accordingly, if the battery is not operated at high temperatures, especially during discharge processes, a better scaling of the cost function is obtained, and, in turn, a better performance of the BESS module is achieved (γ_4 is considered to be 3).

5.2 SIMULATION SETUP

5.2.1 Case-study data

For the analysis of the control strategy presented in Section 5.1, the following case-study has been defined. This overview outlines the various general conditions pertaining to the application - power and temperature - under which the battery is operated, in order to compare the results of the adaptive MPC with the capacity-aware management.

For this purpose, a power profile with which to compare the performance of both controls has first been determined. In light of a hierarchical control structure for modular batteries (Section 2.2), and assuming that the primary or intramodule control layer is already considered when modelling a battery module, it is a matter of formulating the tertiary level management that determines the overall power flow between the application and the modular BESS. This is the power flow that will subsequently be the input to the secondary control layers introduced in the previous section. Since it is not within the scope of this thesis, for the design of this tertiary level of control, the simple, yet functional, solution shown in the flow chart in Figure 5.1a has been suggested. This input power profile for the tertiary control level is based on 11 consecutive, 1 hour charge, 1 hour discharge and 15 minutes rest periods, being the overall charged and discharged energy equal to the 60% of the nominal energy of the modular BESS.

In view of the preceding, with the control strategy presented in 5.1, there are two paths of analysis:

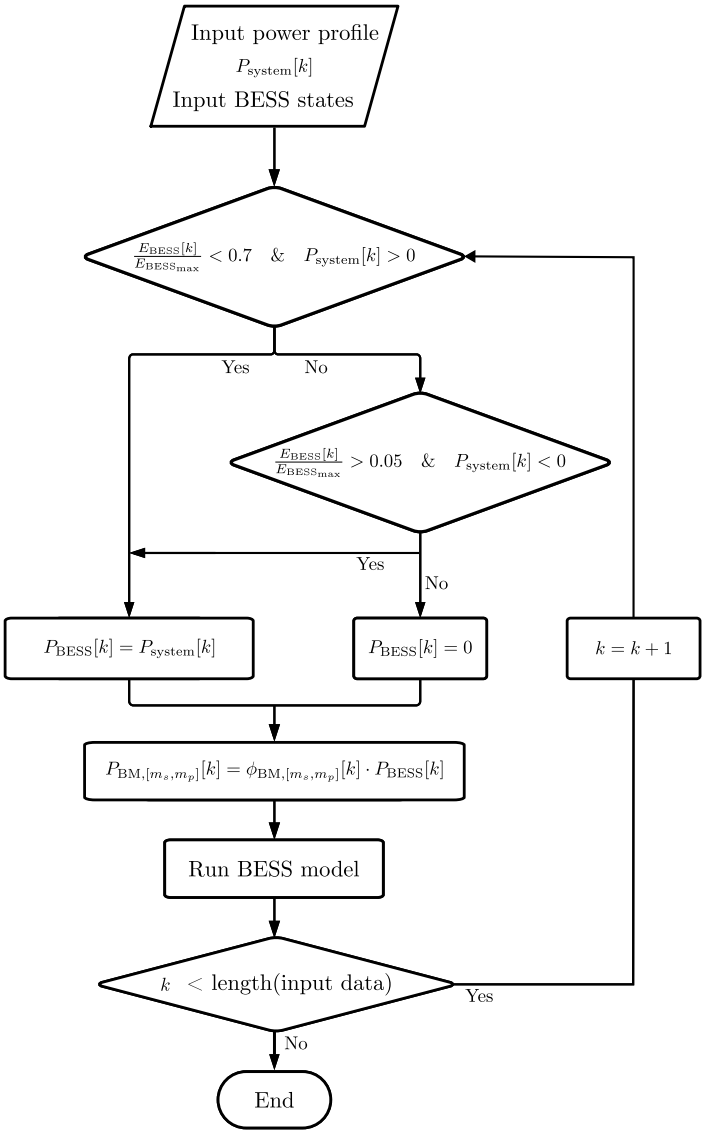

(a)

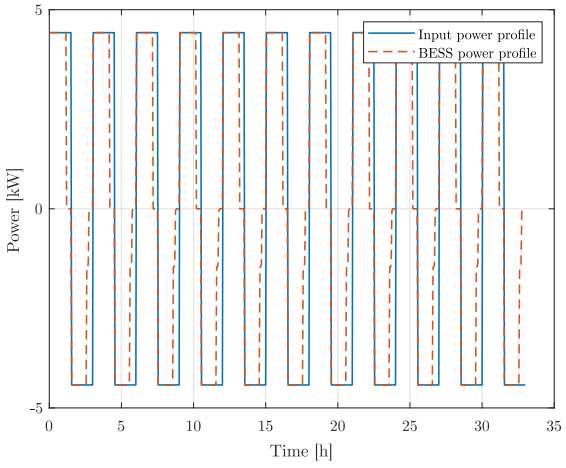

(b)

Figure 5.1: Power profile generation for the modular BESS case-study: a) Flow chart of the tertiary control level, and b) Input power profile of the case-study.

- **Option 1:** First a combination of tertiary control and capacity-aware management has to be analysed. In so doing, there is a power profile for the baseline case, which is, later on, used as the input power profile of the adaptive MPC. This allows a comparison of both controls under the same operating profile, as long as the efficiency of the batteries does not become decisive.
- **Option 2:** The tertiary control level is applied independently to each one of the control algorithms. Although in this case it is also possible to compare the results of both cases, the evolution of the stored energy may reveal different dynamics, making it difficult to compare the two cases.

Between these two options, the first alternative has been chosen with the aim of analysing the impact of operating the same power profile from an economic point of view, as well as from an efficiency perspective. When choosing option 1 it also has to be taken into account that this is the only of the alternatives that enables the straightforward use of the predictive control strategies.

Additionally to the operating power, the ambient temperature conditions are to be determined. Their different values can be decisive for the operation of the battery in one way or another. As per this analysis, three different ambient temperatures have been considered: 5 °C, 25 °C, and 45 °C.

5.2.2 Battery initialisation

With the case-study in place, the subsequent step is to determine the characteristics of the modular BESS. In this instance, it is a modular system based on three modules connected in parallel that require output power control. Both the cell and module models are presented in Chapter 3, and the dimensions of each of the three units are the same as the one already introduced in Section 4.2.2, with an energy of 2.5 kWh (16P16S cell configuration). As for the economic cost model of the BESS, the starting investment is determined to be of 700 $ per module (350 $/kWh, this is a general approach that has been determined for this research) [133–135], and the EoL is met when the SoH of the cell is below 60% of its BoL value. Upon this data set, battery initialisation is performed under the five same premises that have been presented in Section 4.2.2 for the cases set in Table 5.1.

the initial investment is assumed to be of 700 $ (350 $/kWh, this is a general approach that has been determined for this research) [133–135]

Table 5.1: Battery initialisation parameters at different ageing stages for modular BESS analysis.

Parameters	Day 1	Week 1	Month 1	Month 6	Year 1
Ah_{Ch} [Ah]	3	21	90	480	1080
Ah_{Tot} [Ah]	6	42	180	960	2160
time [h]	24	168	720	4320	8640
SoC [-]	0.05	0.05	0.05	0.05	0.05
SoH [-]	1	1	1	1	1

With a view to extending the analysis of the performance of adaptive MPC vs capacity-aware control, differences have been generated among the different characteristics of the modular BESS. Each of them has been analysed independently, under the different conditions of the Table 5.1, and presented below:

- **Balanced modular BESS:** In this instance, the three modules have exactly the same electro-thermal, degradation and cost characteristics.
- **Ageing unbalanced modular BESS:** While the electro-thermal, degradation and cost model remain the same, modules are unbalanced considering that, after a year, one of the three modules fails and gets replaced by a new one. As per this, for analysis, the new cell presents the values of Table 5.1, while the two most degraded cells have a one-year head start.
- **Cost unbalanced modular BESS:** The sole difference between the two first modules and a third is considered to be the cost. The latter agent has a 50% higher cost.
- **Temperature unbalanced modular BESS:** The models of the three modules in this case are the same. Yet, each of them is considered to operate under different ambient temperatures. Precisely, one is at general ambient temperature, another five degrees below, and the third one five degrees above.
- **Capacity unbalanced modular BESS:** This scenario considers that one of the three modules has a 5% lower nominal capacity, while all other characteristics of the cell/module model remain the same for all three modules.

Once the input data concerning the case-study has been provided and the initial conditions, as well as premises, have been defined, the following section outlines the features of the MPC algorithm.

5.2.3 Control settings

With the case-study and module data already defined, the last step in analysing the performance of the control problem, formulated in Section 5.1, is to draw on the control settings presented below. In this instance, as it is a non-linear and non-convex optimisation problem due to the characteristics of the cell model, it is opted to resort to the solver IPOPT using YALMIP [20]. In addition to the solver, more control characteristics, shown in Table 5.2, are needed to be determined for optimisation. On the one hand, there is the step-time discretasitaion, which in this case is set at 3 minutes. To calculate the maximum duration of the optimisation, this same value has been determined. On the other hand, the prediction horizons considered for this analysis are N_p equal to 2 and 5, which is equivalent to 6 or 15 minutes of prediction window. Finally, optimisations are presented using the initial guess, which means that each optimisation considers the current values previously obtained for its initialisation. Additional information on solver tolerances and hardware devices can be found at Table 5.2.

Table 5.2: Optimisation problem settings for the analysis of the modular BESS.

Parameters	Value
Optimisation solver	IPOPT
Prediction horizon (N_p)	2 and 5
Optimisation step time	3 minutes
Initial guess	Yes
Maximum iterations	5e4
Maximum CPU time	3 minutes
Optimal solver tolerance	1e-16
Acceptable solver tolerance	1e-8
CPU	AMD Ryzen 7 7800X3D 4.2 GHz
RAM	32.0 GB

5.3 SIMULATION RESULTS AND DISCUSSION

5.3.1 Balanced modular battery systems

In this section, results obtained in analysing the operation of modules with the same electro-thermal, degradation and cost conditions are displayed. To perform this analysis, a

comparison between the two control strategies presented in Section 5.1 is proposed. In this regard, the initialisation data required for these simulations are illustrated in Section 5.2.

Figures 5.2 and 5.3 present the dynamics of the results obtained for a simulation where N_p=2 and the lifetime is equal to month 6 from Table 5.1. From these it is possible to determine that both the adaptive MPC and the capacity-aware control have identical dynamics. In the two cases, the power is distributed almost identically amongst the modules, although there may be a slight difference for the adaptive MPC as a consequence of the relaxation of the constraints or errors in the solver (see Appendix B). Accordingly, the same power in all the modules implies that the evolution of the electro-thermal and ageing states of the batteries follow the same form. In analysing the dynamics, in the case of the adaptive MPC, it is also interesting to look at the evolution of the solver diagnostics. As shown in Figure 5.4, for this case-study, except in some specific cases, the optimisation is able to solve the problem correctly, with the diagnostics being equal to zero.

If special attention is drawn to the economic cost, the objective of the cost function, its dynamics and final value, all shown in Figure 5.3d, it becomes apparent that there is no significant variation. In fact, the minimal difference that may exist between the results of the two cases, mainly due to the power soft-constraint, presents a dynamic that progresses on a much smaller scale, so that the relevance of this cost difference will get closer and closer to zero.

Finally, when analysing Figures 5.5 and 5.6, it is possible to observe the impact of the adaptive MPC under different temperatures (5°C, 25°C and 45°C) and prediction horizons (N_p=[2;5]) of operation. By analysing these figures, the results suggest that, in case of having modules with the same conditions, a higher prediction horizon does not provide any decisive improvement from an economic point of view. Regarding the results obtained under different thermal conditions, it is observed that as the operating conditions become more severe - lower or higher temperatures - the adaptive MPC continues to perform reasonably well with the modular BESS. If the cost difference percentage is analysed, its mean variation taking into account these 30 simulation - at different prediction horizons, temperatures and ageing conditions - equals 0.06%. Therefore, from an economic point of view, none of the both controls is an option that should be discarded.

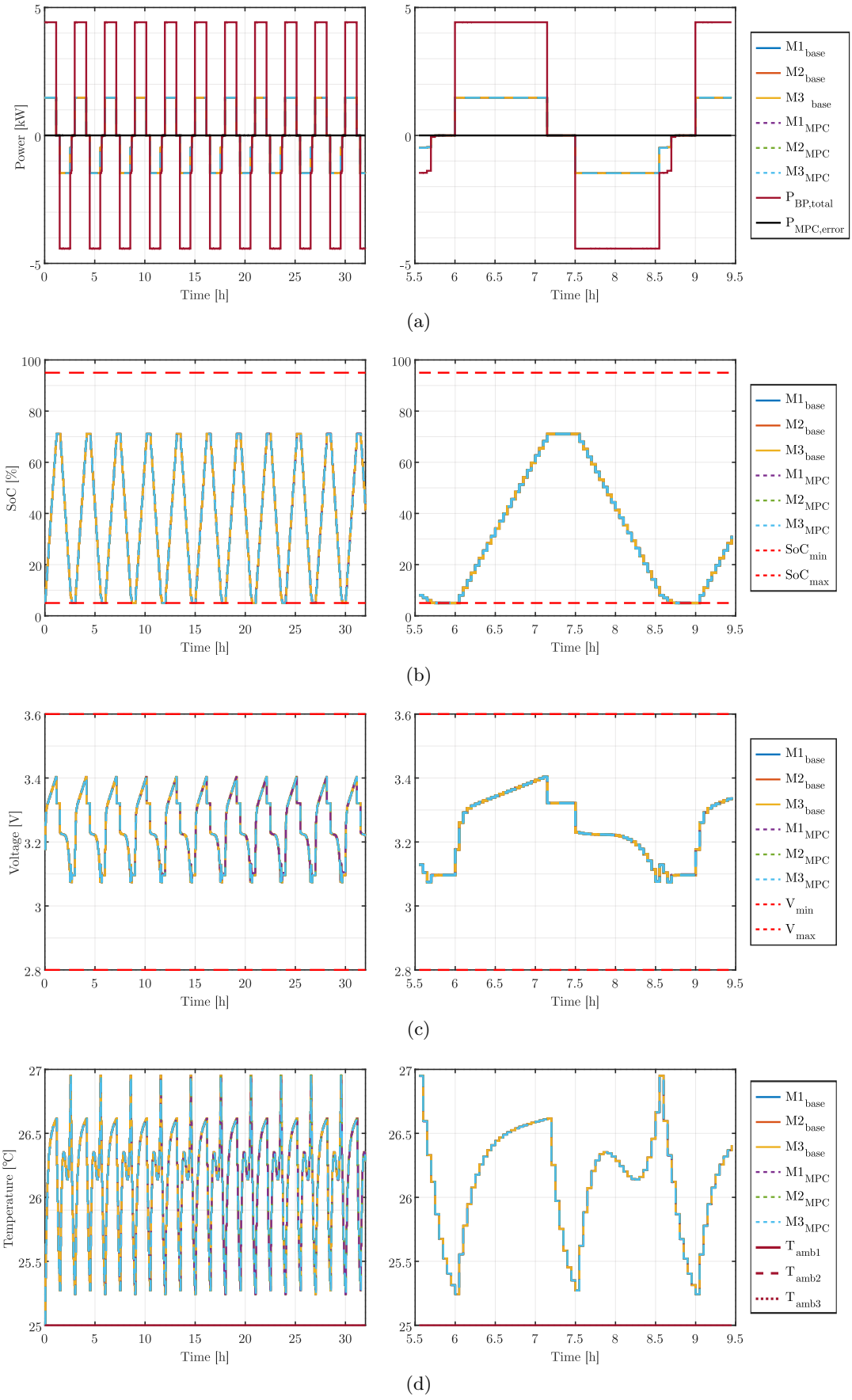

Figure 5.2: Balanced battery system in modular BESS management at month 6: a) Module power, b) Module SoC, c) Cell voltage, and d) Module voltage.

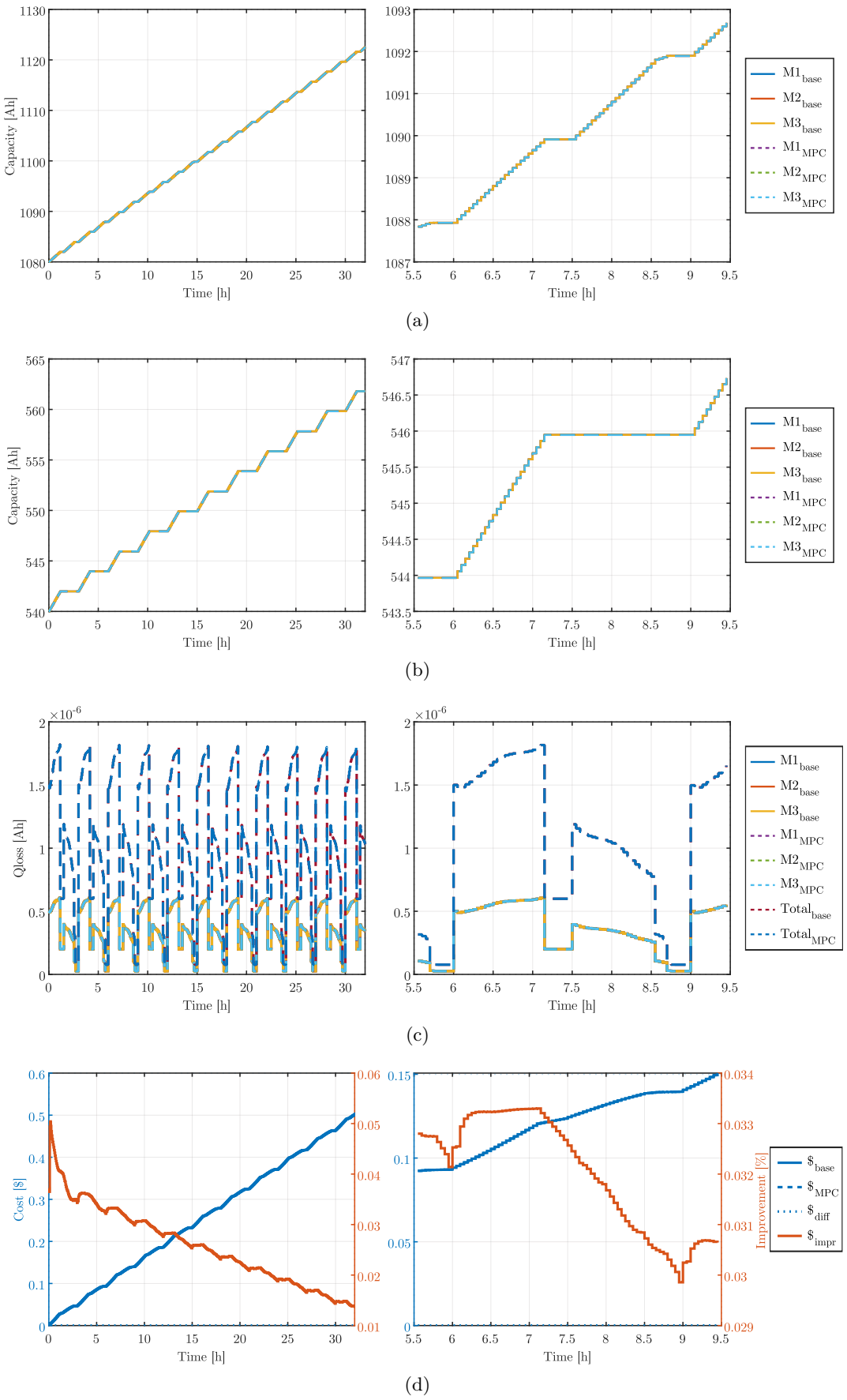

Figure 5.3: Balanced battery system in modular BESS management at month 6: a) Overall cell capacity, b) Charged cell capacity, c) Cell level capacity loss, and d) System level cost.

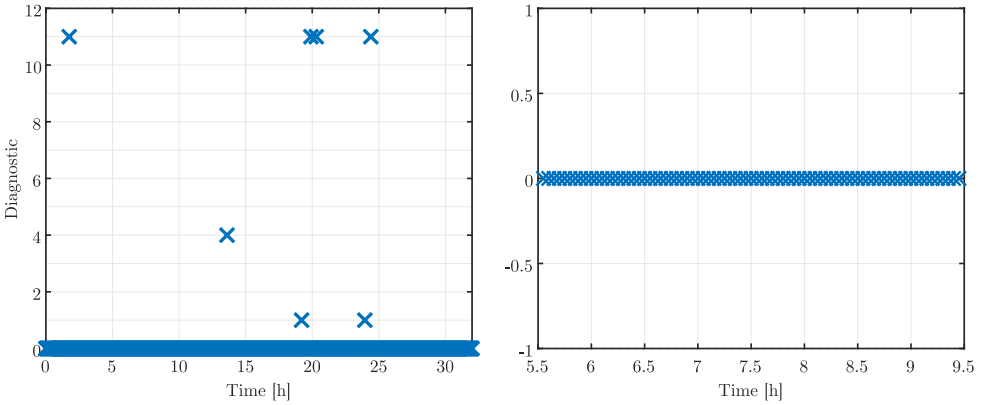

Figure 5.4: Optimisation diagnostics in a balanced modular BESS at month 6.

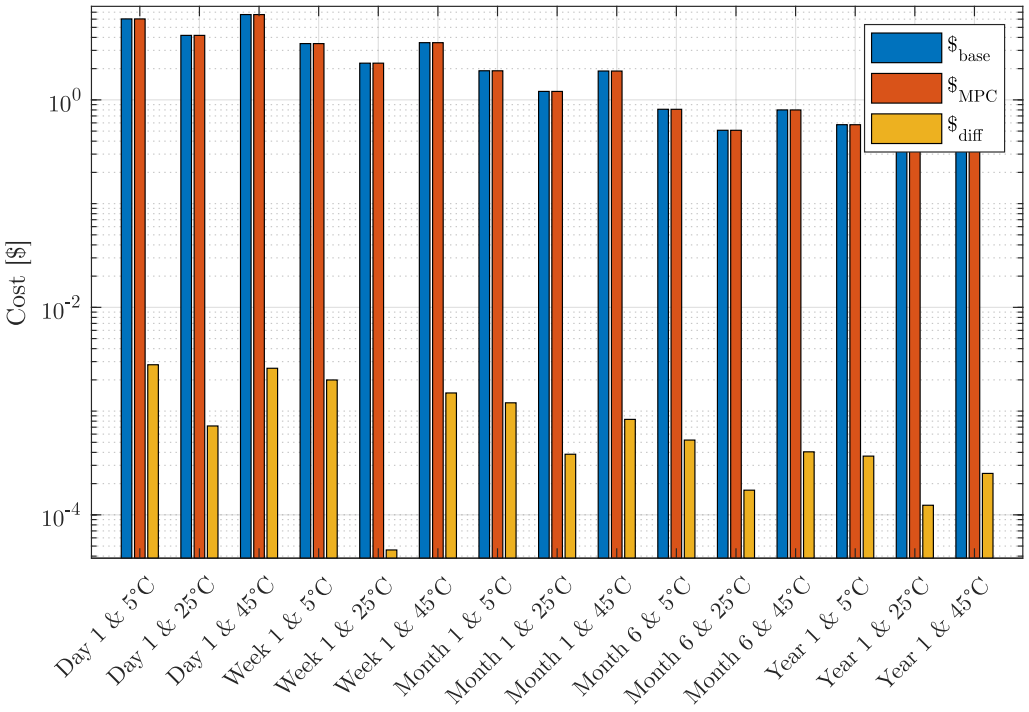

Figure 5.5: Economic cost in a modular BESS case-study with balanced battery capacity at different lifetime and temperature conditions with $N_p = 2$.

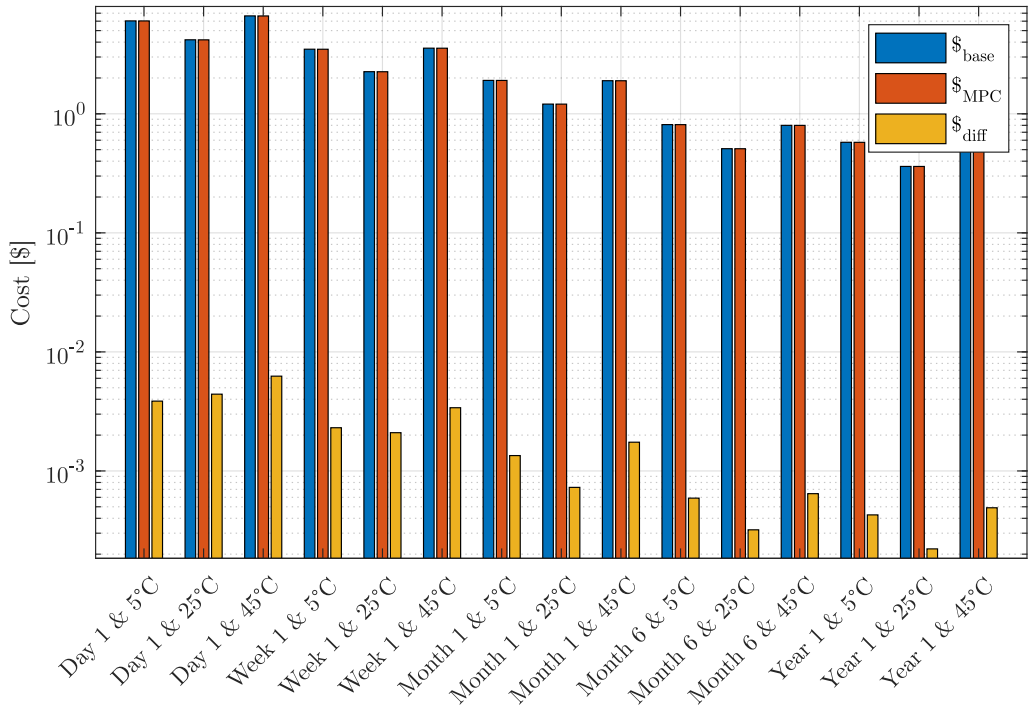

Figure 5.6: Economic cost in a modular BESS case-study with balanced capacity at different lifetime and temperature conditions with $N_p = 5$.

5.3.2 Ageing unbalanced modular battery systems

This section presents the results obtained from the analysis of the findings observed during the operation of modules, having the same electro-thermal and cost characteristics, yet under different degradation conditions. These initialisation characteristics are available in Section 5.2. Further analysis shows, moreover, the comparison between the capacity-aware control and the adaptive MPC presented in the Section 5.1.

Figures 5.7 and 5.8 display the dynamics of the values obtained for a simulation of N_p=2 and the battery lifetime at month 6. From these data, it is possible to identify that there is a clear difference between the dynamics established by the two control algorithms. Regarding the capacity-aware control, as the nominal capacity of the three modules remains equal the power is distributed equally among the three modules. In the case of adaptive MPC, however, having batteries in different states of life, the way they operate is far from equal. Dynamics of the two most degraded modules have the same values in all their operating states, while the third one participates in a more reserved way, especially during discharge, and, thus, its operation shows different battery states. The rationale for the above is identified by analysing Figure 5.8c, where it can be noticed that the adaptive MPC, in contrast to its alternative, tries to equalise the ageing-rate of the three

modules. This implies that, if operating under the same conditions, the newer module has a higher ageing-rate, and therefore, its use should be more limited. During periods where the dynamics of the aged modules are bounded by the control constraints, instead, greater use is made of the newer module.

That said, the strategy of operating the modules heterogeneously is not without its drawbacks, as it has a worse energy efficiency. Figure 5.7a is indicative of this, since it shows that there is a period where the BESS is not able to supply the energy demand when the same baseline charging and discharging power profile is applied. This is so because the adaptive MPC is not capable of forecasting that the increased economic benefit may result in not being able to meet the demand set by the case-study. Although to a lesser extent, soft-constraints also affect the non-compliance with the power profile.

As for the results related to the diagnostics of the optimisation of the Figure 5.9, it is observed that there is a period where the solver is not able to determine an optimal control setpoint. Further, in a large number of cases, this phenomenon is coinciding with the instants where the sign change of the power occurs, and, as a consequence, the diagnostic indicates that the optimisation is infeasible (diagnostic equal to 1). For all these instances, it is necessary to apply the error management of Appendix B, so the advantage of an adaptive MPC is not so much impaired by the optimisation errors.

Figure 5.8d calls for special attention as it compares the economic result of the adaptive MPC with the cost of capacity-aware control. The dynamics indicate that the total balance, at the end of each charging and discharging cycle, favours economic savings, reducing the cost around 3%. Nonetheless, the lack of prediction horizon and the optimisation errors during its development prevent the trend from always being positive.

At last, looking at Figures 5.10 and 5.11, the impact of the adaptive MPC under different temperatures (5°C, 25°C and 45°C) and prediction horizons (N_p=[2;5]) can be observed. The analysis of these figures, where ageing differences between modules are taken into account, makes it clear that a higher prediction horizon does not show any significant improvement from an economic perspective. Nevertheless, if the results gathered under different thermal conditions are compared, it is found that as the operating conditions escalate in severity - lower or higher temperatures - the adaptive MPC keeps maximising the utility of the modular BESS. If the cost difference percentage is analysed, its mean variation taking into account these 30 simulation - at different prediction horizons, temperatures and ageing conditions - equals 17.82%. Hence, the adaptive MPC is beneficial over the baseline in any of the scenarios analysed.

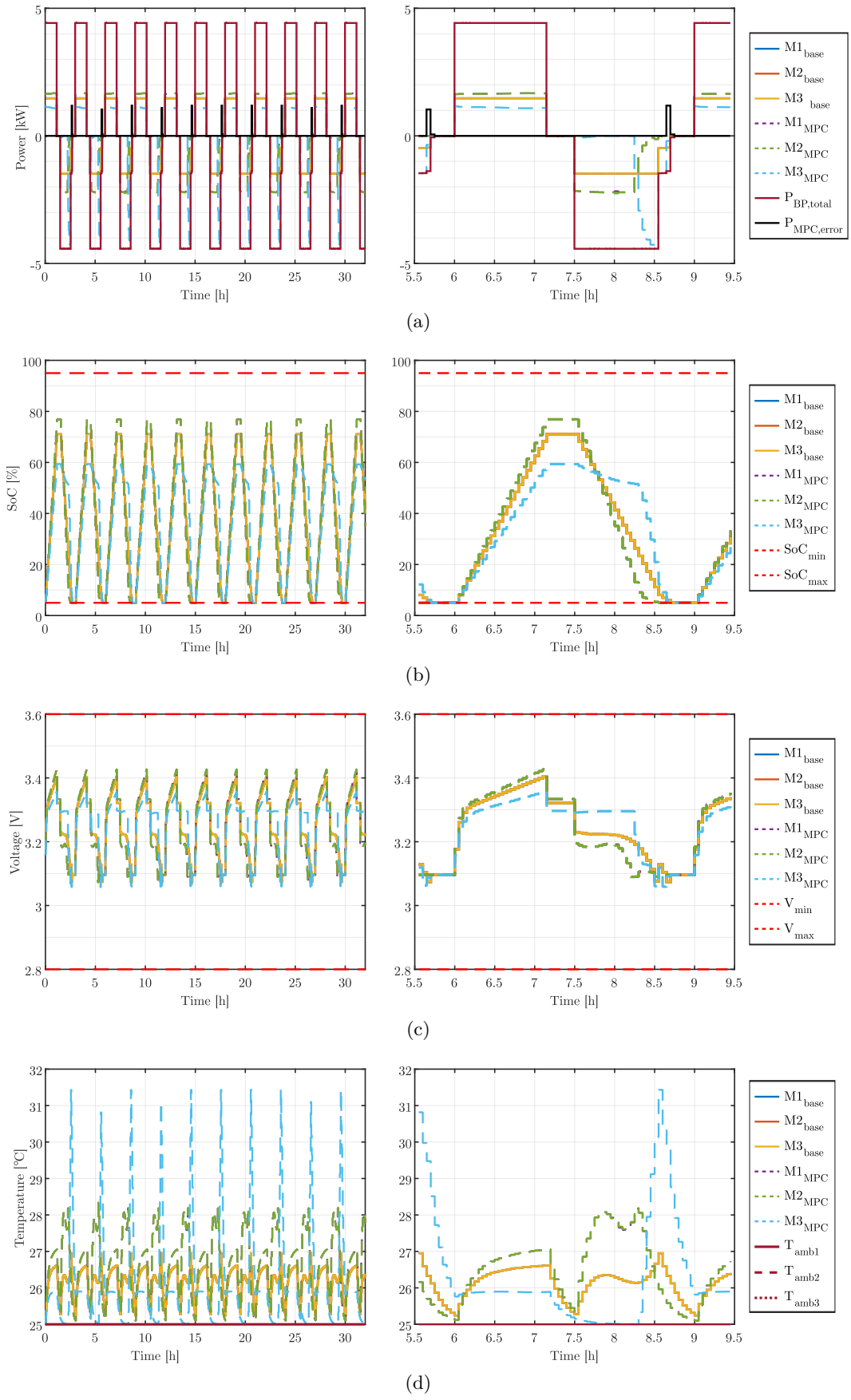

Figure 5.7: Unbalanced battery ageing in modular BESS management at month 6: a) Module power, b) Module SoC, c) Cell voltage, and d) Module voltage.

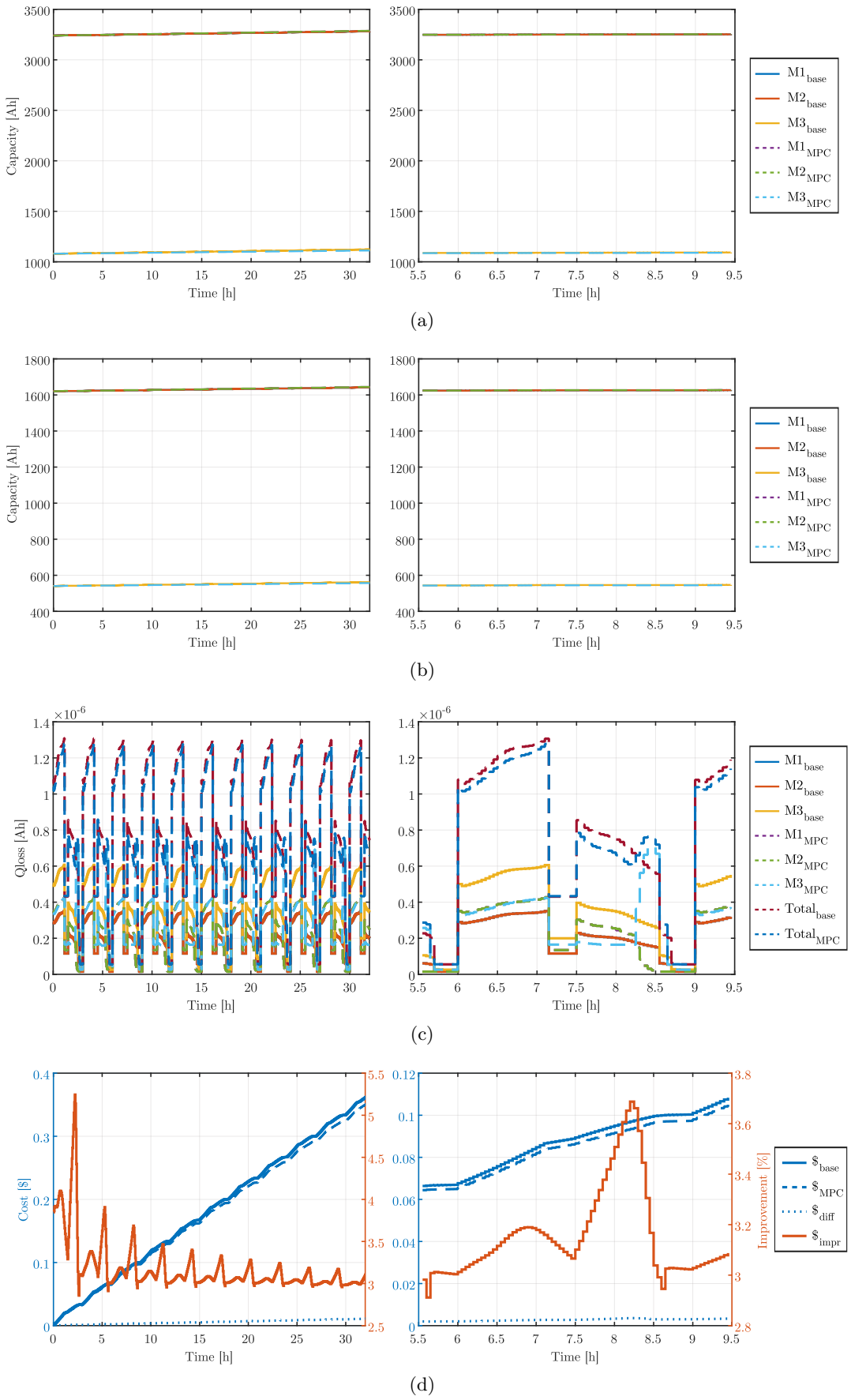

Figure 5.8: Unbalanced battery ageing in modular BESS management at month 6: a) Overall cell capacity, b) Charged cell capacity, c) Cell level capacity loss, and d) System level cost.

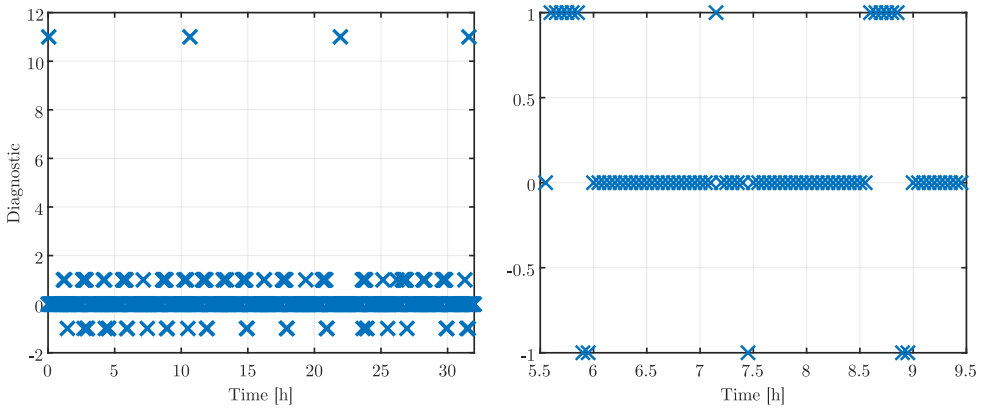

Figure 5.9: Optimisation diagnostics in a modular BESS with unbalanced battery ageing at month 6.

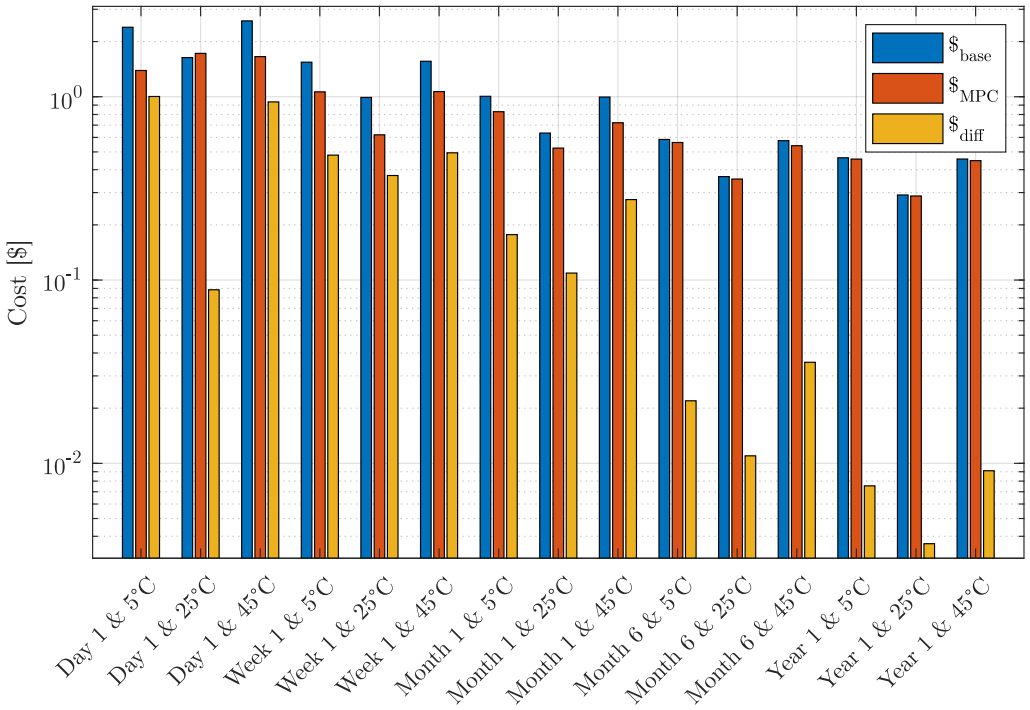

Figure 5.10: Economic cost in a modular BESS case-study with unbalanced battery ageing at different lifetime and temperature conditions with $N_p = 2$.

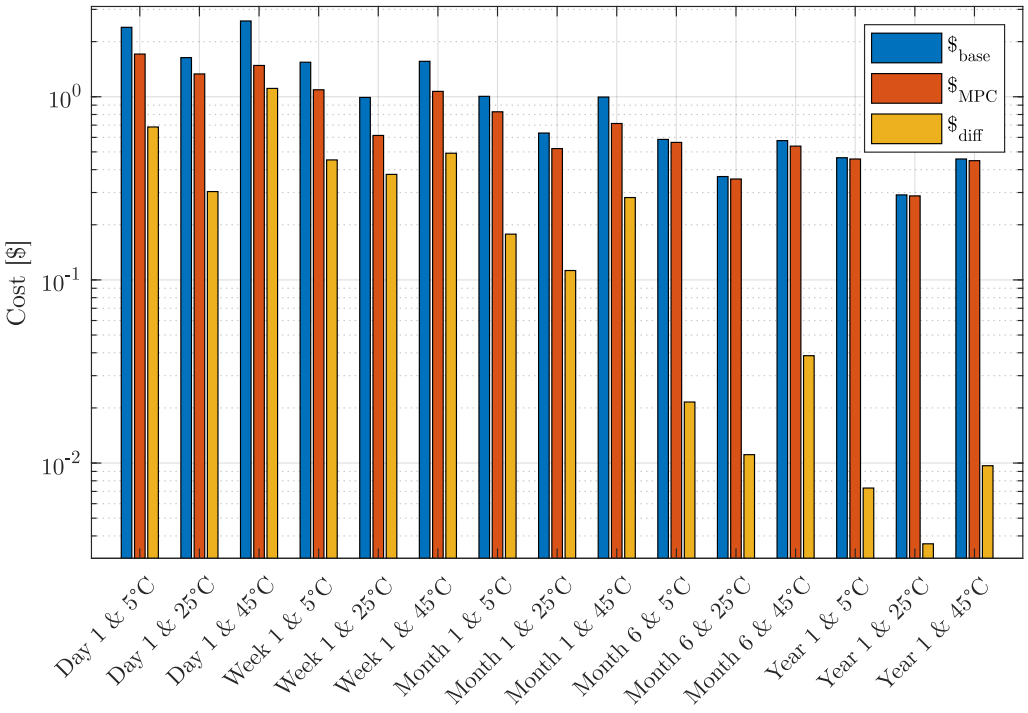

Figure 5.11: Economic cost in a modular BESS case-study with unbalanced battery ageing at different lifetime and temperature conditions with $N_p = 5$.

5.3.3 Cost unbalanced modular battery systems

This section, as implied by its name, presents the results obtained in analysing the findings generated by operating modules which, despite having the same electro-thermal and degradation conditions, diverge in terms of economic cost. These data have already been presented in Section 5.2. This analysis compares the two control strategies presented in Section 5.1.

Figures 5.12 and 5.13 depict the dynamics of the findings inferred for a simulation of N_p=2 and the lifetime at month 6. In these, a clear difference can be identified between the dynamics established by the two control algorithms. As for the capacity-aware control, the power is distributed equally among the three modules and, consequently, having identical initial electro-thermal and ageing conditions, the evolution of the different battery states is the same. By contrast, in the case of the adaptive MPC, having CBMs with different economic costs, the way of operating them is far from being equal. The dynamics of the two cheapest modules have the same values in all their operating states, while the third one performs in a rather reserved capacity, especially during discharge. The cause underlying these trends lies in Figure 5.13c, where it appears that the adaptive MPC, unlike its alternative, strives to generate differences in the ageing-rates of the modules with the aim

of balancing the cost-rate. In fact, it is interesting to note that the control favours a higher capacity loss in order to meet its objective. During periods where the dynamics of the cheaper modules are bounded by the control constraints, the only solution is to resort to the more expensive module.

With the strategy of operating the modules based on the adaptive MPC, however, the energy efficiency of operating the modular BESS is reduced. As shown in Figure 5.12a, this comes about because, at certain time periods, the BESS is not able to supply the same power profile that is applied to the capacity-aware management strategy. The main reason is related to the lack of prediction horizon to anticipate the impact of BESS efficiency. In a lesser extent, but the power soft-constraint also influences the results.

Regarding the outcomes on optimisation diagnostics presented in Figure 5.14, it can be observed that there is a period in which the solver is not capable of finding an optimal result. In a high number of instances, this phenomenon matches the moments in which the sign change of the power takes place, resulting in an unfeasible optimisation (diagnosis equal to 1). The error management of Appendix B must be applied for all these scenarios, with a view to ensuring that the advantage of an adaptive MPC is not so adversely affected by optimisation errors.

Figure 5.13d requires close attention in comparing the economic result of the adaptive MPC with the cost of capacity-aware control. The dynamics suggest that the overall balance after each charge and discharge cycle is conducive to economic savings.

To conclude, upon examining Figures 5.15 and 5.16, the impact of the adaptive MPC under different temperatures (5°C, 25°C and 45°C) and prediction horizons (N_p=[2;5]) of operation can be assessed. From the analysis of these figures it can be noted that, if there are cost differences between modules, a higher prediction horizon fails to yield any determining improvement in cost. However, if results obtained from various thermal conditions are examined, it is noted that as the operating conditions become increasingly challenging - lower or higher temperatures -, the adaptive MPC leverages the modular BESS more efficiently, especially at higher temperatures. If the cost difference percentage is analysed, its average variation taking into account these 30 simulation - at different prediction horizons, temperatures and ageing conditions - equals 2.58%. As such, the utility of the adaptive MPC appears to be favourable under any of the considered settings.

5.3.4 Temperature unbalanced modular battery systems

This section analyses the results obtained during the simulation of modules with the same electrical, degradation and cost conditions, albeit with different thermal conditions. In this case, a scenario where each of the modules operates under different ambient temperature conditions is considered. Further details on these data are available in Section 5.2. This analysis provides a comparative analysis between the two control strategies introduced in Section 5.1.

Figures 5.17 and 5.18 display the dynamics of the results obtained for a simulation of N_p=2 and the battery lifetime at month 6. From them it is possible to identify that, regardless of whether the modules operate under the same ratio of the total power or not, the evolution of all the battery states is heterogeneous. This difference is especially accentuated when, during discharge with the adaptive MPC, the operation of any of the modules is limited by the operating constraints at different moments. This is so because, at discharge time, higher temperatures become more critical from a cost point of view, and, therefore, the adaptive MPC attempts to avoid their usage as long as it is not strictly necessary. Its impact is seen in the sudden dynamics depicted in Figure 5.18c, which may be a consequence of an insufficient prediction horizon.

With the strategy of operating the modules with the adaptive MPC, however, the energy efficiency of operating the BESS is again reduced. Figure 5.17a is indicative of this, since at the end of each discharge it is not able to supply the energy demand, which is not the case with capacity-aware control. This arises from the fact that the prediction window of the adaptive MPC is not able to contemplate the impact beyond its prediction horizon. In a lesser extent, but the power soft-constraint also influences the results.

As for the diagnostics of the optimisation, Figure 5.19 points out that, whenever the BESS approaches a period with a change of sign of the power, the algorithm has convergence issues. Such challenges may render the problem infeasible (diagnostic equal to 1). The error management of Appendix B must be applied for all these scenarios, with a view to ensuring that the advantage of an adaptive MPC is not so adversely affected by optimisation errors.

Figure 5.18d requires special attention. It shows the evolution and the final value of the economic cost. In this case it is possible to identify a favourable economic cost trend for the adaptive MPC.

Finally, in examining Figures 5.20 and 5.21, the impact of the adaptive MPC under different temperature (5°C, 25°C and 45°C) and prediction horizons (N_p=[2;5]) of operation

can be monitored. It becomes clear from the analysis of these figures that a higher prediction horizon does not lead to any major improvement in cost. Yet, if results under different thermal conditions are analysed, it is remarkable that as the operating conditions grow more severe - lower or higher temperatures - the adaptive MPC optimises the use of the modular BESS, especially at low temperatures. If the cost difference percentage is analysed, its average variation taking into account these 30 simulation - at different prediction horizons, temperatures and ageing conditions - equals 2.09%. Consequently, the utility of the adaptive MPC turns out to be beneficial under any of the discussed scenarios.

5.3.5 Capacity unbalanced modular balanced systems

This section analyses the results obtained in the simulation of modules with the same thermal, degradation and cost conditions, yet different in terms of electrical characteristics. In this particular case, a scenario in which one of the modules operates with a 5% lower nominal capacity is considered. More details on these data are available in Section 5.2. This analysis draws a comparison between the two control strategies presented in Section 5.1.

Figures 5.22 and 5.23 show the dynamics of the results obtained for a simulation of N_p=2 and the lifetime at month 6. They indicate that, while the adaptive MPC opts for a similar power distribution for the three modules, which only causes notable divergences in the SoC, the capacity-aware management generates a heterogeneous power distribution equalising the SoC values, although not the temperature values. On the contrary to the previously analysed scenarios, though, by operating the modules in a balanced way, the SoC constraints limit the operation of the three modules at the same instant. Any scenario with aggressive charging and discharging dynamics that could increase the cost of operating the BESS is therefore avoided. When analysing the results and the feasibility of the adaptive MPC, the correct operation of the optimisation depicted in Figure 5.24 must also be considered. Interpretation of these results indicates that, while operating the modules with different nominal capacity may generate some convergence issues, this is an isolated phenomenon, as most solver diagnostics indicate correct operation.

Figure 5.23d demands careful consideration. It provides the evolution and the final value of the economic cost. In this case it is possible to identify a favourable trend for the adaptive MPC, although it should be noted that the scale of the benefit is at least two orders of magnitude lower.

At last, on analysing Figures 5.25 and 5.26, the impact of the adaptive MPC under different temperature (5°C, 25°C and 45°C) and prediction horizons (N_p=[2;5]) of operation can be observed. Through the analysis of these figures, a higher prediction horizon does not reveal any overall cost improvement at the end of the different simulations. Simultaneously, in analysing the results obtained under different thermal conditions, the adaptive MPC and the capacity-aware management show similar behaviours. If the cost difference percentage is analysed, its mean variation taking into account these 30 simulation - at different prediction horizons, temperatures and ageing conditions - equals 0.08%. Therefore, from control objective point of view, none of the both controls is an option that should be discarded.

5.4 SUMMARY AND CONCLUSIONS

The objective of this chapter was to formulate a control algorithm that enables the performance optimisation of modular BESSs. To this end, the first section introduces, on the one hand, the formulation of the ageing-aware management by means of an economic MPC, and, on the other hand, a power-sharing strategy for battery modules based on their nominal capacity. The data used, including a tertiary level control, is then defined, followed by simulations showing the results of the two control alternatives. Thus, it is possible to make a comparison between adaptive MPC and capacity-aware management to determine the advantages and disadvantages of using each of the solutions.

The comparison of these two energy management strategies is based on comparing both the operating dynamics of the two cases and the economic cost results at the end of each simulation. Moreover, for a better understanding of the performance of the two controls at different scenarios, heterogeneous modules in factors such as degradation, temperature, the economic cost of each module and its nominal capacity are simulated. Analysing the results obtained in each of the scenarios, one by one, the dynamics indicate the following: a) as long as the states of all modules remain identical or similar from a nominal capacity point of view, a proportional power allocation can be enough; b) when the battery operating parameters change, so that the ageing-rate is slightly affected - such as in the case of cost and temperature unbalance - the quadratic cost function tends to equalise the cost-rate (calculated by means of the ageing-rate and the battery cost), thus reducing the overall cost; c) when differences in the ageing-rate become more critical like in Section 5.3.2, this is reflected in the cost, and while capacity-aware management distributes power equally, the adaptive MPC modulates power sharing in a completely heterogeneous way. Due to this

heterogeneous power-sharing, it is possible to improve the cost for a similar input power profile. That said, it should be noted that an insufficient prediction horizon, as well as the soft-constraints, may cause efficiency losses, and therefore not yield the same power profile with the adaptive MPC. If the results are analysed from an end-of-simulation point of view, except for some specific occasions where the error management has a greater presence, the adaptive MPC presents an economic gain. This economic improvement, at times, may seem minimal, yet these differences over its useful life can turn out to be really competitive.

From the foregoing, it is safe to conclude that the modular BESS management strategy, based on a battery ageing-aware adaptive economic MPC, presents better results and a higher potential for improvement, even in scenarios where the solver is a possible source of problems and, hence, a fully heuristic error management strategy is required. Indeed, data collection and analysis reveals that the adaptability of this control to different scenarios, mainly due to the feature of predicting the impact of operating each module in any of the circumstances, is crucial for the optimal performance of a modular BESS.

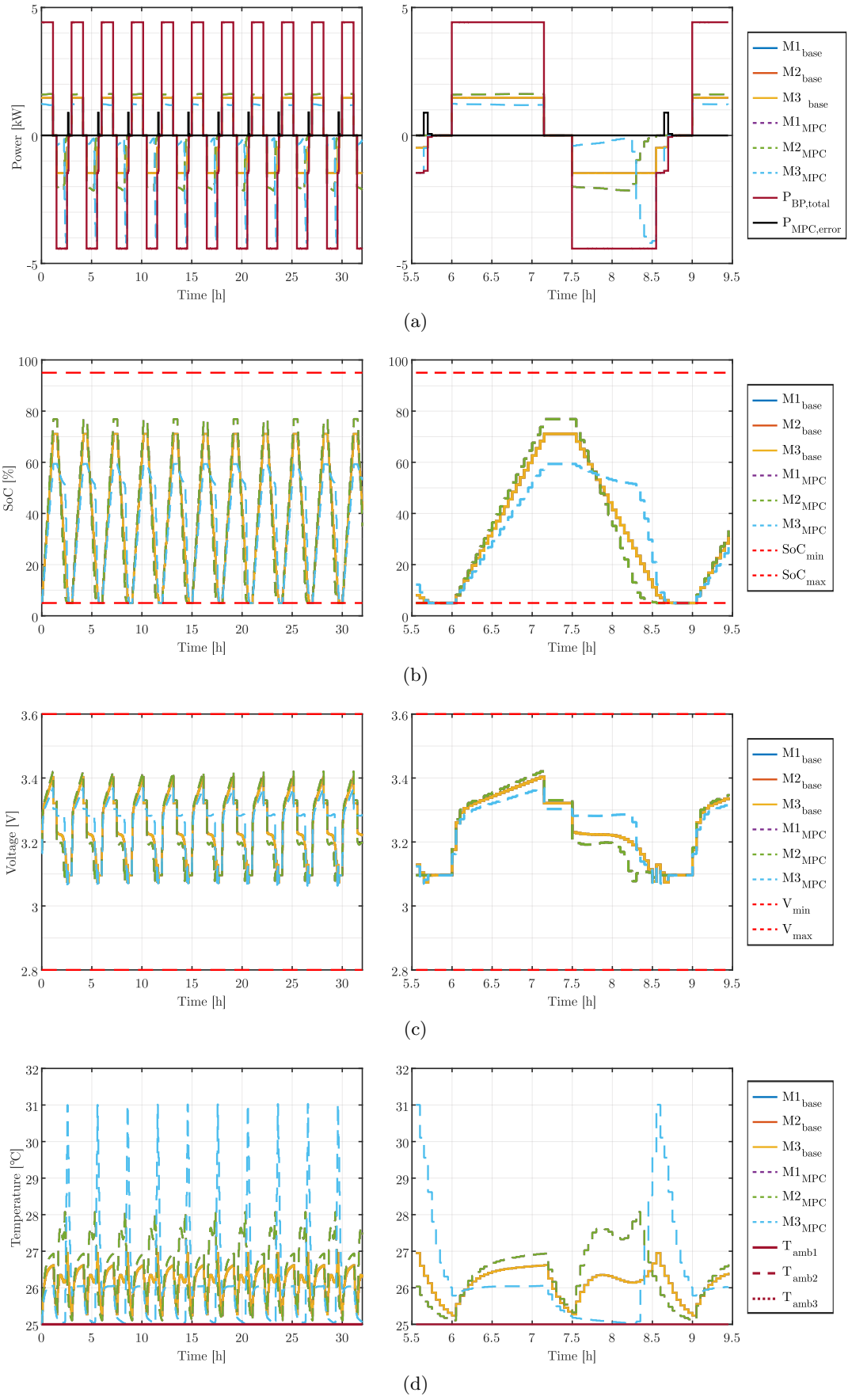

Figure 5.12: Unbalanced battery cost in modular BESS management at month 6: a) Module power, b) Module SoC, c) Cell voltage, and d) Module voltage.

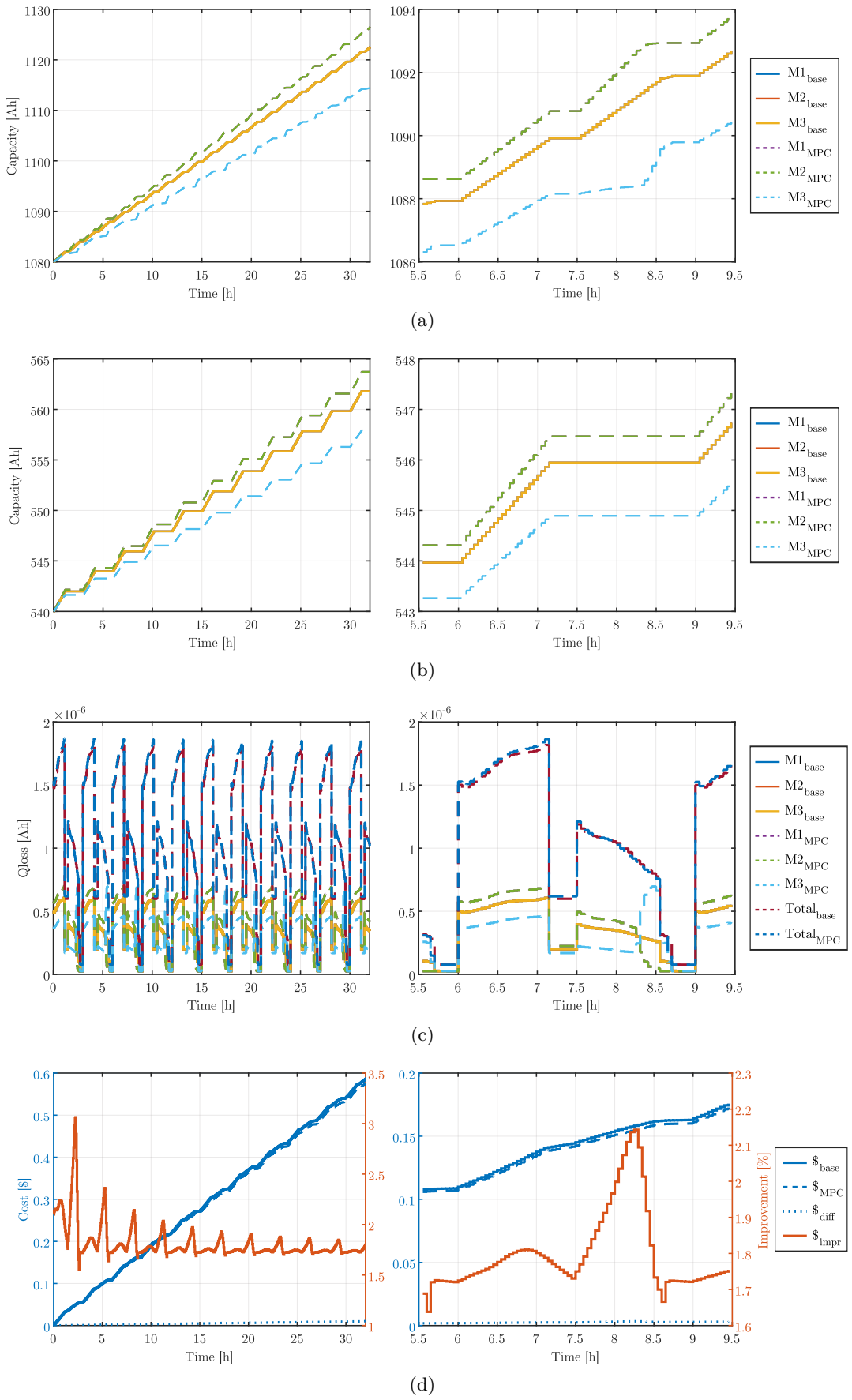

Figure 5.13: Unbalanced battery cost in modular BESS management at month 6: a) Overall cell capacity, b) Charged cell capacity, c) Cell level capacity loss, and d) System level cost.

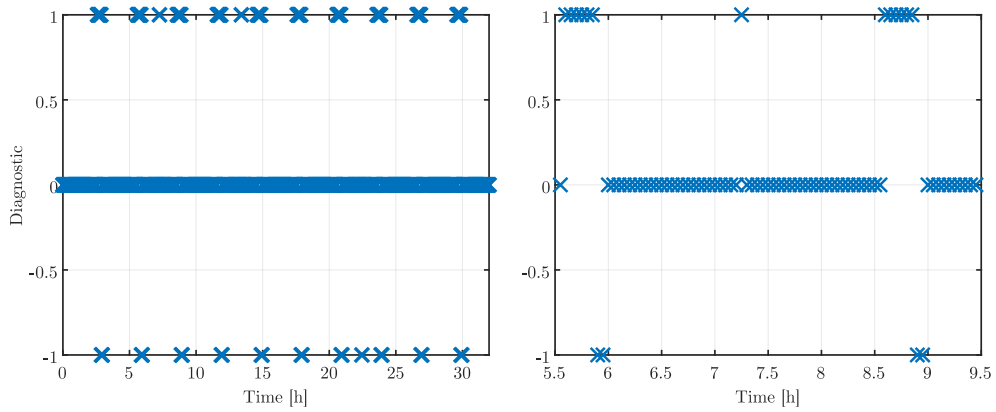

Figure 5.14: Optimisation diagnostics in a modular BESS with unbalanced cost at month 6.

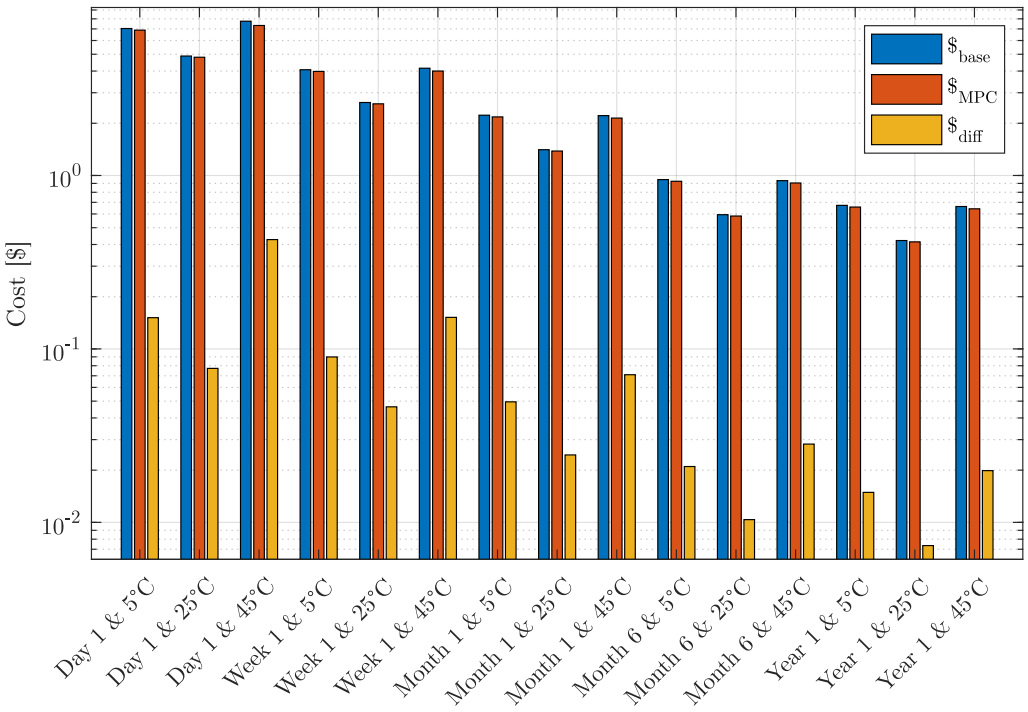

Figure 5.15: Economic cost in a modular BESS case-study with unbalanced battery cost at different lifetime and temperature conditions with $N_p = 2$.

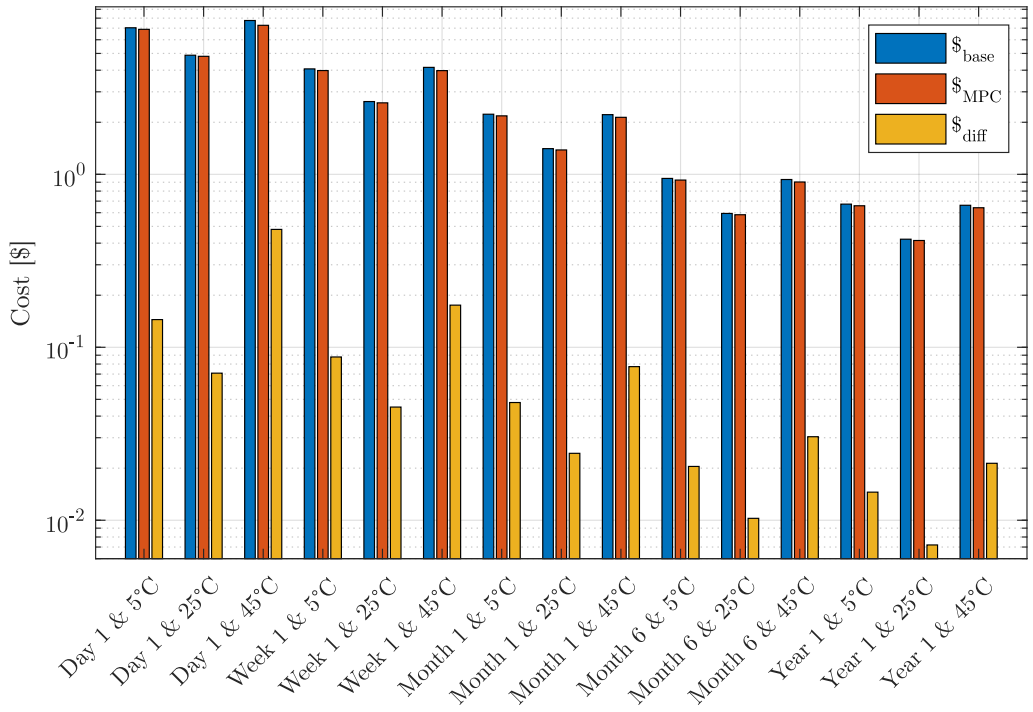

Figure 5.16: Economic cost in a modular BESS case-study with unbalanced battery cost at different lifetime and temperature conditions with $N_p = 5$.

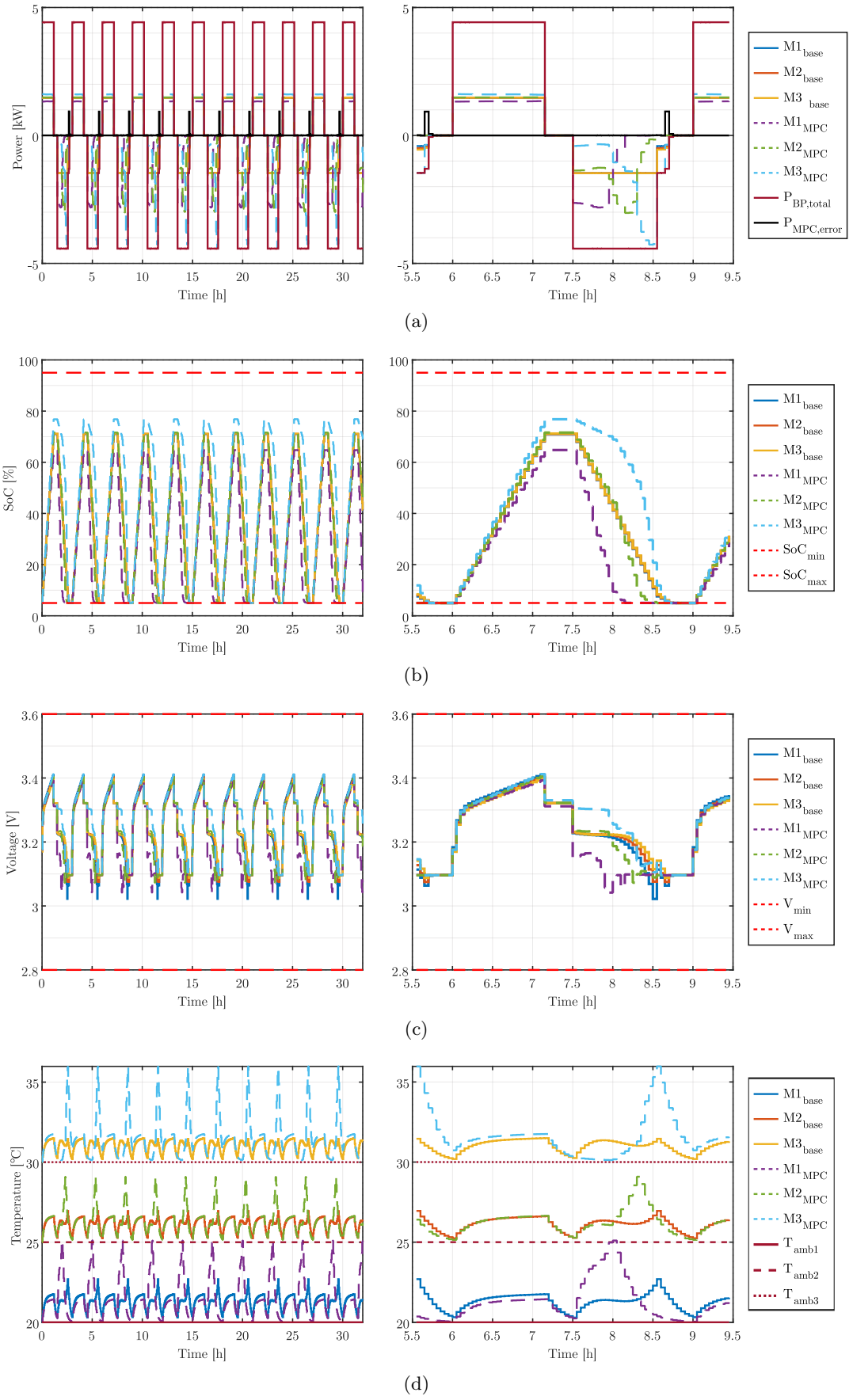

Figure 5.17: Unbalanced ambient temperature in modular BESS management at month 6: a) Module power, b) Module SoC, c) Cell voltage, and d) Module voltage.

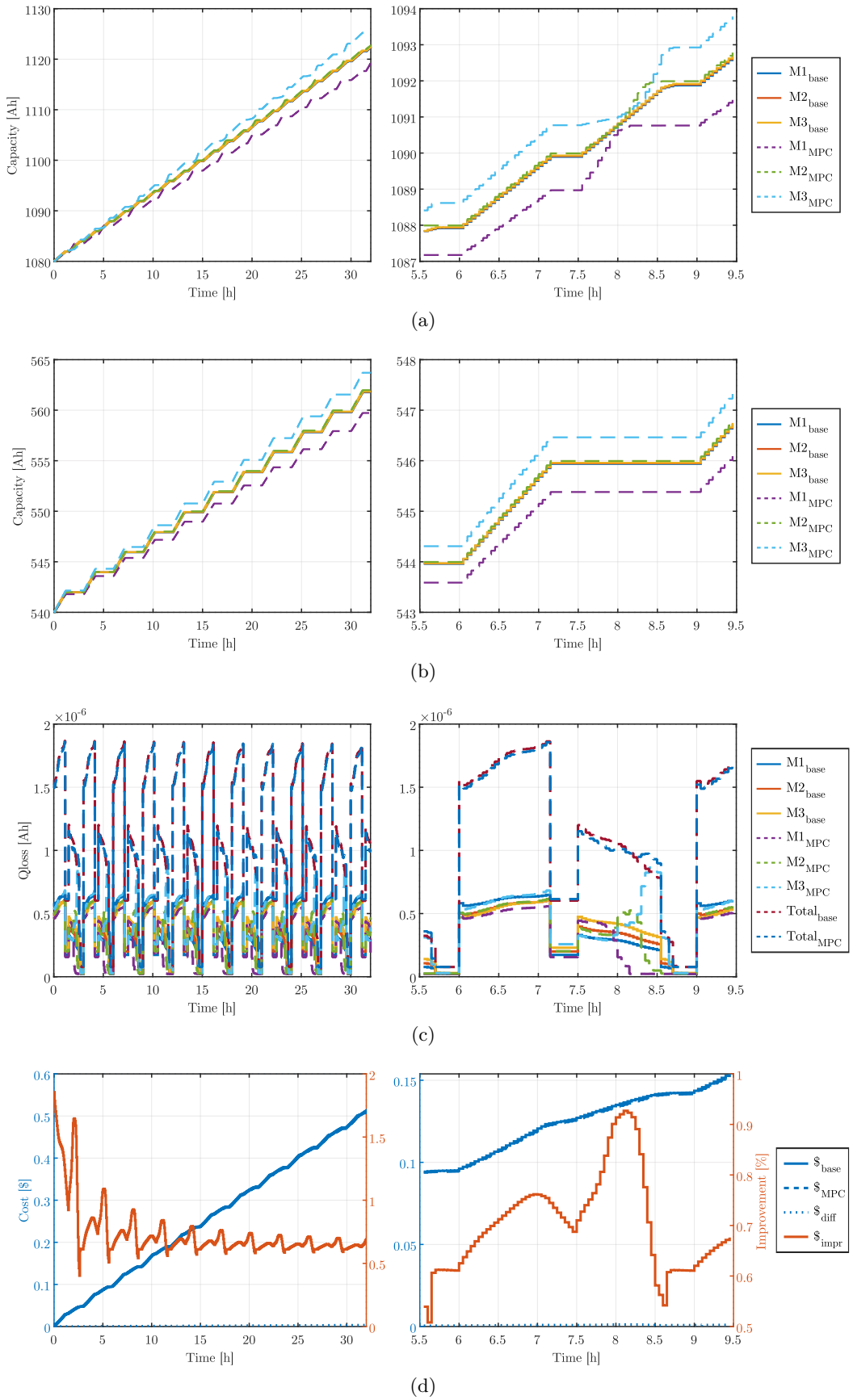

Figure 5.18: Unbalanced ambient temperature in modular BESS management at month 6: a) Overall cell capacity, b) Charged cell capacity, c) Cell level capacity loss, and d) System level cost.

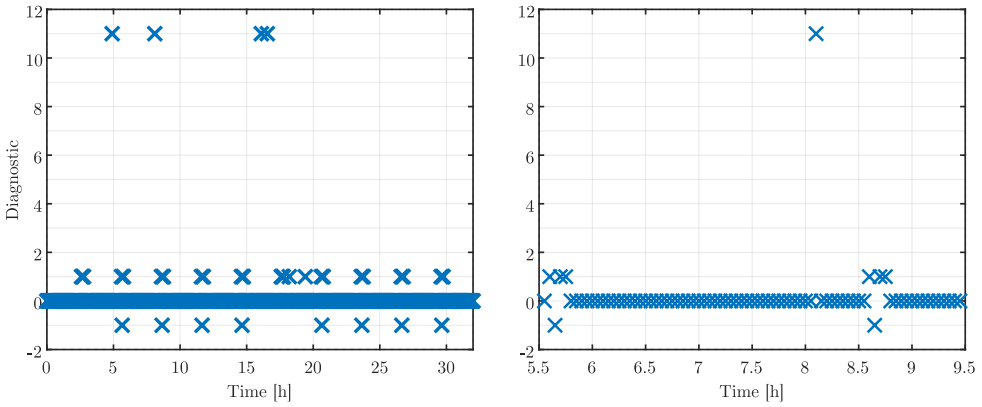

Figure 5.19: Optimisation diagnostics in a modular BESS with unbalanced ambient temperature at month 6.

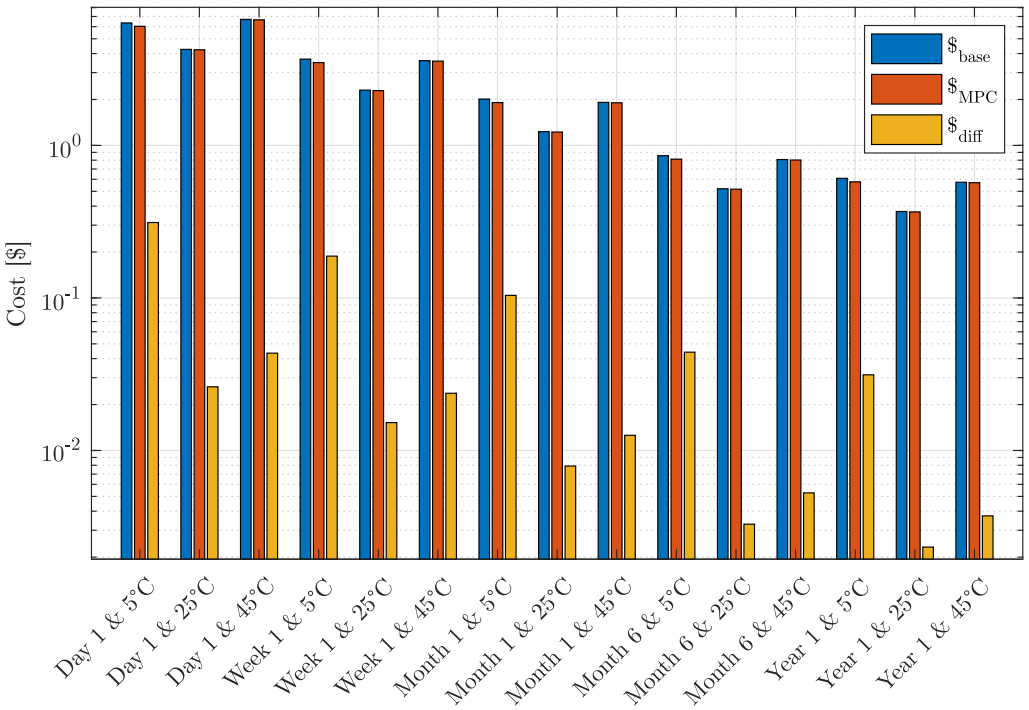

Figure 5.20: Economic cost in a modular BESS case-study with unbalanced battery temperature at different lifetime and temperature conditions with $N_p = 2$.

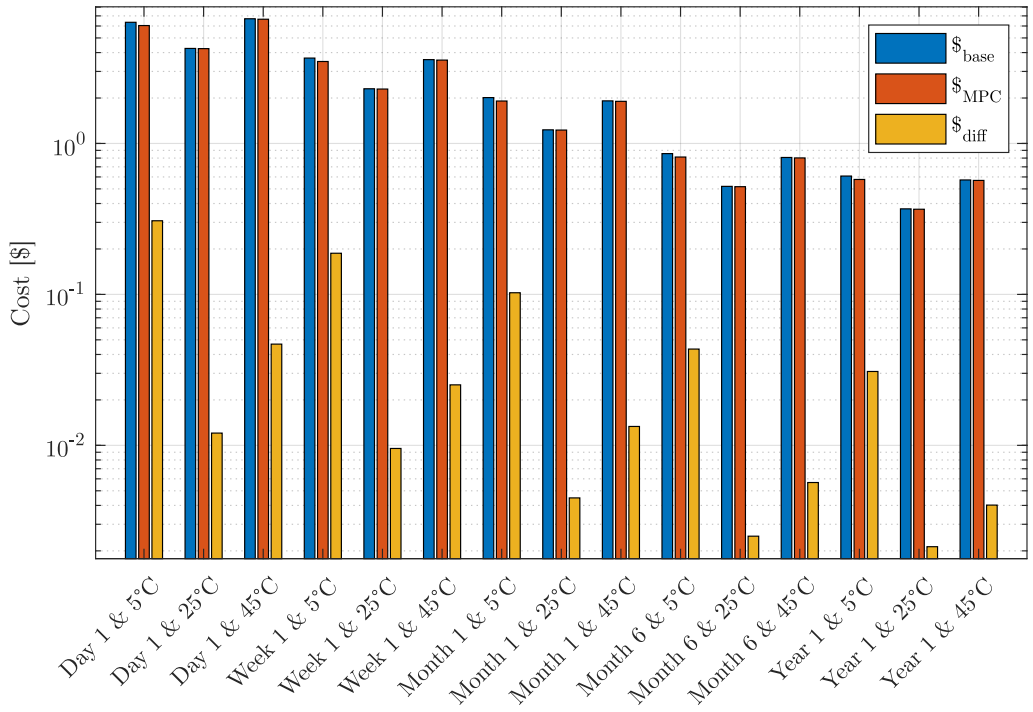

Figure 5.21: Economic cost in a modular BESS case-study with unbalanced battery temperature at different lifetime and temperature conditions with $N_p = 5$.

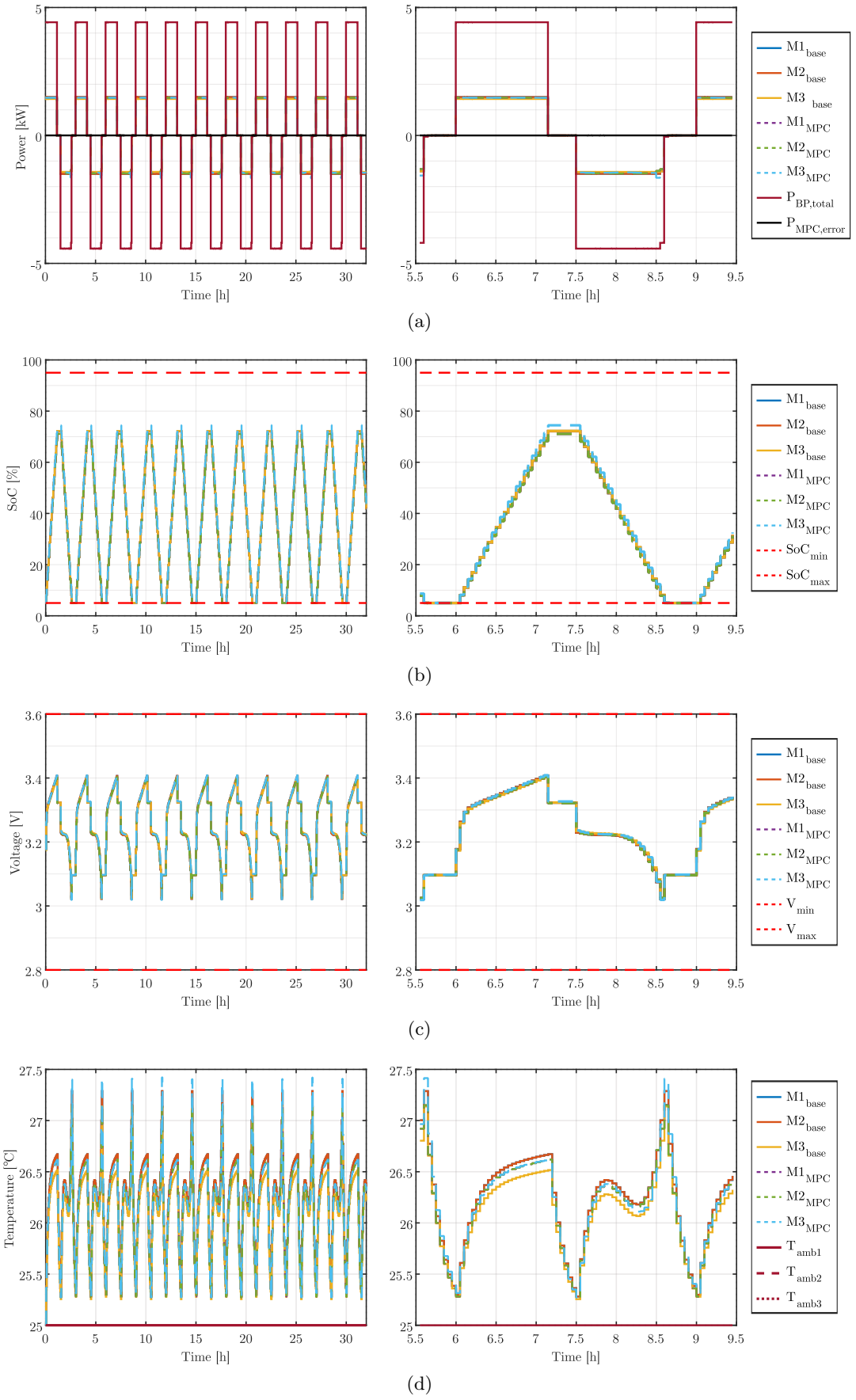

Figure 5.22: Unbalanced battery capacity in modular BESS management at month 6: a) Module power, b) Module SoC, c) Cell voltage, and d) Module voltage.

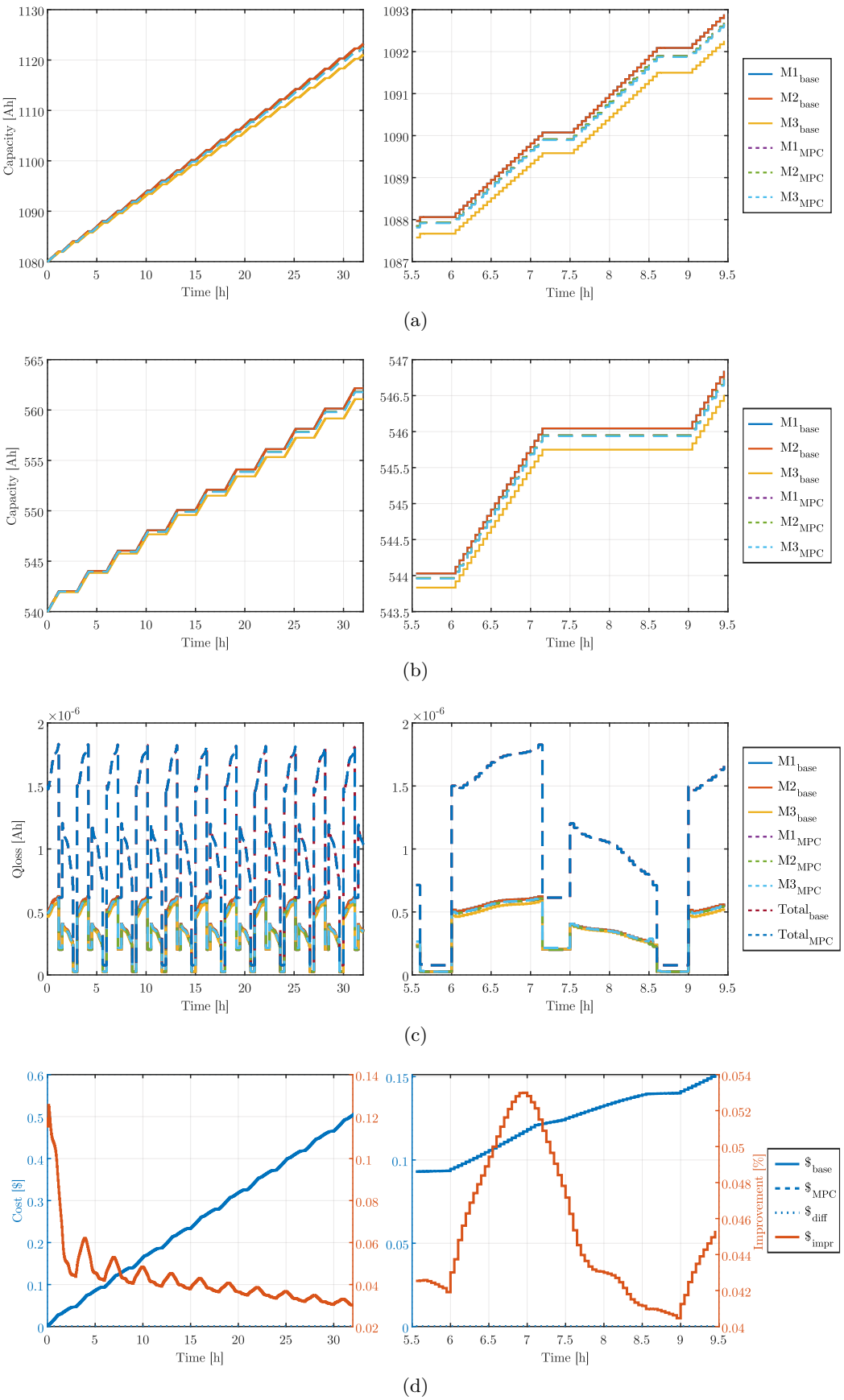

Figure 5.23: Unbalanced battery capacity in modular BESS management at month 6: a) Overall cell capacity, b) Charged cell capacity, c) Cell level capacity loss, and d) System level cost.

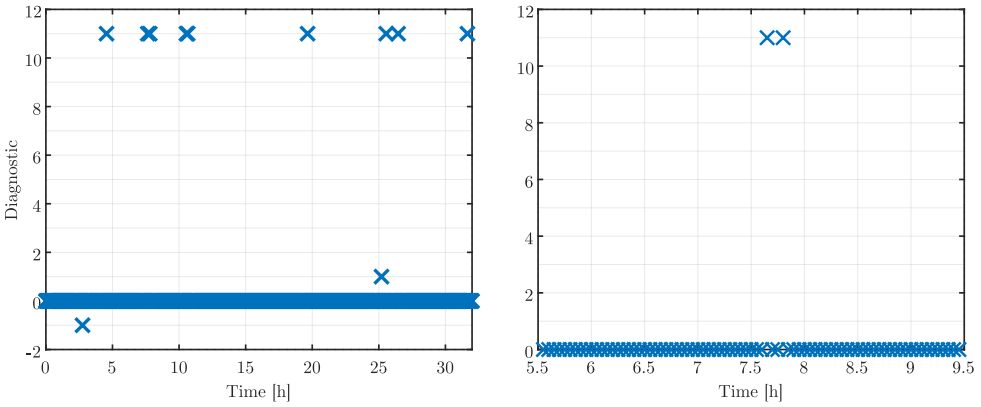

Figure 5.24: Optimisation diagnostics in a modular BESS with unbalanced battery capacity at month 6.

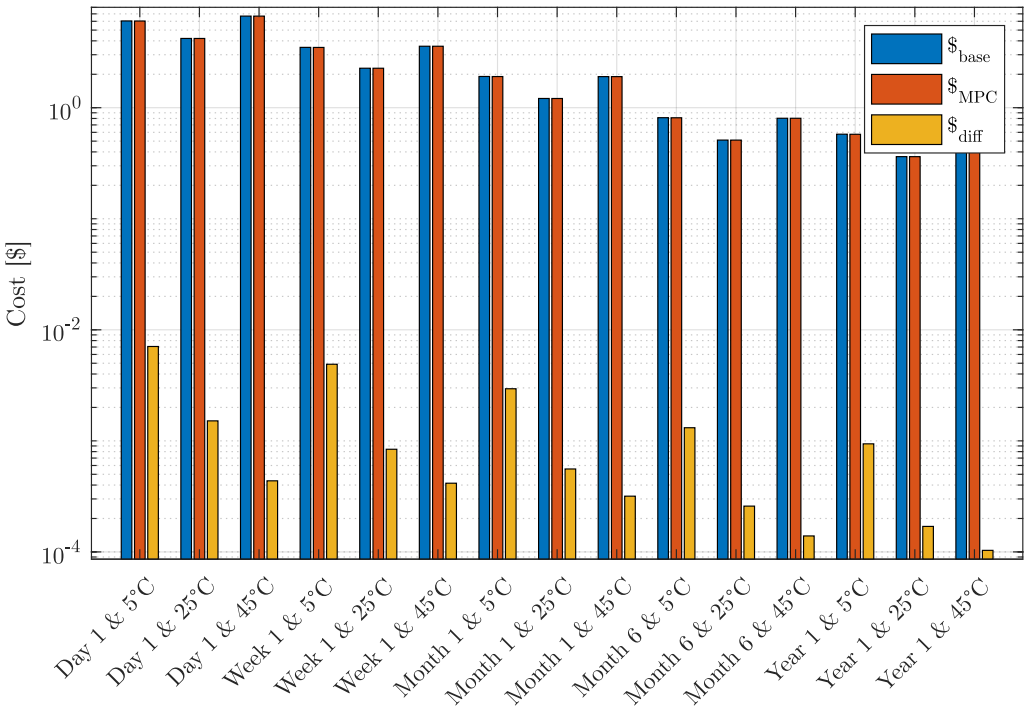

Figure 5.25: Economic cost in a modular BESS case-study with unbalanced battery capacity at different lifetime and temperature conditions with $N_p = 2$.

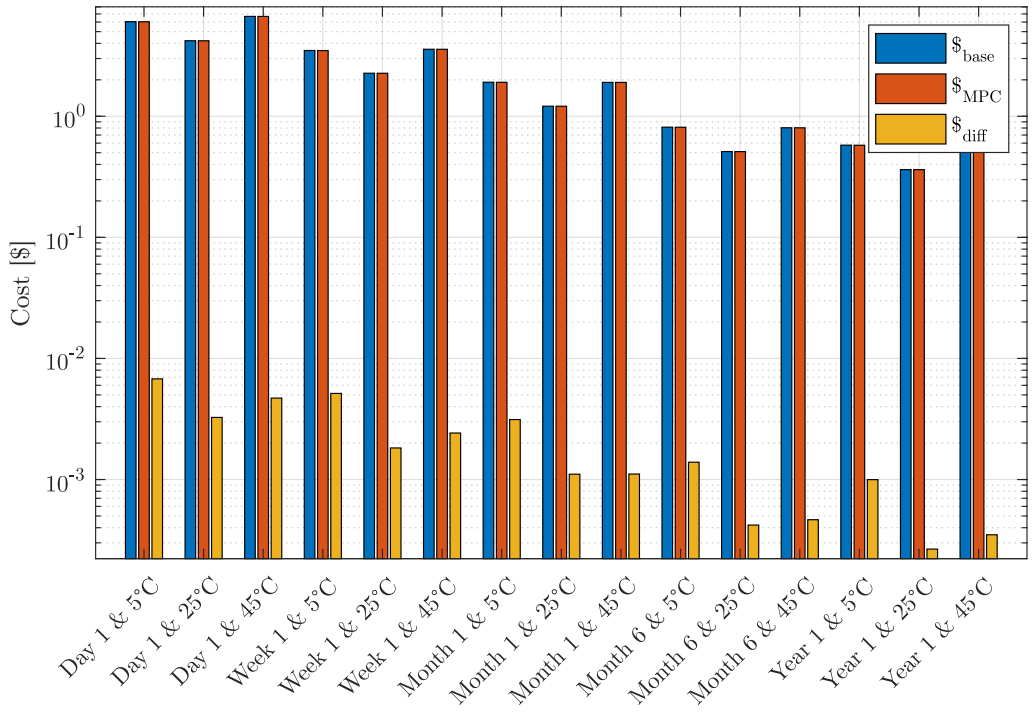

Figure 5.26: Economic cost in a modular BESS case-study with unbalanced battery capacity at different lifetime and temperature conditions with $N_p = 5$.

Chapter 6

CONCLUSIONS AND FUTURE LINES

Having developed the control strategy that provides a power-sharing algorithm for modular BESSs, built on a model-based ageing-aware solution that relies on a nonlinear economic MPC, this chapter draws the main conclusions and future lines of work. These concluding remarks and opportunities for further investigation are intended to respond to the research question formulated at the outset of the thesis, whilst suggesting new lines for following research studies.

6.1 CONCLUSIONS

With the research question aimed at optimising the performance and extending the lifespan of the modular BESS, this research seeks to develop a new control algorithm that improves the characteristics presented by the baseline of the literature. For this purpose, a battery model-based ageing-aware adaptive nonlinear economic MPC has been formulated to improve the performance of the system within the prediction window. The comparison of these two alternatives led to the conclusion that, alongside better results, the adaptive MPC has a greater potential to boost the performance of modular systems to the next level. However, it is important to understand that these results completely depend on the model used, therefore, changing the cell model does not guarantee the same performance.

In pursuit of this main objective, a first approach to both, the model-based ageing-aware management and the MPC algorithm, has been introduced in Chapter 4. In this first approximation, instead of formulating a complex system with the possibility of having multiple agents/modules and a high degree of complexity, a case-study focused on the use of a single battery unit, together with a PV system in a grid-connected residential dwelling, has been chosen. By enabling an easy identification of the different dynamics of each actor in the system, this proposal has proved to be key to the correct understanding of the battery model and its application in an MPC algorithm. Evidence of this are the results obtained by means of the ageing-aware adaptive factor (α and β) of the tertiary control level which, being an economic MPC, presents the greatest cost benefit among the three energy management strategies compared. This being so, this first phase has demonstrated that it is possible to formulate a model-based SOO problem for predictive battery management.

From an experimental analysis of the adaptive MPC via an RCP system, it has also been possible to conclude that its real-time operation is correct, insofar as the economic cost difference between the results does not exceed an average variation of 2.81%. That said, there are two lessons to be drawn from this experimental approximation of the real system: first, the differences between the prediction model and its operation in a real system indicate that determining a power-sharing factor can be of greater use than setting only the electrical current value of the BESS, so that the power-sharing ratio is established, which is, in turn, useful for cases where there may be power oscillations that the MPC cannot predict; second, it is necessary to implement advanced solutions to estimate the

battery states, such as the SoC, since a small error in its measurement over time can lead the MPC to make erroneous decisions.

Drawing on the knowledge and conclusions gathered from this first study, a control strategy could be formulated to address each of the research questions presented in Section 2.3.2. This strategy relies on both information related to the battery model and the ability to predict its performance, in order to optimise the final result and propose the use of a SOO problem by means of a quadratic economic cost function. Through its analysis, the following findings have been concluded with regard to the dynamics of operation and the final results:

- **Analysis of the dynamics:** The comparison between the results of adaptive MPC and capacity-aware management indicates that, while the latter option always seeks to distribute the power based on capacity-aware "fixed" power-sharing ratios, the control proposed in this study resorts to the generation of imbalances, either in SoC or temperature, for example, so as to obtain a better result. This suggests that minimising the economic cost calls for prioritising the ageing-rate and the cost-rate balancing and not the divergences between the different variables of the system, such as temperature and SoC. Therefore, solutions based on such heuristics that promise to minimise degradation may be exerting counterproductive control.

- **Analysis at the end of simulation:** The comparison based on the end of each simulation leads to the formulation of system level conclusions. From an economic point of view, adaptive MPC outperforms capacity-aware management, regardless of the scale at which economic savings are being made. For the worst case, after analysing its performance under different conditions of temperature, prediction horizon and lifetime stage, it has been found that the adaptive MPC is able to replicate the results of capacity-aware management. As for the best results, as imbalances increase, the adaptive MPC is still able to adapt to the characteristics of the system to minimise the cost, thus obtaining an average cost that is up to 17.82% lower. In terms of total system lifetime predictions, it is common practice in the literature to extrapolate the results beyond the period analysed. From the analysis performed at different lifetime points, however, it has been concluded that, in this case, such practice is not adequate, given the difference that may exist between the results at different ageing conditions.

Despite its great advantages, the adaptive MPC also hides an efficiency challenge. By prioritising the discharge of the cheaper modules, a benefit is achieved, yet when these units

subsequently reach a constraint, such as the SoC, which forces the system to operate the remaining more expensive modules in a demanding manner, higher losses are generated, for instance due to the Joule effect. As a consequence, this can lead as well to a higher overall capacity loss and economic cost. Therefore, in order to better address this challenge, it is concluded that the prediction horizon and the weighting factors require closer attention and a more detailed study, since their use could minimise the impact of efficiency loss and excessively accelerated discharges.

Finally, before concluding this section, mention should be made of the difficulty of implementing the type of system formulated. On the one hand, the battery model depends on non-continuous and non-linear functions that are also non-convex. On the other hand, tuning an MPC requires heuristic knowledge beyond the more technical aspects. This may result in the formulation of a single centralised MPC, for the control of a large number of modules, becoming a difficult task. All things considered, it is concluded that a new cell model, that is easier to implement and is as accurate or even more precise as the one used for this study, as well as a non-centralised control to split the problem and, thus, reduce its dimensions and difficulty of optimisation, can boost the use of this type of controls.

6.2 FUTURE LINES

Having successfully tested the feasibility of the formulated control at a simulation and RCP level, it is worth comparing this system with other alternatives available in the literature. The comparison of the appropriate KPIs would contribute to assessing whether the option presented by this research has better characteristics and greater potential than current solutions, in terms of promoting the development and adoption of BESSs based on CBMs.

Beyond the extensive comparison between this control strategy and the baseline, there are several challenges, still to be answered, that could be addressed in future research in greater detail. Below, I introduce those future lines of research that have been considered as the most relevant and with the greatest potential.

First of all, in order to formulate this type of control, a coupled electro-thermal and ageing battery model, along with an economic cost model, is mandatory to predict and optimise the performance of the BESSs. As for the electrical, thermal and degradation aspects, the results are completely dependent on each battery model, as well as on the accuracy of the ECM, PBM or Data-driven model selected. Hence, it would be interesting

to repeat the development of this control with a different cell model, together with another modelling strategy, such as PBMs which are gaining momentum due to the increasing interest on the internal physical characteristics. By doing so, it would demonstrate both the adaptability of the control strategy to any scenario, and also that this is not an isolated case. As for the modelling of the cost of each cell/module, there is a wide research window. Currently, this work predicts battery cost in a "simplistic" but useful way that facilitates the formulation of a cost function, while allowing all number of modules to operate. Still, a cost function that takes a more detailed and up-to-date look at the economics of a module can help to improve the cost prediction, and, in turn, the techno-economic performance of individual modules and the BESS. This would enable the optimisation of both CAPEX and OPEX, key indicators from an industrial adoption and expansion point of view.

Second, in this research, it is presumed that the power converters have the required voltage amplification at 100% efficiency, and, as such, the analysis is limited to the configuration of parallel modules. As the application voltage increases, however, this approach can turn into a challenge that cannot be met with parallel modules alone. This means that future work may consider "matrix" module configurations, where series and parallel connections are combined. With this type of systems, nevertheless, it is imperative to reformulate the equations for power distribution among modules. In this regard, account must be taken of the fact that parallel connections still serve the same function of supplying a given demand, whereas series connections require consideration of the impact of the power flow on the output voltage. On this premise, the current modular configuration could be scaled up to larger structures.

Third, as far as the control algorithm is concerned, there are several possible areas of future research interest. On the one hand, the hierarchical control of the BESS requires a better understanding of how the interactions between the different control layers make an impact. Especially when these control layers can and often do differ in cell models, control objectives and actuation times. On the other hand, the control architecture of the current solution is centralised, yet, as mentioned throughout this paper, both decentralised and distributed options have potential for improvement. With this in mind, it would be worth considering new alternatives, i.e. a distributed MPC, to try to improve the characteristics of the current control. Moreover, the current control algorithm is not adapted to a faulty module scenario. That said, as this is a functionality of the modular BESSs of great interest, it would be desirable to find means to adapt the control, so that it can offer this improvement, by for example, limiting the current constraints of the faulty module to zero

until the faulty module is repaired. Additionally, the diagnostics of each simulation show the computational difficulty of the control algorithm under some operating specifications. Given the above, it is crucial to devote efforts in future work to try to solve these control algorithm limitations, in order to achieve better results and avoid an error management system.

Finally, to stimulate wider adoption of this or similar control strategies, it is necessary to validate the simulation results experimentally. For this purpose, it is worth developing an experimental setup in the laboratory, covering aspects ranging from the cell model and its initial conditions, to the power converters that regulate the power, via the BMS unit, with a view to monitoring the operation and safety of each module as well as the entire BESS. This experimental validation also involves dumping the control algorithm on a control board with sufficient computational capacity, for the implementation of this system in a real environment.

Appendix A

CELL MODELLING DETAILS

A.1 ELECTRICAL RESISTANCE

In the following, Equations A.1 and A.2 display the polynomials that have been fitted to represent the behaviour of the electrical resistance of charge $f_{R_{ch}}$ and discharge $f_{R_{dch}}$, respectively. In the fitting process conducted by means of the MATLAB® *curvefitter* tool, the dependencies of both the temperature and the SoC have been factored in. The impact of each of these variables in predicting the resistance value is defined using polynomials with various degrees. As such, these degrees of dependence are defined in the sub-indices of the coefficients p, and the value corresponding to each of them is provided in Tables A.1 and A.2.

$$f_{R_{\text{ch}}} = p_{0,0} + p_{1,0} \cdot T_{\text{cell}} + p_{0,1} \cdot q + p_{2,0} \cdot T_{\text{cell}}^2 + p_{1,1} \cdot T_{\text{cell}} \cdot q_{\text{cell}} \tag{A.1}$$

$$\begin{aligned} f_{R_{\text{dch}}} =& p_{0,0} + p_{1,0} \cdot T_{\text{cell}} + p_{0,1} \cdot q_{\text{cell}} + p_{2,0} \cdot T_{\text{cell}}^2 + p_{1,1} \cdot T_{\text{cell}} \cdot q_{\text{cell}} + p_{0,2} \cdot q_{\text{cell}}^2 \\ &+ p_{3,0} \cdot T_{\text{cell}}^3 + p_{2,1} \cdot T_{\text{cell}}^2 \cdot q_{\text{cell}} + p_{1,2} \cdot T_{\text{cell}} \cdot q_{\text{cell}}^2 + p_{0,3} \cdot q_{\text{cell}}^3 + p_{4,0} \cdot T_{\text{cell}}^4 \\ &+ p_{3,1} \cdot T_{\text{cell}}^3 \cdot q_{\text{cell}} + p_{2,2} \cdot T_{\text{cell}}^2 \cdot q_{\text{cell}}^2 + p_{1,3} \cdot T_{\text{cell}} \cdot q_{\text{cell}}^3 + p_{0,4} \cdot q_{\text{cell}}^4 \end{aligned} \tag{A.2}$$

Implementing this type of non-continuous function in the control algorithm, however, can be a challenge. Bearing this in mind, an adjustment has been made to convert the electrical resistance calculation into a continuous function. This has been possible through the use of hyperbolic tangents (tanh) as represented in Equation A.3.

Table A.1: Coefficients for charging electrical resistance.

T \ q	0	1	2
0	0,0685	-0,0012	8,098 e-6
1	0,0169	-1,5148 e-4	-
2	-	-	-

Table A.2: Coefficients for discharging electrical resistance.

T \ q	0	1	2	3	4
0	0,5347	-0,0228	3,833 e-4	2,775 e-6	7,275 e-9
1	-2,0843	0,0576	-5,505 e-4	1,743 e-6	-
2	3,5503	-0,0537	2,2186 e-4	-	-
3	-2,6416	0,0168	-	-	-
4	0,7168	-	-	-	-

$$R_{\text{cell}} = R_{\text{ch}} + R_{\text{dch}} \begin{cases} R_{\text{ch}} = \frac{\tanh(1e3u)+1}{2} f_{R_{\text{ch}}}(q_{\text{cell}}, T_{\text{cell}}) \\ R_{\text{dch}} = \frac{\tanh(-1e3u)+1}{2} f_{R_{\text{dch}}}(q_{\text{cell}}, T_{\text{cell}}) \end{cases} \tag{A.3}$$

A.2 AGEING MODEL

In formulating the control algorithm, a change has been introduced to the means of calculating the stress factor required for the determination of the capacity loss $Q_{\text{Cyc,LowT\&HighSoC}}$. This change consists of replacing the *sgn* function used to identify the sign of the SoC by the *tanh* function, as shown in Equation A.4.

$$\begin{aligned} & k_{\text{Cyc,LowT\&HighSoC}}\left(q_{\text{cell}}, T_{\text{cell}}, I_{\text{Ch}}\right) \\ & = k_{\text{Cyc,LowT\&HighSoC,Ref}} \cdot \exp\left[\frac{E_{\text{a,Cyc,LowT\&HighSoC}}}{R_{\text{g}}}\left(\frac{1}{T_{\text{cell}}} - \frac{1}{T_{\text{Ref}}}\right)\right] \\ & \quad \cdot \exp\left[\beta_{\text{LowT\&HighSoC}} \cdot \frac{I_{\text{Ch}} - I_{\text{Ch,Ref}}}{C_0}\right] \\ & \quad \cdot \left(\frac{\left(\tanh\left(1e2\left(q_{\text{cell}} - q_{\text{cell,Ref}}\right)\right)\right) + 1}{2}\right) \end{aligned} \tag{A.4}$$

Appendix B

OPTIMISATION SOLVER

B.1 SOLVER DIAGNOSTICS

Upon completion of each optimisation, the solver returns a diagnostic to identify the type of error that may have occurred during its execution. If the optimisation completes the calculations correctly, the diagnostic indicator equals zero.

- -9 Specified solver name not recognised
- -8 Problem does not satisfy geometric programming rules
- -7 Solver does not return error codes
- -6 Search space not bounded (bound all variables)
- -5 License problems in solver
- -4 Solver not applicable
- -3 Solver not found
- -2 No suitable solver
- -1 Unknown error
- 0 Successfully solved
- 1 Infeasible problem
- 2 Unbounded objective function
- 3 Maximum iterations exceeded

- 4 Numerical problems
- 5 Lack of progress
- 6 Initial solution infeasible
- 7 YALMIP sent incorrect input to solver
- 8 Feasibility cannot be determined
- 9 Unknown problem in solver
- 10 bigM failed (increase sp.Mfactor)
- 11 Other identified error
- 12 Infeasible or unbounded
- 13 YALMIP cannot determine status in solver
- 14 Model creation failed
- 15 Problem either infeasible or unbounded
- 16 User terminated
- 17 Presolve recovery failed

B.2 ERROR MANAGEMENT

When it comes to operating the modules optimally, the control introduced in Section 5.1 determines how to proceed with the power-sharing. Yet, it is worth mentioning that the solver, at the end of each optimisation, indicates, by means of different diagnostics, that the final result obtained is not always optimal or acceptable. When this occurs, a non-optimal power setpoint can counteract any previous benefit. Therefore, an extra control layer is considered to be of interest for the proposed control in Chapter 5. Its function is to identify any solver diagnostic that is not equal to zero, to apply the heuristics-based management shown in Figure 5 and, in turn, determine a new operating setpoint.

Upon identifying any errors, this strategy distributes the power based on the same power-sharing factor previously used. At the same time, when an optimal setpoint is not obtained, all the initial guess current values are set to zero for the warm-start of the following optimisation. Next, the control is conducted to ensure that the constraints of

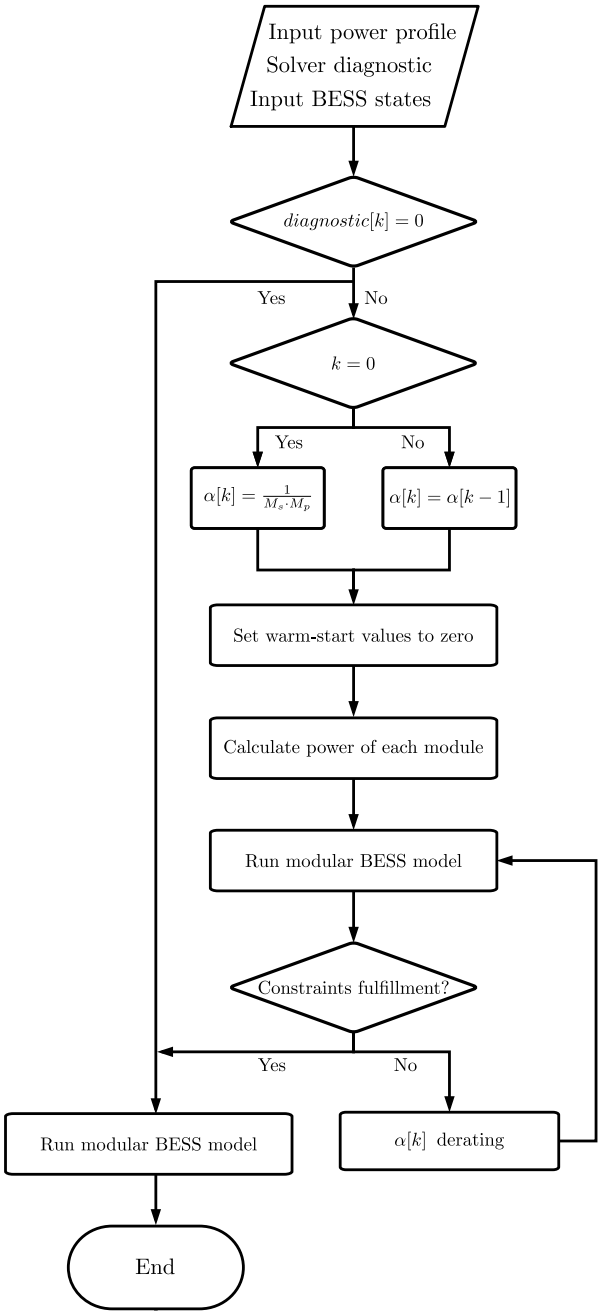

Figure B.1: Optimisation error management for the modular BESS.

the battery are met. If necessary, new power-sharing values are determined to guarantee compliance. Finally, with a view to ensuring correct operation after this possible adaptation, this result is compared with the power setpoint established by the system, in an attempt to respond to the demand.

B.3 CONSTRAINT ADAPTATIONS

To facilitate the optimisation conducted by the solver, a series of adaptations have been made, as detailed below:

- The fulfillment of Equation 5.1a, which plays the role of hard-constraint in the MPC, makes the optimisation work more difficult. To facilitate the calculation of the optimal power-sharing setpoint, the soft-constraint presented in Equation B.1 is applied, by using P_{relax} as the relaxation factor. In this case its value is equal to 1 W, which is established after analysing a series of simulations with different values.

$$-P_{\text{relax}} \leq P_{\text{BESS}}[k] - \sum_{m_s=1}^{M_s} \sum_{m_p=1}^{M_p} P_{\text{BM},[m_s,m_p]}[k] \leq P_{\text{relax}} \tag{B.1}$$

- The analysis of a series of simulations performed to determine the correct functioning of hard-constraints has indicated that formulating the following limitations also facilitates the optimisation problem to be solved by the IPOPT. In this regard, Equation B.2 shows the hard-constraints that are related to the capacity calculation, while Equation B.3 refers to the different stress factors associated with degradation.

$$\begin{bmatrix} \varphi_{\text{Ch},[m_s,m_p]}[k+1] \\ \varphi_{\text{Tot},[m_s,m_p]}[k+1] \end{bmatrix} \geq \begin{bmatrix} \varphi_{\text{Ch},[m_s,m_p]}[k] \\ \varphi_{\text{Tot},[m_s,m_p]}[k] \end{bmatrix} \tag{B.2}$$

$$\begin{bmatrix} 10 \\ 10 \\ 10 \\ 10 \end{bmatrix} \cdot \begin{bmatrix} k_{\text{Cal},[m_s,m_p]}[k] \\ k_{\text{Cyc,HighT},[m_s,m_p]}[k] \\ k_{\text{kCyc,LowT},[m_s,m_p]}[k] \\ k_{\text{kCyc,LowT\&HighSoC},[m_s,m_p]}[k] \end{bmatrix} \geq \begin{bmatrix} 0 \\ 0 \\ 0 \\ 0 \end{bmatrix} \tag{B.3}$$

Appendix C

RAPID CONTROL PROTOTYPING

The schematic of the RCP system, employed in this research to analyse the differences between a simulation and a system closer to any experimental solution, is introduced in Figure C.1. While this approach allows the adaptive MPC to be kept in the MATLAB/Simulink® environment, the cell model used to represent the real battery operation is transferred to an experimental environment, along with all the required measurement systems. In this regard, the following three main components are required for the operation of this system:

- **Control Unit:** This is the device (CPU: Intel Core i7-8700 3.2 GHz; RAM: 16 GB) where the control algorithm for the BESS is located. Therefore, this unit determines with which current each cell is to be operated. The Control Unit also shares information about the ambient temperature with the battery model.
- **Battery emulator:** This system is divided into two parts. On the one hand, there is the F28379d launchpad of Texas Instruments (TI), where the cell and battery model are located. This board receives the operating instructions from the Control Unit. On the other hand, there are the digital to analogue converter boards, which transform the PWM output of the TI board into a constant output voltage. These enable the measurement and safety tasks to be carried out.
- **BMS:** This element is made up of two parts: first, there is the BMS slave, in this instance, based on an LTC6811IG-1 DC2259A evaluation board; and, second, there is the BMS master, based on an Arduino Mega 2560, which communicates all the measurements with the Control Unit.

In order to understand how it works in detail, the most relevant dynamics and characteristics are introduced below:

- Before undertaking the analysis, it is crucial to correctly determine the initial conditions of the system, not only for the Control Unit, but also for the battery emulator.
- Upon the start-up of the RCP, both the battery emulator and the BMS are in standby for the first three minutes. During this period, the control algorithm determines how to operate the cell and the battery. Once the initial standby period of 180 seconds is over, the control unit will send the current and ambient temperature reference to the TI board where the cell model is located.
- While the MATLAB/Simulink® program monitors the BMS measurements every second, the system optimisation starts 12 minutes after each current setpoint update. At this point, with the measurements taken at that moment, and predicting the evolution of the system over the next 180 seconds, the next optimisation begins.
- When the current setpoint, updated every 15 minutes, reaches the TI board, this operates in real-time. As a result, it is possible to dynamically represent the voltage and temperature of the cell. These values are updated by varying different PWMs at the output of the board, which are, subsequently, passed through the matching system. At the output, these boards are converted into constant voltage values, so that measurements can be carried out correctly with the BMS.
- Measurements are taken at the output of the matching boards with a sampling period of one second. The evaluation board of the LTC6811IG-1 DC2259A performs the cell voltage measurement prior to communicating this data to the Arduino Mega 2560. Meanwhile, the current and temperature are measured directly by the Arduino Mega 2560. Once the measurements are completed, the data is transferred to the Control Unit for its use in the control algorithm.

In the development of this system, however, an inaccurate current measurement can be critical in predicting the SoC. This prediction error, a posteriori, can lead to improper operation. Therefore, a future challenge is to include an estimator, such as Kalman Filter, to reduce the impact on the current measurement. In the meantime, it has been opted to directly feedback the current setpoint for the SoC prediction.

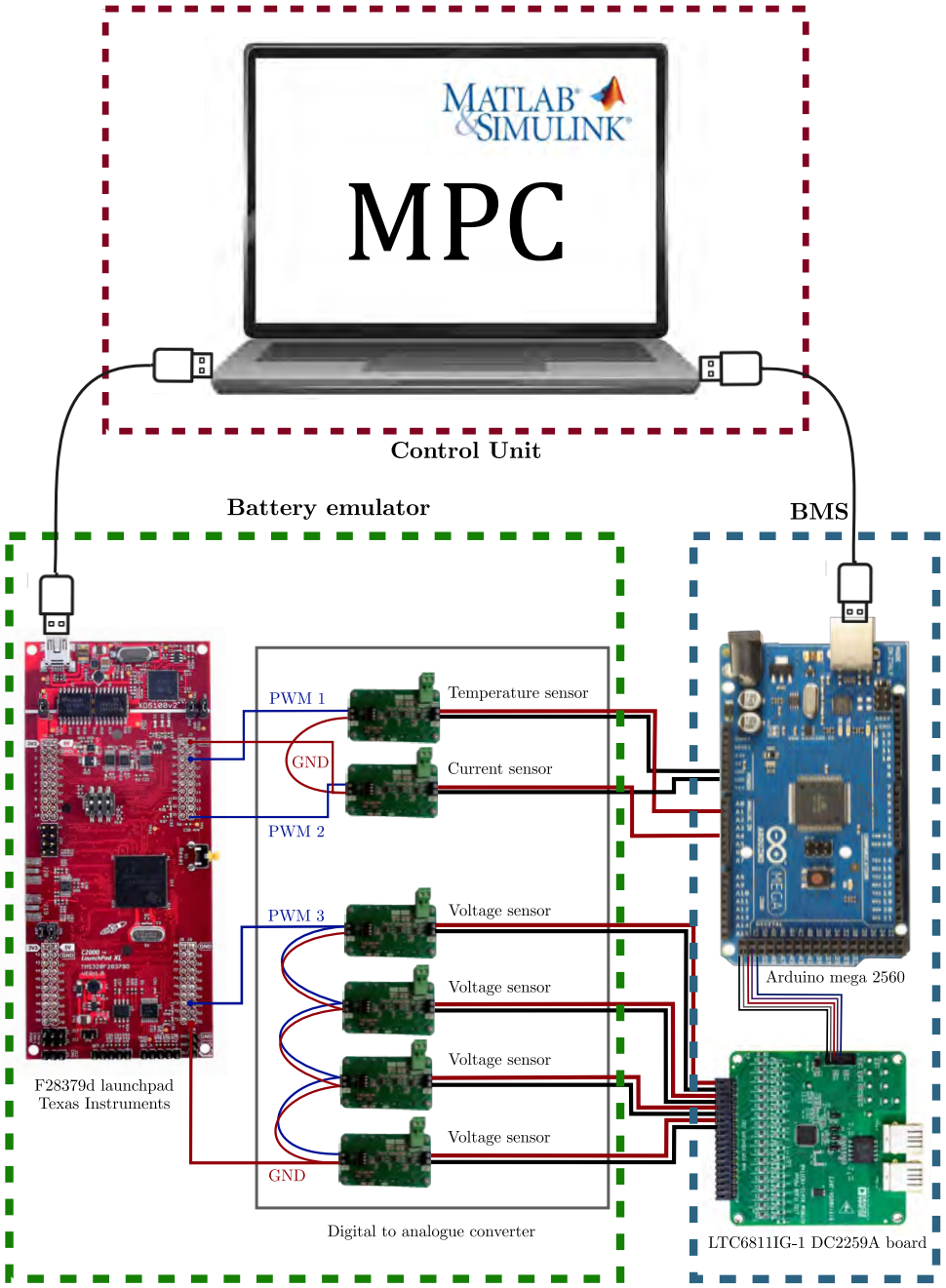

Figure C.1: RCP system scheme.

LIST OF FIGURES

LIST OF TABLES

REFERENCES

[1] UN General Assembly, "70/1. transforming our world: the 2030 agenda for sustainable development transforming our world: the 2030 agenda for sustainable development preamble. a/res/70/1," October 21, 2015.

[2] G. Zubi, R. Dufo-López, M. Carvalho, and G. Pasaoglu, "The lithium-ion battery: State of the art and future perspectives," *Renewable and Sustainable Energy Reviews*, vol. 89, pp. 292–308, 2018.

[3] European Commission, Directorate-General for Mobility and Transport. Sustainable and smart mobility strategy – putting european transport on track for the future. Accessed: January 8th, 2024. [Online]. Available: https://eur-lex.europa.eu/legal-content/EN/TXT/?uri=CELEX:52020DC0789

[4] H. Kawamura, M. LaFleur, K. Iversen, and H. W. J. Cheng, "Frontier technology issues: Lithium-ion batteries: a pillar for a fossil fuel-free economy?" July, 2021. [Online]. Available: https://www.un.org/development/desa/dpad/publication/frontier-technology-issues-lithium-ion-batteries-a-pillar-for-a-fossil-fuel-free-economy/

[5] F. Duffner, M. Wentker, M. Greenwood, and J. Leker, "Battery cost modeling: A review and directions for future research," *Renewable and Sustainable Energy Reviews*, vol. 127, p. 109872, 2020.

[6] J. Wen, D. Zhao, and C. Zhang, "An overview of electricity powered vehicles: Lithium-ion battery energy storage density and energy conversion efficiency," *Renewable Energy*, vol. 162, pp. 1629–1648, 2020.

[7] I. Hasa, S. Mariyappan, D. Saurel, P. Adelhelm, A. Y. Koposov, C. Masquelier, L. Croguennec, and M. Casas-Cabanas, "Challenges of today for na-based batteries of the future: From materials to cell metrics," *Journal of Power Sources*, vol. 482, p. 228872, 2021.

[8] Y. Xiao, Y. Wang, S.-H. Bo, J. C. Kim, L. J. Miara, and G. Ceder, "Understanding interface stability in solid-state batteries," *Nature Reviews Materials*, vol. 5, no. 2, pp. 105–126, 2020.

[9] T. Lombardo, M. Duquesnoy, H. El-Bouysidy, F. Årén, A. Gallo-Bueno, P. B. Jørgensen, A. Bhowmik, A. Demortière, E. Ayerbe, F. Alcaide, M. Reynaud, J. Carrasco, A. Grimaud, C. Zhang, T. Vegge, P. Johansson, and A. A. Franco, "Artificial intelligence applied to battery research: Hype or reality?" *Chemical Reviews*, vol. 122, no. 12, pp. 10 899–10 969, 2022, pMID: 34529918.

[10] G. L. Plett, *Battery Management Systems, Volume I: Battery Modeling*. Artech House, 2015, vol. I.

[11] ——, *Battery Management Systems, Volume II: Equivalent-Circuit Methods*. Artech House, 2016, vol. II.

[12] I. Lopetegi, G. L. Plett, M. S. Trimboli, L. Oca, E. Miguel, and U. Iraola, "A new battery soc/soh/esoh estimation method using a pbm and interconnected spkfs: Part ii. soh and esoh estimation," *Journal of The Electrochemical Society*, vol. 171, no. 3, p. 030518, mar 2024.

[13] H. Ruan, J. V. Barreras, T. Engstrom, Y. Merla, R. Millar, and B. Wu, "Lithium-ion battery lifetime extension: A review of derating methods," *Journal of Power Sources*, vol. 563, p. 232805, 2023.

[14] Y. Yang, S. Bremner, C. Menictas, and M. Kay, "Battery energy storage system size determination in renewable energy systems: A review," *Renewable and Sustainable Energy Reviews*, vol. 91, pp. 109–125, 2018.

[15] J. Zhang, S. Ci, H. Sharif, and M. Alahmad, "Modeling discharge behavior of multicell battery," *IEEE Transactions on Energy Conversion*, vol. 25, no. 4, pp. 1133–1141, 2010.

[16] M. Dubarry, C. Pastor-Fernández, G. Baure, T. F. Yu, W. D. Widanage, and J. Marco, "Battery energy storage system modeling: Investigation of intrinsic cell-to-cell variations," *Journal of Energy Storage*, vol. 23, pp. 19–28, 2019.

[17] R. de Castro, H. Pereira, R. E. Araújo, J. V. Barreras, and H. C. Pangborn, "qtsl: A multilayer control framework for managing capacity, temperature, stress, and losses

in hybrid balancing systems," *IEEE Transactions on Control Systems Technology*, vol. 30, no. 3, pp. 1228–1243, 2022.

[18] M. M. U. Rehman, "Modular, scalable battery systems with integrated cell balancing and dc bus power processing," Ph.D. dissertation, Utah State University, 2018.

[19] D. Frost, "Battery management systems with active loading and decentralised control," Ph.D. dissertation, University of Oxford, 2017.

[20] J. Löfberg, "Yalmip : A toolbox for modeling and optimization in matlab," in *In Proceedings of the CACSD Conference*, Taipei, Taiwan, 2004.

[21] X. Dorronsoro, E. Garayalde, U. Iraola, and M. Aizpurua, "Modular battery energy storage system design factors analysis to improve battery-pack reliability," *Journal of Energy Storage*, vol. 54, p. 105256, 2022.

[22] ——, "Modular battery systems' accessible energy analysis," in *Seminario Anual de Automática, Electrónica Industrial e Instrumentación*, 2022.

[23] X. Dorronsoro, I. Lopetegi, E. Garayalde, U. Iraola, and J. Yeregui, "Modular battery energy storage systems for available energy increase," in *2022 IEEE Vehicle Power and Propulsion Conference (VPPC)*, 2022, pp. 1–7.

[24] X. Dorronsoro, R. De Castro, J. V. Barreras, E. Garayalde, and U. Iraola, "Model predictive control for ev chargers coupling electro-thermal and degradation battery models," in *2023 IEEE Vehicle Power and Propulsion Conference (VPPC)*, 2023, pp. 1–7.

[25] I. Aghabali, J. Bauman, P. J. Kollmeyer, Y. Wang, B. Bilgin, and A. Emadi, "800-V Electric Vehicle Powertrains: Review and Analysis of Benefits, Challenges, and Future Trends," *IEEE Trans. Transp. Electrif.*, vol. 7, no. 3, pp. 927–948, 2021.

[26] D. Knuth. Useable battery capacity of electric vehicles. [Online]. Available: https://ev-database.org/uk/cheatsheet/useable-battery-capacity-electric-car

[27] J. Tian, Y. Fan, T. Pan, X. Zhang, J. Yin, and Q. Zhang, "A critical review on inconsistency mechanism, evaluation methods and improvement measures for lithium-ion battery energy storage systems," *Renewable and Sustainable Energy Reviews*, vol. 189, p. 113978, 2024.

[28] T. Baumhöfer, M. Brühl, S. Rothgang, and D. U. Sauer, "Production caused variation in capacity aging trend and correlation to initial cell performance," *Journal of Power Sources*, vol. 247, pp. 332–338, 2014.

[29] A. Zimmerman, "Self-discharge losses in lithium-ion cells," *IEEE Aerospace and Electronic Systems Magazine*, vol. 19, no. 2, pp. 19–24, 2004.

[30] Y. Shi, K. Smith, R. Zane, and D. Anderson, "Life prediction of large lithium-ion battery packs with active and passive balancing," in *2017 American Control Conference (ACC)*, 2017, pp. 4704–4709.

[31] G. Piombo, S. Fasolato, R. Heymer, M. Hidalgo, M. Faraji Niri, S. Onori, and J. Marco, "Unveiling the performance impact of module level features on parallel-connected lithium-ion cells via explainable machine learning techniques on a full factorial design of experiments," *Journal of Energy Storage*, vol. 84, p. 110783, 2024.

[32] I. Aizpuru, U. Iraola, J. M. Canales, M. Echeverria, and I. Gil, "Passive balancing design for li-ion battery packs based on single cell experimental tests for a cccv charging mode," in *2013 International Conference on Clean Electrical Power (ICCEP)*, 2013, pp. 93–98.

[33] N. Ghaeminezhad, Q. Ouyang, X. Hu, G. Xu, and Z. Wang, "Active cell equalization topologies analysis for battery packs: A systematic review," *IEEE Transactions on Power Electronics*, vol. 36, no. 8, pp. 9119–9135, 2021.

[34] I. Lopetegi, G. L. Plett, M. S. Trimboli, A. K. de Souza, L. Oca, E. Miguel, and U. Iraola, "A new battery soc/soh/esoh estimation method using a pbm and interconnected spkfs: Part i. soc and internal variable estimation," *Journal of The Electrochemical Society*, vol. 171, no. 3, p. 030519, mar 2024.

[35] J. V. Barreras, R. de Castro, Y. Wan, and T. Dragicevic, "A consensus algorithm for multi-objective battery balancing," *Energies*, vol. 14, no. 14, 2021.

[36] N. Ghaeminezhad, Q. Ouyang, X. Hu, G. Xu, and Z. Wang, "Active cell equalization topologies analysis for battery packs: A systematic review," *IEEE Transactions on Power Electronics*, vol. 36, no. 8, pp. 9119–9135, 2021.

[37] H. Chen, L. Zhang, and Y. Han, "System-theoretic analysis of a class of battery equalization systems: Mathematical modeling and performance evaluation," *IEEE Transactions on Vehicular Technology*, vol. 64, no. 4, pp. 1445–1457, 2015.

[38] F. Chen, J. Yuan, C. Zheng, C. Wang, Z. Li, and X. Zhou, "A state-of-charge based active ev battery balancing method," in *Proceedings of the 2018 2nd International Conference on Electrical Engineering and Automation (ICEEA 2018)*. Atlantis Press, 2018/03, pp. 70–73.

[39] Q. Ouyang, W. Han, C. Zou, G. Xu, and Z. Wang, "Cell balancing control for lithium-ion battery packs: A hierarchical optimal approach," *IEEE Transactions on Industrial Informatics*, vol. 16, no. 8, pp. 5065–5075, 2020.

[40] Q. Ouyang, Z. Wang, K. Liu, G. Xu, and Y. Li, "Optimal charging control for lithium-ion battery packs: A distributed average tracking approach," *IEEE Transactions on Industrial Informatics*, vol. 16, no. 5, pp. 3430–3438, 2020.

[41] C.-S. Lim, K.-J. Lee, N.-J. Ku, D.-S. Hyun, and R.-Y. Kim, "A modularized equalization method based on magnetizing energy for a series-connected lithium-ion battery string," *IEEE Transactions on Power Electronics*, vol. 29, no. 4, pp. 1791–1799, 2014.

[42] Y. Chen, X. Liu, Y. Cui, J. Zou, and S. Yang, "A multiwinding transformer cell-to-cell active equalization method for lithium-ion batteries with reduced number of driving circuits," *IEEE Transactions on Power Electronics*, vol. 31, no. 7, pp. 4916–4929, 2016.

[43] Z. Zhang, H. Gui, D.-J. Gu, Y. Yang, and X. Ren, "A hierarchical active balancing architecture for lithium-ion batteries," *IEEE Transactions on Power Electronics*, vol. 32, no. 4, pp. 2757–2768, 2017.

[44] S. Ci, N. Lin, and D. Wu, "Reconfigurable battery techniques and systems: A survey," *IEEE Access*, vol. 4, pp. 1175–1189, 2016.

[45] S. Muhammad, M. U. Rafique, S. Li, Z. Shao, Q. Wang, and X. Liu, "Reconfigurable battery systems: A survey on hardware architecture and research challenges," *ACM Trans. Des. Autom. Electron. Syst.*, vol. 24, no. 2, Mar. 2019.

[46] S. Rothgang, H. Nordmann, C. Schäper, and D. U. Sauer, "Challenges in battery pack design," in *2012 Electrical Systems for Aircraft, Railway and Ship Propulsion*, 2012, pp. 1–6.

[47] S. Ci, N. Lin, and D. Wu, "Reconfigurable battery techniques and systems: A survey," *IEEE Access*, vol. 4, pp. 1175–1189, 2016.

[48] F. Baronti, G. Fantechi, R. Roncella, and R. Saletti, "Design of a module switch for battery pack reconfiguration in high-power applications," in *2012 IEEE International Symposium on Industrial Electronics*, 2012, pp. 1330–1335.

[49] T. Kim, W. Qiao, and L. Qu, "Power electronics-enabled self-x multicell batteries: A design toward smart batteries," *IEEE Transactions on Power Electronics*, vol. 27, no. 11, pp. 4723–4733, 2012.

[50] A. Manenti, A. Abba, A. Merati, S. M. Savaresi, and A. Geraci, "A new bms architecture based on cell redundancy," *IEEE Transactions on Industrial Electronics*, vol. 58, no. 9, pp. 4314–4322, 2011.

[51] L. He, L. Gu, L. Kong, Y. Gu, C. Liu, and T. He, "Exploring adaptive reconfiguration to optimize energy efficiency in large-scale battery systems," in *2013 IEEE 34th Real-Time Systems Symposium*, 2013, pp. 118–127.

[52] H. Kim and K. G. Shin, "Desa: Dependable, efficient, scalable architecture for management of large-scale batteries," *IEEE Transactions on Industrial Informatics*, vol. 8, no. 2, pp. 406–417, 2012.

[53] V. Sukumar, M. Alahmad, K. Buck, H. Hess, H. Li, D. Cox, F. N. Zghoul, J. Jackson, S. Terry, B. Blalock, M. Mojarradi, W. West, and J. Whitacre, "Switch array system for thin film lithium microbatteries," *Journal of Power Sources*, vol. 136, no. 2, pp. 401–407, 2004.

[54] S. Ci, J. Zhang, H. Sharif, and M. Alahmad, "A novel design of adaptive reconfigurable multicell battery for power-aware embedded networked sensing systems," in *IEEE GLOBECOM 2007 - IEEE Global Telecommunications Conference*, 2007, pp. 1043–1047.

[55] H. Kim and K. G. Shin, "On dynamic reconfiguration of a large-scale battery system," in *2009 15th IEEE Real-Time and Embedded Technology and Applications Symposium*, 2009, pp. 87–96.

[56] F. Altaf, B. Egardt, and L. Johannesson Mårdh, "Load management of modular battery using model predictive control: Thermal and state-of-charge balancing," *IEEE Transactions on Control Systems Technology*, vol. 25, no. 1, pp. 47–62, 2017.

[57] D. F. Frost and D. A. Howey, "Completely decentralized active balancing battery management system," *IEEE Transactions on Power Electronics*, vol. 33, no. 1, pp. 729–738, 2018.

[58] F. Altaf, "On modeling and optimal control of modular batteries," Ph.D. dissertation, Chalmers University of Technology, 2016.

[59] A. Xu, L. Rui, L. Chang, C. Qiang, L. Xiaolin, L. Bo, C. Man, L. Yongqi, G. Haifeng, L. Jianlin, Y. Bo, G. Jianghua, and L. Guanjun, "Transformerless high-voltage power conversion system for battery energy storage system and the first demonstration application in world," *Proceedings of the CSEE*, vol. 387, pp. 200–211, 2020.

[60] C.-S. Moo, K. S. Ng, and Y.-C. Hsieh, "Parallel operation of battery power modules," *IEEE Transactions on Energy Conversion*, vol. 23, no. 2, pp. 701–707, 2008.

[61] L. Koltermann, M. Celi Cortés, J. Figgener, S. Zurmühlen, and D. U. Sauer, "Power curves of megawatt-scale battery storage technologies for frequency regulation and energy trading," *Applied Energy*, vol. 347, p. 121428, 2023.

[62] K. Jacqué, L. Koltermann, J. Figgener, S. Zurmühlen, and D. U. Sauer, "The influence of frequency containment reserve on the efficiency of a hybrid stationary large-scale storage system," *Journal of Energy Storage*, vol. 52, p. 104961, 2022.

[63] Z. Ma, M. Jia, L. Koltermann, A. Blömeke, R. W. De Doncker, W. Li, and D. U. Sauer, "Review on grid-tied modular battery energy storage systems: Configuration classifications, control advances, and performance evaluations," *Journal of Energy Storage*, vol. 74, p. 109272, 2023.

[64] E. Unamuno and J. A. Barrena, "Hybrid ac/dc microgrids—part ii: Review and classification of control strategies," *Renewable and Sustainable Energy Reviews*, vol. 52, pp. 1123–1134, 2015.

[65] N. Ghorbani, A. Kasaeian, A. Toopshekan, L. Bahrami, and A. Maghami, "Optimizing a hybrid wind-pv-battery system using ga-pso and mopso for reducing cost and increasing reliability," *Energy*, vol. 154, pp. 581–591, 2018.

[66] M. Sedghi, A. Ahmadian, and M. Aliakbar-Golkar, "Optimal storage planning in active distribution network considering uncertainty of wind power distributed generation," *IEEE Transactions on Power Systems*, vol. 31, no. 1, pp. 304–316, 2016.

[67] A. Tomaszewska, Z. Chu, X. Feng, S. O'Kane, X. Liu, J. Chen, C. Ji, E. Endler, R. Li, L. Liu, Y. Li, S. Zheng, S. Vetterlein, M. Gao, J. Du, M. Parkes, M. Ouyang, M. Marinescu, G. Offer, and B. Wu, "Lithium-ion battery fast charging: A review," *eTransportation*, vol. 1, p. 100011, 2019.

[68] B. Zhou, G. Fan, Y. Wang, Y. Liu, S. Chen, Z. Sun, C. Meng, J. Yang, and X. Zhang, "Life-extending optimal charging for lithium-ion batteries based on a multi-physics model and model predictive control," *Applied Energy*, vol. 361, p. 122918, 2024.

[69] M. Mühlbauer, "Evaluation of power flow control strategies for heterogeneous battery energy storage systems," Ph.D. dissertation, Universität Bayreuth, 2022.

[70] F. Garrett, M. James, M. Jesse, and T. Hervé, "The economics of battery energy storage: How multi-use, customer-sited batteries deliver the most services and value to customers and the grid," Rocky Mountain Institute, Tech. Rep., September 2015. [Online]. Available: http://www.rmi.org/electricity_battery_value

[71] A. Pozzi, M. Zambelli, A. Ferrara, and D. M. Raimondo, "Balancing-aware charging strategy for series-connected lithium-ion cells: A nonlinear model predictive control approach," *IEEE Transactions on Control Systems Technology*, vol. 28, no. 5, pp. 1862–1877, 2020.

[72] F. Feng, X. Hu, J. Liu, X. Lin, and B. Liu, "A review of equalization strategies for series battery packs: variables, objectives, and algorithms," *Renewable and Sustainable Energy Reviews*, vol. 116, p. 109464, 2019.

[73] M. Schimpe, J. V. Barreras, B. Wu, and G. J. Offer, "Battery degradation-aware current derating: An effective method to prolong lifetime and ease thermal management," *Journal of The Electrochemical Society*, vol. 168, no. 6, p. 060506, jun 2021.

[74] S. (2008). Nasa/tp-2003–212242 instructions for eee parts selection,screening, qualification, and derating. Accessed: 08.05.2023. [Online]. Available: https://nepp.nasa.gov/docuploads/FFB52B88-36AE-4378-A05B2C084B5EE2CC/EEE-INST-002_add1.pdf

[75] L. Patnaik, A. V. J. S. Praneeth, and S. S. Williamson, "A closed-loop constant-temperature constant-voltage charging technique to reduce charge time of lithium-ion batteries," *IEEE Transactions on Industrial Electronics*, vol. 66, no. 2, pp. 1059–1067, 2019.

[76] G. Angenendt, S. Zurmühlen, H. Axelsen, and D. U. Sauer, "Comparison of different operation strategies for pv battery home storage systems including forecast-based operation strategies," *Applied Energy*, vol. 229, pp. 884–899, 2018.

[77] A. Chahbaz, F. Meishner, W. Li, C. Ünlübayir, and D. Uwe Sauer, "Non-invasive identification of calendar and cyclic ageing mechanisms for lithium-titanate-oxide batteries," *Energy Storage Materials*, vol. 42, pp. 794–805, 2021.

[78] Y. Gao, J. Jiang, C. Zhang, W. Zhang, Z. Ma, and Y. Jiang, "Lithium-ion battery aging mechanisms and life model under different charging stresses," *Journal of Power Sources*, vol. 356, pp. 103–114, 2017.

[79] S. S. Sebastian, B. Dong, T. Zerrin, P. A. Pena, A. S. Akhavi, Y. Li, C. S. Ozkan, and M. Ozkan, "Adaptive fast charging methodology for commercial li-ion batteries based on the internal resistance spectrum," *Energy Storage*, vol. 2, no. 4, p. e141, 2020.

[80] B. Liu, J.-G. Zhang, and W. Xu, "Advancing lithium metal batteries," *Joule*, vol. 2, no. 5, pp. 833–845, 2018.

[81] Y. Yin, Y. Hu, S.-Y. Choe, H. Cho, and W. T. Joe, "New fast charging method of lithium-ion batteries based on a reduced order electrochemical model considering side reaction," *Journal of Power Sources*, vol. 423, pp. 367–379, 2019.

[82] M. Bibinsha and P. Sivraj, "Machine learning based battery aging management strategy for electric vehicles," in *2021 Second International Conference on Electronics and Sustainable Communication Systems (ICESC)*. IEEE, 2021, pp. 128–134.

[83] M. Ye, H. Gong, R. Xiong, and H. Mu, "Research on the battery charging strategy with charging and temperature rising control awareness," *IEEE Access*, vol. 6, pp. 64 193–64 201, 2018.

[84] U. R. Koleti, C. Zhang, R. Malik, T. Q. Dinh, and J. Marco, "The development of optimal charging strategies for lithium-ion batteries to prevent the onset of lithium plating at low ambient temperatures," *Journal of Energy Storage*, vol. 24, p. 100798, 2019.

[85] J. Sieg, J. Bandlow, T. Mitsch, D. Dragicevic, T. Materna, B. Spier, H. Witzenhausen, M. Ecker, and D. U. Sauer, "Fast charging of an electric vehicle lithium-ion battery

at the limit of the lithium deposition process," *Journal of Power Sources*, vol. 427, pp. 260–270, 2019.

[86] U. R. Koleti, C. Zhang, R. Malik, T. Q. Dinh, and J. Marco, "The development of optimal charging strategies for lithium-ion batteries to prevent the onset of lithium plating at low ambient temperatures," *Journal of Energy Storage*, vol. 24, p. 100798, 2019.

[87] C.-H. Lee, Z.-Y. Wu, S.-H. Hsu, and J.-A. Jiang, "Cycle life study of li-ion batteries with an aging-level-based charging method," *IEEE Transactions on Energy Conversion*, vol. 35, no. 3, pp. 1475–1484, 2020.

[88] Z. Guo, B. Y. Liaw, X. Qiu, L. Gao, and C. Zhang, "Optimal charging method for lithium ion batteries using a universal voltage protocol accommodating aging," *Journal of Power Sources*, vol. 274, pp. 957–964, 2015.

[89] A. R. Mandli, S. Ramachandran, A. Khandelwal, K. Y. Kim, and K. S. Hariharan, "Fast computational framework for optimal life management of lithium ion batteries," *International Journal of Energy Research*, vol. 42, no. 5, pp. 1973–1982, 2018.

[90] S. Su, W. Li, A. Garg, and L. Gao, "An adaptive boosting charging strategy optimization based on thermoelectric-aging model, surrogates and multi-objective optimization," *Applied Energy*, vol. 312, p. 118795, 2022.

[91] H. Zhou, M. Erol-Kantarci, Y. Liu, and H. V. Poor, "A survey on model-based, heuristic, and machine learning optimization approaches in ris-aided wireless networks," *IEEE Communications Surveys & Tutorials*, 2023.

[92] H. Pourbabak, T. Chen, and W. Su, "1 - centralized, decentralized, and distributed control for energy internet," in *The Energy Internet*, W. Su and A. Q. Huang, Eds. Woodhead Publishing, 2019, pp. 3–19.

[93] W. Ren and R. W. Beard, *Distributed consensus in multi-vehicle cooperative control*. Springer, 2008, vol. 27, no. 2.

[94] A. X. Sun, D. T. Phan, and S. Ghosh, "Fully decentralized ac optimal power flow algorithms," in *2013 IEEE Power & Energy Society General Meeting*, 2013, pp. 1–5.

[95] H. Pourbabak, T. Chen, B. Zhang, and W. Su, "Control and energy management system in microgrids," *arXiv preprint arXiv:1705.10196*, 2017.

[96] T. Senjyu, R. Kuninaka, N. Urasaki, H. Fujita, and T. Funabashi, "Power system stabilization based on robust centralized and decentralized controllers," in *2005 International Power Engineering Conference*. IEEE, 2005, pp. 905–910.

[97] H. Pourbabak, S. Xu, T. Chen, Z. Liang, and W. Su, "Distributed control algorithm for optimal power allocation of ev parking lots," in *2017 IEEE Power & Energy Society General Meeting*. IEEE, 2017, pp. 1–5.

[98] S. Xu, H. Pourbabak, and W. Su, "Distributed cooperative control for economic operation of multiple plug-in electric vehicle parking decks," *International Transactions on Electrical Energy Systems*, vol. 27, no. 9, p. e2348, 2017.

[99] Y. Zheng, M. Ouyang, X. Han, L. Lu, and J. Li, "Investigating the error sources of the online state of charge estimation methods for lithium-ion batteries in electric vehicles," *Journal of Power Sources*, vol. 377, pp. 161–188, 2018.

[100] E. Miguel, G. L. Plett, M. S. Trimboli, I. Lopetegi, L. Oca, U. Iraola, and E. Bekaert, "Electrochemical model and sigma point kalman filter based online oriented battery model," *IEEE Access*, vol. 9, pp. 98 072–98 090, 2021.

[101] G. Dos Reis, C. Strange, M. Yadav, and S. Li, "Lithium-ion battery data and where to find it," *Energy and AI*, vol. 5, p. 100081, 2021.

[102] S. Passerini, L. Barelli, M. Baumann, J. Peters, and M. Weil, *Emerging Battery Technologies to Boost the Clean Energy Transition: Cost, Sustainability, and Performance Analysis*. Springer Nature, 2024.

[103] Q. Mayemba, R. Mingant, A. Li, G. Ducret, and P. Venet, "Aging datasets of commercial lithium-ion batteries: A review," *Journal of Energy Storage*, vol. 83, p. 110560, 2024.

[104] M. Schimpe, M. E. von Kuepach, M. Naumann, H. C. Hesse, K. Smith, and A. Jossen, "Comprehensive modeling of temperature-dependent degradation mechanisms in lithium iron phosphate batteries," *Journal of The Electrochemical Society*, vol. 165, no. 2, p. A181, jan 2018.

[105] J. Sowe, J. Varela Barreras, M. Schimpe, B. Wu, C. Candelise, J. Nelson, and S. Few, "Model-informed battery current derating strategies: Simple methods to extend battery lifetime in islanded mini-grids," *Journal of Energy Storage*, vol. 51, p. 104524, 2022.

[106] M. Schimpe, M. Naumann, N. Truong, H. C. Hesse, S. Santhanagopalan, A. Saxon, and A. Jossen, "Energy efficiency evaluation of a stationary lithium-ion battery container storage system via electro-thermal modeling and detailed component analysis," *Applied Energy*, vol. 210, pp. 211–229, 2018.

[107] N. Padmanabhan, M. Ahmed, and K. Bhattacharya, "Battery energy storage systems in energy and reserve markets," *IEEE Transactions on Power Systems*, vol. 35, no. 1, pp. 215–226, 2020.

[108] Y. Shi, B. Xu, Y. Tan, D. Kirschen, and B. Zhang, "Optimal battery control under cycle aging mechanisms in pay for performance settings," *IEEE Transactions on Automatic Control*, vol. 64, no. 6, pp. 2324–2339, 2019.

[109] E. Thomas, I. Bloom, J. Christophersen, and V. Battaglia, "Rate-based degradation modeling of lithium-ion cells," *Journal of Power Sources*, vol. 206, pp. 378–382, 2012.

[110] M. Safari and C. Delacourt, "Modeling of a commercial graphite/lifepo4 cell," *Journal of The Electrochemical Society*, vol. 158, no. 5, p. A562, mar 2011.

[111] N. Collath, B. Tepe, S. Englberger, A. Jossen, and H. Hesse, "Aging aware operation of lithium-ion battery energy storage systems: A review," *Journal of Energy Storage*, vol. 55, p. 105634, 2022.

[112] S. P. Boyd and L. Vandenberghe, *Convex optimization*. Cambridge university press, 2004.

[113] H. C. Hesse, V. Kumtepeli, M. Schimpe, J. Reniers, D. A. Howey, A. Tripathi, Y. Wang, and A. Jossen, "Ageing and efficiency aware battery dispatch for arbitrage markets using mixed integer linear programming," *Energies*, vol. 12, no. 6, 2019.

[114] J. Cai, H. Zhang, and X. Jin, "Aging-aware predictive control of pv-battery assets in buildings," *Applied Energy*, vol. 236, pp. 478–488, 2019.

[115] N. Li, F. Gao, T. Hao, Z. Ma, and C. Zhang, "Soh balancing control method for the mmc battery energy storage system," *IEEE Transactions on Industrial Electronics*, vol. 65, no. 8, pp. 6581–6591, 2018.

[116] W.-W. Kim, J.-S. Shin, S.-Y. Kim, and J.-O. Kim, "Operation scheduling for an energy storage system considering reliability and aging," *Energy*, vol. 141, pp. 389–397, 2017.

[117] S. Englberger, A. Jossen, and H. Hesse, "Unlocking the potential of battery storage with the dynamic stacking of multiple applications," *Cell reports physical science*, vol. 1, no. 11, 2020.

[118] L. Grne and J. Pannek, *Nonlinear model predictive control: theory and algorithms*. Springer Publishing Company, Incorporated, 2013.

[119] A. H. K. de Souza, "Physics-based modeling, estimation and control for lithium-ion and lithium-metal batteries," Ph.D. dissertation, University of Colorado Colorado Springs, 2023.

[120] G. L. Plett and M. S. Trimboli, *Battery Management Systems, Volume 3: Physics-Based Methods*. Artech House, 2024, vol. 3.

[121] A. Kawakita de Souza, W. Hileman, M. S. Trimboli, and G. L. Plett, "A control-oriented reduced-order model for lithium-metal batteries," *IEEE Control Systems Letters*, vol. 7, pp. 1165–1170, 2023.

[122] B. Zhou, G. Fan, Y. Wang, Y. Liu, S. Chen, Z. Sun, C. Meng, J. Yang, and X. Zhang, "Life-extending optimal charging for lithium-ion batteries based on a multi-physics model and model predictive control," *Applied Energy*, vol. 361, p. 122918, 2024.

[123] R. Du, X. Hu, S. Xie, L. Hu, Z. Zhang, and X. Lin, "Battery aging- and temperature-aware predictive energy management for hybrid electric vehicles," *Journal of Power Sources*, vol. 473, p. 228568, 2020.

[124] G. Pozzato, M. Müller, S. Formentin, and S. M. Savaresi, "Economic mpc for online least costly energy management of hybrid electric vehicles," *Control Engineering Practice*, vol. 102, p. 104534, 2020.

[125] S. East and M. Cannon, "Optimal power allocation in battery/supercapacitor electric vehicles using convex optimization," *IEEE Transactions on Vehicular Technology*, vol. 69, no. 11, pp. 12 751–12 762, 2020.

[126] A. B. Kordabad, W. Cai, and S. Gros, "Multi-agent battery storage management using mpc-based reinforcement learning," in *2021 IEEE Conference on Control Technology and Applications (CCTA)*, 2021, pp. 57–62.

[127] C. Le Floch, S. Bansal, C. J. Tomlin, S. J. Moura, and M. N. Zeilinger, "Plug-and-play model predictive control for load shaping and voltage control in smart grids," *IEEE Transactions on Smart Grid*, vol. 10, no. 3, pp. 2334–2344, 2019.

[128] B. Banfield, D. A. Robinson, and A. P. Agalgaonkar, "Comparison of economic model predictive control and rule-based control for residential energy storage systems," *IET Smart Grid*, vol. 3, no. 5, pp. 722–729, 2020.

[129] M. Schlemminger, T. Ohrdes, E. Schneider, and M. Knoop, "Dataset on electrical single-family house and heat pump load profiles in germany," *Scientific data*, vol. 9, no. 1, p. 56, 2022.

[130] D. Kucevic, B. Tepe, S. Englberger, A. Parlikar, M. Mühlbauer, O. Bohlen, A. Jossen, and H. Hesse, "Standard battery energy storage system profiles: Analysis of various applications for stationary energy storage systems using a holistic simulation framework," *Journal of Energy Storage*, vol. 28, p. 101077, 2020.

[131] Jrc photovoltaic geographical information system (pvgis) - european commission. Accessed: 08.05.2023. [Online]. Available: https://re.jrc.ec.europa.eu/pvg_tools/en/

[132] Energyonline®. Accessed: 08.05.2023. [Online]. Available: http://www.energyonline.com/Data/GenericData.aspx?DataId=20&CAISO___Average_Price

[133] F. Duffner, M. Wentker, M. Greenwood, and J. Leker, "Battery cost modeling: A review and directions for future research," *Renewable and Sustainable Energy Reviews*, vol. 127, p. 109872, 2020.

[134] L. Mauler, F. Duffner, W. G. Zeier, and J. Leker, "Battery cost forecasting: a review of methods and results with an outlook to 2050," *Energy & Environmental Science*, vol. 14, no. 9, pp. 4712–4739, 2021.

[135] W. Cole, A. W. Frazier, and C. Augustine, "Cost projections for utility-scale battery storage: 2021 update," National Renewable Energy Lab. (NREL), Tech. Rep., 6 2021.

[136] S. Jacobitz, S. Scherler, and X. Liu-Henke, "Model-based design of a scalable battery management system by using a low-cost rapid control prototyping system," in *2018 Thirteenth International Conference on Ecological Vehicles and Renewable Energies (EVER)*, 2018, pp. 1–7.

[137] D. G. Jimenez, "A hybrid methodology for fault detection and diagnosis in railway traction systems: Integrating data-driven and physics-based models," Ph.D. dissertation, Mondragon Unibertsitatea, 2023.

[138] M. Mühlbauer, O. Bohlen, and M. A. Danzer, "Analysis of power flow control strategies in heterogeneous battery energy storage systems," *Journal of Energy Storage*, vol. 30, p. 101415, 2020.

[139] F. Altaf, B. Egardt, and L. Johannesson Mårdh, "Load management of modular battery using model predictive control: Thermal and state-of-charge balancing," *IEEE Transactions on Control Systems Technology*, vol. 25, no. 1, pp. 47–62, 2017.

[140] M. Bauer, M. Muehlbauer, O. Bohlen, M. A. Danzer, and J. Lygeros, "Power flow in heterogeneous battery systems," *Journal of Energy Storage*, vol. 25, p. 100816, 2019.